

Journal of Experimental Biology

Colonial Architecture Modulates the Speed and Efficiency of Multi-Jet Swimming in Salp Colonies

--Manuscript Draft--

| | |
|------------------------------------|--|
| Manuscript Number: | |
| Article Type: | Research Article |
| Full Title: | Colonial Architecture Modulates the Speed and Efficiency of Multi-Jet Swimming in Salp Colonies |
| Abstract: | <p>Salps are marine pelagic tunicates with a complex life cycle including a solitary and colonial stage. Salp colonies are composed of asexually budded individuals that coordinate their swimming by multi-jet propulsion. Colonies develop into species-specific architectures with distinct zooid orientations. These distinct colonial architectures vary in how frontal area scales with the number of propeller zooids in the colony. Based on findings from other jet-propelled systems, we hypothesize that differences in frontal area drive differences in swimming speed and that increased swimming speed leads to higher cost of transport in salps. We (1) compare swimming speed across salp species and architectures, (2) evaluate how swimming speed scales with the number of zooids in the colony in architectures with a constant motion-orthogonal frontal area as well as in those where this area increases with the number of zooids, and (3) compare the metabolic cost of transport across different species and how it scales with swimming speed. To measure swimming speeds, we recorded swimming salp colonies using <i>in situ</i> videography while SCUBA diving in the open ocean. To estimate the cost of transport, we measured the respiration rates of swimming and anesthetized salps collected <i>in situ</i> using jars equipped with non-invasive oxygen sensors. We found that linear colonies generally swim faster due to their differential advantage in frontal area scaling with an increasing number of zooids. While cost of transport generally did not differ significantly between architectures, we did find that higher swimming speeds predict lower costs of transport in salps. These findings underscore the importance of considering propeller arrangement to optimize speed and energy efficiency in bioinspired underwater vehicle design, leveraging lessons learned from the diverse natural laboratory provided by salp diversity.</p> |
| Corresponding Author: | Alejandro Damian-Serrano, Ph.D. University of Oregon Oregon Institute of Marine Biology Eugene, OR UNITED STATES |
| Other Authors: | Kaiden A. Walton, B.S. Anneliese Bishop-Perdue, B.S. Sophie Bagoye Kevin T. Du Clos, Ph.D. Bradford J. Gemmell, Ph.D. Sean P. Colin, Ph.D. John H. Costello, Ph.D. Kelly R. Sutherland, Ph.D. |
| Keywords: | salps; colonial architecture; multi-jet propulsion; swimming; cost of transport |
| Manuscript Classifications: | Invertebrate; Biomechanics - locomotion |
| Suggested Reviewers: | Moira Décima mdecima@ucsd.edu Salp physiology expertise Joshua Stone jpstone@vims.edu salp swimming and respiration expertise Michael Stukel |

| | |
|--|--|
| | mstukel@fsu.edu Salp migratory behavior and zooplankton ecology expertise |
| Opposed Reviewers: | |
| Additional Information: | |
| Question | Response |
| Companion Paper | No |
| Is your paper a companion paper (part of a group of papers being submitted)? | |
| Editor Suggestions You may request that your submission is assigned to a specific editor . Please suggest no more than three editor names in order of preference. Although you may suggest an editor for your submission, the journal will make the final assignment. If you do not request an editor, your submission will be assigned to the most appropriate editor as determined by the editorial staff. | Sheila Patek (previous editor for first submission) |
| Special Issue | No, this article is not part of a special themed issue |
| Open Access | Green Open Access |
| Please check your funder requirements carefully and select the appropriate Open Access publication route below. A quote for your Open Access publication charges will be available to view on the final submission page, revealing any institutional discounts and providing you with another chance to select Open Access. See Instructions for further information. | |
| Word Count | 9045 |
| Number of Figures | 6 |
| Number of Tables | 0 |

Dear JEB editors,

Please find our revised and resubmitted manuscript titled "Colonial Architecture Modulates Speed and Efficiency of Multi-Jet Swimming in Salp Colonies" to be considered for publication as a Research Article in the Journal of Experimental Biology. We believe we have now addressed the reviewers' concerns.

Aquatic animals swim via a variety of propulsive strategies. While studies on pulsed jets date back to the 1970s, multi-jet propulsion is one of the least studied modes of aquatic locomotion, found in understudied colonial gelatinous invertebrates such as salps and siphonophores. Previous studies have shown that multi-jet propulsion is an efficient strategy that confers mechanical advantages over single-jet propulsion and provides a promising avenue for bioinspired underwater vehicle design. Salp colonies develop into different species-specific architectures with distinct zooid orientations. This morphological diversity presents a natural laboratory to explore and understand the hydrodynamic implications of different multi-jet arrangement designs.

Salps inhabit remote open ocean environments with great bottom depths, posing unique challenges for accessing and observing them. Moreover, salps are extremely fragile and cannot be collected intact with nets nor maintained alive in containers for extended periods. To overcome these challenges, we embarked on diurnal and nocturnal SCUBA diving expeditions in the open ocean off the coast of Hawaii, where we found a broad diversity of salp species across all colonial architectures. Here we used state-of-the-art methods to record the swimming behavior and measure their respiratory physiology from 18 species of salp.

Our results indicate that linear colonies generally swim faster and more efficiently, as a result of a more hydrodynamic arrangement of their zooids, underscoring the importance of propeller arrangement. By leveraging lessons learned from salp diversity, this research builds a foundation for optimizing speed and energy efficiency in underwater multi-jet propulsion systems.

Salps play a crucial role in the oceanic carbon cycle, exporting large quantities of fixed carbon into the deep sea. Our study sheds light on the distribution of their ecological impact across the diversity of salp species as it relates to their respiration rates and their locomotory ability to perform long-distance vertical migrations. Further, this study follows up with our prior work on the evolutionary history of salp colonial architecture, testing many of the hypotheses generated by the reconstructed evolutionary transitions on the phylogeny.

We believe that our study advances our understanding of multi-jet locomotion and salp ecophysiology, as well as provides insights into bioinspired underwater vehicle design. We are confident that our cross-disciplinary study will be of interest to the broad readership of JEB.

Thank you for considering our manuscript.

Sincerely,

Alejandro Damian-Serrano, Ph.D.

As you will see, the reviewers raised a number of substantial criticisms that require me to reject your paper. While the reviewers (and I) were very impressed with the scope of the dataset, there were a considerable number of issues with the manuscript that make it unclear as to whether it could be revised sufficiently to be publishable. These issues range from statistics to calculations to the framing of the study and its claims. Perhaps a substantially rewritten manuscript with new analyses could be acceptable, but it is not clear to me whether or not that is feasible. My one broad suggestion is to align the goals of the study with a feasible set of questions that can be robustly addressed with the dataset in hand and appropriate statistics. This may narrow the scope, but it may also allow for a more rigorous study in the end.

A thoroughly revised manuscript might warrant further consideration, but it will require that you make extensive amendments to your paper, including the re-analysis or collection of new data. Even in this case, however, it may not be possible to address the most substantial concerns raised by the reviewers. We are currently under great pressure for space and it takes two very enthusiastic recommendations by the reviewers for a manuscript to be accepted.

>We thank the editor for the helpful feedback.

Reviewer 1 Comments for the Author:

Summary:

This paper tests whether linearly configured (streamlined) colonial invertebrates are faster and more efficient than other architectures. The motivation for the work stated in the paper is bio-inspired design of vehicles. The idea itself is an interesting one, and there are some interesting results in the paper itself.

>We thank Reviewer 1 for their kind feedback.

Overview:

In general, I found two main issues with the paper that need to be addressed in order to strengthen the results and the stated conclusions.

The first issue is that the conclusions in the abstract and the discussion are inconsistent with one another.

>We reworked the abstract to match the discussion (see specifics in replies to other comments below)

Part of the issue is that the hypotheses seem interdependent in some places, so it isn't easy to test them independently.

>We removed the interdependence structure of the primary hypotheses by switching the angle of inquiry on the second hypothesis (whether COT should decrease with speed) away from the

results from the first hypothesis test, and toward previous research (such as Bi & Zhang 2019) predicting that COT should increase with speed in jet-propelled systems.

There is also never a quantitative argument relating either of them explicitly to frontal drag, which is the crux of the paper.

>We removed our claims on drag from the introduction and added some discussion of the relevant forces in the discussion section.

The second is the need for post-hoc analysis to explore the driving source of significance in the results where it was found. Addressing the second point could help with the first one, as the driving sources might explain some of the unexpected results.

>We omitted the t-tests and replaced them with ANOVAs with Tukey post hoc contrasts (to explore the source of significance) with adjusted p-values. We added two supplemental tables S4 and S5 for architecture ANOVAs on the swimming speed and COT data respectively.

Below are some of the main questions and comments that I had while reading the paper.

Questions/Comments:

Lines 23-26 (Summary Statement): Reading the rest of the paper, the results were mixed in some cases (see below). This reads more like a hypothesis than a summary statement of what was found, and the results were more complex than expected. Is this what is intended?

>We edited the Significance Statement to: “Linear arrangements in multi-jet propelled marine colonial invertebrates are faster than less streamlined architectures without incurring higher costs of transport, offering insights for bioinspired underwater vehicle design.”

Lines 32-36 (Abstract): What is meant by swimming performance? Performance can mean many things; since this is part of the hypothesis to be tested, the specific metric should be clearly stated.

>We rephrased swimming performance to swimming speed.

As written, the second hypothesis reads that faster-swimming taxa are more energetically efficient because the drag is lower. What is being compared here? Similarly streamlined taxa? Similarly swimming taxa? Again, this may be clarified in the main paper. Still, the ambiguity in the abstract generates immediate skepticism, as there are many reasons why something might swim faster but be less efficient. In both of these cases, I suggest being more precise in stating the hypotheses so that the reader

has a clear sense of the paper's aims and what is specifically being tested in each case.

>We rewrote the hypothesis structure in the Abstract: "We hypothesize that colonial architecture drives differences in swimming speed between salps due to differences in how frontal area scales with the number of propeller zooids in the colony. Based on findings from other jet-propelled systems, we hypothesize that swimming speed leads to higher cost of transport in salps."

Lines 43-47: The abstract reads with much stronger statements than the results and sometimes omits that the authors' hypotheses weren't supported. In multiple places, for example: lines 357-358, 409-410, 421-423, 559-561, they explicitly state that the results are incongruent with one or more hypotheses. None of this is reflected in the abstract. The abstract should accurately reflect both the congruent and incongruent results, especially when the incongruences are in multiple places and in some cases completely contrary to the hypothesis.

>We edited the abstract results section to: "We found that linear colonies generally swim faster due to their differential advantage in frontal area scaling with an increasing number of zooids. While we did not find any significant differences in cost of transport between architectures, we found that higher swimming speeds predict lower costs of transport in salps". Some of the line examples provided refer to results addressing secondary hypotheses (such as the relationships with pulsation rate) which are not the primary goal of the manuscript and thus don't belong in the abstract.

Lines 43-46 and 80-113: The authors claim that frontal drag accounts for the differences in swimming speeds, but it doesn't appear that the drag was measured/calculated.

>Measuring drag falls outside the scope of the study. We narrowed down our claims to the effects of relative frontal area (streamlinedness) on swimming speeds, which incorporates any underlying forces involved.

In addition, the hypothesis relies entirely on the assumption that frontal drag is the dominant energetic contributor to the system.

>The independent effect of varying relative frontal area can be accounted for even in the presence of additional sources of variation. We only rely on the assumption that frontal-area-driven resistance forces are a non-zero contributor with direct predictable relationships with colonial architecture. Other factors are likely to explain the residual unexplained variation. We added lines to the Discussion delineating alternative explanatory factors, inviting future studies to unravel their influence on salp swimming.

When considering length of chains, for example, other considerations, such as vortex shedding and added mass along the lateral sides, can contribute to energetic cost and can also scale with length. There is also an assumption that the system's stability and efficiency are independent of the chain's length, which is not necessarily true and impacts efficiency. Some of these effects could account for some of the unexpected results mentioned in the paper.

>We added further discussion on factors that may impair performance/efficiency due to an increased number of linear propellers (skin/friction drag, vortex drag). "The questions addressed in this study focus on the effect of frontal area of colonial architectures on swimming speed. This effect may be associated with form and pressure drag differences between more and less streamlined colony shapes. In order to test whether these are the forces responsible for differences in swimming speed, drag would have to be measured or calculated, which is beyond the scope of this study. Other unaccounted forces may be significant energetic contributors to the system that explain the remainder of the observed variation. Chain length for the streamlined forms (helical, linear, and bipinnate chains) could have negative effects on swimming speeds that may partially counteract the positive effect of increased propeller thrust. For example, skin drag increases proportionally to the surface area of the system, and the smoothness of the chain may increase pressure drag through vortex shredding (Vogel 1981). While added (virtual) mass could also be an issue, asynchronously swimming colonies do not suffer as much from these acceleration-related costs, since their speed is maintained near constant while cruising. Chain length could also lead to reduced stability and efficiency, though some linear species capitalize on this by swimming in corkscrew orbital spirals (Sutherland et al. 2024). However, if friction drag, chain stability, or vortex shredding were indeed more important contributors than frontal form drag, we would predict that linear chains would appear slower than other more stable and compact architectures. Future studies may unravel these potential confounding effects on the biomechanics of colonial salp swimming."

Even if linear architectures are shown to be faster and more efficient, I'm not sure you can claim it is due to frontal drag unless you somehow quantify and compare the drag in the analysis. It would be a more substantial claim if the authors addressed why factors other than frontal drag can be ignored or controlled for and tie frontal drag to the quantitative results.

>We added further discussion (see above) of the unaccounted mechanical factors that may confound the results. If friction drag, chain stability, and vortex shredding were more important than frontal form drag, we predict that linear chains would appear slower than other more stable and compact architectures.

For the statistical analysis throughout: the R² values and the linear equations should be given, I didn't see that they were anywhere?

>We added adjusted R² values for each regression. We also made the equations used for each regression more explicit.

In the cases where significance was found, post hoc analysis should be done to determine what

drives the significance. In particular, there is quite a bit of variation in the linear species, and I wonder if one of the taxa is driving a good deal of the significance.

>We changed the t-tests to ANOVAs with post-hoc pairwise analyses to identify the drivers of significance.

Also, a table of the number of individuals collected for each species for each type of measurement for clarity. If I read the SI correctly, the samples for non-linear architectures were, in many cases, much lower than linear architectures, some only having 1-2 specimens. Even when there were several specimens available, it would be helpful to know the relative sample sizes and have it summarized in a table.

>We added Supplementary Table S3 summarizing Ns and other key variables across both the video/speed data and the respirometry experiment data.

Widely varying numbers of taxa and specimens will affect statistical considerations such as p-value thresholds and, in turn, the strength of the statements. In cases where there were only one or two specimens, it might be more appropriate to report the analyses without those taxa and only add them where they can provide significant information.

>Even when sample sizes were low for certain species, we chose not to omit data and instead, we've made our sample sizes and comparisons transparent (see Table S3). Owing to the challenges of working with fragile and patchily occurring open ocean jelly plankton we think it is important to include all of the data.

Generally, the idea of the research is very interesting and could be quite useful for bio-inspired design if the sources of significance and overall results are clearly and consistently reported to the reader in each section of the paper.

>We thank Reviewer 1 for their generous feedback.

Reviewer 2 Comments for the Author:

Damian-Serrano et al. have performed kinematic and energetic measurements upon a variety of sulp species to evaluate how differences in the morphology of these colonies relates to their swimming. The central idea is that colonies organized in a linear arrangement offer less projected area to the oncoming flow, which results in faster and more economical swimming.

The authors' present a tour-de-force of experimental measurements from 17 species, collected in the field, under highly challenging conditions. The data collected here are truly impressive and offer a real gem to the literature, especially given the difficulty to find and work with these animals.

>We thank Reviewer 2 for their generous feedback.

As itemized below, the trouble with this study comes from the analysis of the measurements. There are numerous statements of findings not supported by any statistics, and the statistical comparisons between morphological categories are evaluated by t-tests without mention of standard adjustments like a Bonferroni correction.

>We removed anecdotal comparison statements from the text. We changed the T-tests to ANOVAs with post-hoc pairwise analyses and reported the adjusted p-values for those instead.

There are lesser issues, such as the sample sizes (though itemized in the supplemental materials) are largely not mentioned in the manuscript, and values are not plotted in the figures.

>We added a table to supplement (S3) with a sample size summary per species and some mean values of descriptive variables such as swimming speeds and zooid sizes. We also reported sample sizes in the Methods: "We analyzed the swimming behavior of salp colonies arranged in linear (six species, 64 specimens), bipinnate (three species, 17 specimens), whorl (three species, 10 specimens), cluster (two species, eight specimens), and transversal (one species, two specimens) architectures, with oblique and helical architectures represented by a single specimen."

There is mention of evolutionary trends in the Discussion, but it is unclear to what extent shared ancestry factors into the measured patterns. It is not necessarily a requirement (in my opinion) to perform independent contrast analysis, or some other way of correcting for phylogeny, but a consideration of phylogeny would help inform the extent to which the measurements (especially those related to COT) are due to ancestral relationships.

>We agree that the PICs are not a requirement in this case, since the relationships between "traits" are mechanical and thus can be considered present-time-driven. At no point do we assume or expect the relationships between speed, shape, or efficiency to be a result of them co-evolving with one another along the branches, but rather a product of present mechanics derived from colonial form. We added details in the discussion around potential phylogenetic signal in the residuals or in the error terms for other unaccounted variables.

In short, the statistics employed in this study are not up to contemporary standards to the extent that I am not convinced of any of the findings. Fortunately, I know these investigators are capable of a rigorous data analysis and I hope they are willing to revise this work.

SPECIFIC COMMENTS

L38 - Unclear meaning of "scaling frontal cross-sectional area,"

>We changed it to “architectures with a constant motion-orthogonal frontal area as well as in those where this area increases with the number of zooids,”

L57 - Perhaps “neurophysiologically” or “nervous” instead of “neurologically”. “Neurology” has biomedical connotations.

>**We changed it to neurophysiologically**

It is difficult to make out from figure 1 where the oral and atrial siphons are located. What are the open circles and closed circles on the zooid shapes?

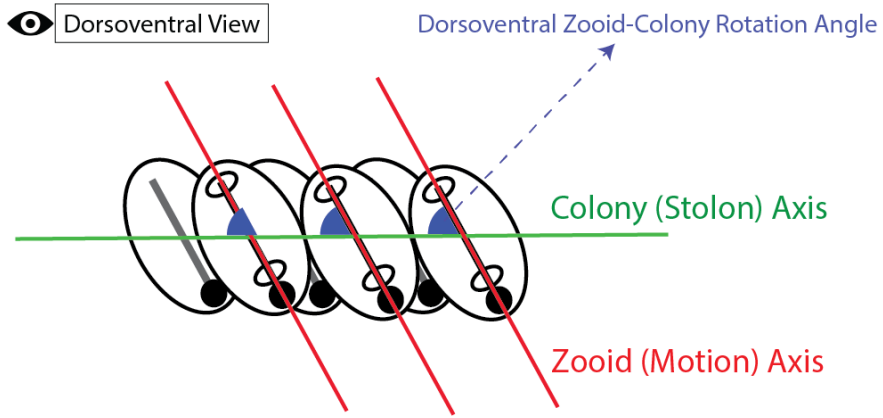
>**We added in the caption an indication that the full black circles are viscera and the open circles are siphons.**

L80-105 - There is an issue with the consideration of frontal area with respect to drag here and in the rest of the paper. The thesis offered here is that more zooids serve to enhance thrust, but their arrangement with respect to the prevailing direction of motion determines the frontal area, and hence, drag on the colony. However, I think readers can reasonably wonder what the implications of the colony arrangement are for the hydrodynamic interactions between zooids, which could affect thrust and drag production. For example, isn't it not possible that a zooid in a chain encounters enhanced drag due (as opposed to a cluster, for example) the jet of the zooid in front of it? It seems to me that the arrangement of zooids could have adverse or beneficial effects on thrust production as well. Your working hypothesis is fine, but you should acknowledge the complexity that it neglects. Alternatively, you may have evidence from prior work for rejecting this complexity, which should be explained.

>We cited Sutherland et al 2024 & Sutherland & Weihs 2017 paper in the Discussion while explaining how jet plumes are non-interacting in linear chains. Non-linear colonies have far broader separation (visibly so) between jet plumes than linear chains (personal observation from several coauthors while diving and imaging jet plumes using fluorescein).

L134- It is not clear on what plane and with respect to what axis these angles are defined. A schematic drawing would help.

>**We added a supplementary figure with the schematic of the DV zooid-colony rotation angle (Fig. S10).**



Faster motion is generally associated with a higher cost of transport, which may hold true for some jetters (e.g., 10.1088/1748-3190/ab57e4). I think I get why that might not be expected here, but it would be helpful for readers if you explained why that expectation may not hold true in this case. It would additionally be helpful to describe relationships between COT and speed in other jet-propelled animals.

>We added a paragraph to the Introduction stating that “In some single-jetters, swimming speed can be directly proportional to the cost of transport (Bi & Zhu 2019) due to a highly inefficient refill phase in the jetting cycle which requires costly acceleration forces to reach high swimming speeds. Since salps are also jet-propelled swimmers, we hypothesize that faster-swimming salps will incur higher costs of transport than their slower counterparts.”

L179 - These systems need to be described in greater detail. Are they all two-camera systems? How were the two cameras synced? In what volume can they interrogate? What are their frame rates and spatial resolution?

>We added details on the two-camera stereovideography system: “The primary stereovideography system was comprised of two synchronized high-resolution cameras (Z Cam E2 and Sync Cable; 4K at 60 or 120 fps) with 17mm f/1.8 lenses (Olympus M.Zuiko Digital) housed in custom aluminum housings (Sexton Company). Each field of view was 23 x 42 mm and in-focus depth was 20-25 mm. The image from the right-hand camera was viewed using an external monitor (Aquatica Digital), and illumination was provided with two 10,000-lumen lights (Keldan). An L-shaped plastic framer helped the videographer position colonies in the field of view of both cameras. Before diving, the stereo system was calibrated in a swimming pool using a cube with reflective landmarks. Calibration images were processed using the CAL software package (SeaGIS measurement science).” + “These two-dimensional videos were collected using a Sony FDR-AX700 4K Camcorder (3840x2160 pixels, 60-120 fps) with a Gates Underwater Housing using brightfield illumination (Colin et al 2022) or darkfield illumination.”

L185 - How were the positions in EventMeasure recorded? How was the 3D spatial calibration performed?

>We added details on how the calibration was performed (see above) and on how the points were selected in EventMeasure in the Methods.

L219 - Explain that coordinates were selected manually (if true).

>We added an explanation of the manual selection to the text.

L298 - It is unclear to me how t-tests could resolve differences between so many species. If they were performed in all possible pairwise comparisons, then that approach would lack statistical power and something like an ANOVA (with post-hoc comparisons) or a mixed-effects model would be better. If I am misunderstanding the design, then please explain in the text.

>We switched from t-tests to ANOVA with post hoc comparisons for both speed and COT comparisons across colonial architectures and reported the adjusted p-values in Tables S4 and S5.

When there were repeated measures, were the mean values used for a species? It should have been or there would be pseudo replication in the analysis. A statistical analysis that takes advantage of those repeated measures would offer a more powerful approach for resolving a significant trend.

>Each specimen was measured only under a single “treatment”, no colonies were measured at different swimming speeds or colony sizes, thus there are no repeated measures across the different factors (colonial architecture, zooid number etc.).

Since the sample sizes are so variable among the species, it would be helpful to report them along with each mean value and p-value provided in the text, or perhaps a new table.

>We reported sample sizes for speed and respirometry across species in the new Table S3 in the supplement.

L317-327 - Since you have not performed stats to demonstrate differences between species, then you cannot offer statements about the relative speed of species. Those differences could be merely due to chance and not a species-specific signal.

>We removed non-supported claims on species differences.

An issue with either comparisons between species of colony formation is that you have not taken into account shared ancestry. In the absence of phylogenetic information, it could very well be that the differences in formation observed may be attributed to unmeasured traits that have to do with similarity in relatedness. Given contemporary expectations for comparative methods, the authors should

address these concerns either by incorporating considerations of phylogeny in the statistics or by discussing the possible role played by the relatedness of the species later in the paper.

>A complete phylogenetic analysis of ancestral states of colony formation was reported in Damian-Serrano et al (2023) IOB. While colonial architecture is phylogenetically structured, we assume its effects on swimming are independent of phylogeny, thus the contrasts within the scope of this study are independent of evolutionary effects. We added a portion to the discussion on the potential role of relatedness in the unexplained variation and on the evolutionary history of colonial architecture.

L336 - It increasing looks problematic that t-tests were used for the statics in these p-values (see concerns above).

>Those are not t-tests, those are slopes in a linear regression and their p-values. We clarified this in the text and added adjusted R² values. We removed the t-test asterisks and brackets from the box and bar plot the figures, and added supplementary tables S4 and S5 with the ANOVA Tukey posthoc contrasts and their adjusted p values.

L397 - This should be explained in Methods, not here. How does the model handle repeated measures? Species?

>We removed these redundant Methods from the Results. We explain in the Methods how we use multiple experiments (and specimens) from each species to obtain multiple values of the differences between variable swimming rates and a single (mean point) anesthetized rate value. We reworked the text in the Methods to make it clearer: "To capture variability within species, we calculated the mean respiration rate of anesthetized specimens for each species and subtracted it from each intact specimen's total respiration rate to get multiple swimming-specific rate values within each species.". Each swimming specimen is independent of each other (they are different specimens collected separately, not the same one under multiple measures) within each species. We did perform paired analyses (intact and anesthetized within the same individual at different times) for sensitivity purposes, finding that using different specimens is just as reliable, but the results from those analyses are not included in manuscript.

L389-419 - As for speed, you cannot offer statements about differences in energetics between species without stats because these values could merely reflect chance events.

>We removed these anecdotal claims, only including statistically supported claims.

L422 - Under what test?

>We used the linear regression non-zero vs. zero slope p-value included in the summary of the lm() function output in R. This comes from an internal t-test on the least-square values of the data points relative to the line under a flat slope vs an inclined one.

In the interest of data transparency, the figure legends should make the sample sizes clear and ideally should also plot the individual measurements.

>We overlaid semitransparent points with the individual measurements onto the specimen mean-collapsed regression plots in Figures 3,4, and 6. We also added the individual specimen points (with jitter and semitransparent) to the species-mean bar plots in Figure 5. The box plots in Figure 2 already show dispersal well and were constructed using the individual points, thus we did not add individual measurement points to those. We included information on sample sizes in a new table (S3).

L569-582 - Incorporating these phylogenetic patterns into your analysis would be very helpful. e.g. how many independent evolutions are included in the species that you sampled? For the species that you considered, it would be informative to know if their ancestors were linear or not.

>We added details from our prior study, Damian-Serrano et al. (2023), to answer that question in the discussion. “Linear chain architectures evolved independently in *M. hexagona*, *S. zonaria*, *I. punctata*, and before the common ancestor of *lasis* and *Salpa*.” and “slower swimmers (such as transversal chains, helical chains, whorls, and clusters in the genus *Pegea* and the Cyclosalpidae family) had also evolved from oblique and linear ancestors.”

1
2
3
4
5
6
7
8
9
10
11 1 **Title: Colonial Architecture Modulates the Speed and**
12
13 2 **Efficiency of Multi-Jet Swimming in Salp Colonies**

14 3
15
16 4 **Authors:** Alejandro Damian-Serrano¹, Kai A. Walton¹, Anneliese Bishop-Perdue¹, Sophie
17
18 5 Bagoye¹, Kevin T. Du Clos², Bradford J. Gemmell³, Sean P. Colin^{4,5}, John H. Costello⁶, Kelly R.
19
20 6 Sutherland¹

21 7
22
23 8 **Author Affiliations:**
24
25
26 9

27
28 10 (1) Institute of Ecology and Evolution, Department of Biology, University of Oregon. 473 Onyx
29 Bridge, 5289 University of Oregon, Eugene, OR 97403-5289, USA.
30
31 12 (2) Louisiana Universities Marine Consortium, 8124 Highway 56, Chauvin, LA 70344, USA.
32
33 13 (3) Department of Integrative Biology, University of South Florida, 4202 East Fowler Avenue,
34
35 14 Tampa, FL 33620, USA.
36
37 15 (4) Marine Biology and Environmental Science, Roger Williams University, Bristol, RI 02809, USA.
38
39 16 (5) Whitman Center, Marine Biological Laboratory, Woods Hole, MA 02543, USA.
40
41 17 (6) Biology Department, Providence College, Providence, RI 02918, USA.

42
43 19 **Running title:** Architecture Modulates Salp Swimming

44
45 20
46 21 **Summary Statement (30 words)**

47
48 22
49
50 23 Linear arrangements in multi-jet propelled marine colonial invertebrates are faster ~~and more~~
51
52 24 ~~energetically efficient~~ than less streamlined architectures without incurring in higher costs of
53
54 25 transport, offering insights for bioinspired underwater vehicle design.

1
2
3
4
5
6
7
8
9
10
11 26
12
13 27 **Abstract**
14 28
15
16 29 Salps are marine pelagic tunicates with a complex life cycle including a solitary and colonial stage.
17
18 30 Salp colonies are composed of asexually budded individuals that coordinate their swimming by
19 31 multi-jet propulsion. Colonies develop into species-specific architectures with distinct zooid
20
21 32 orientations. These distinct colonial architectures vary in how frontal area scales with the number
22
23 33 of propeller zooids in the colony. Based on findings from other jet-propelled systems, we
24
25 34 hypothesize that differences in frontal area drive differences in swimming speed and that
26
27 35 increased swimming speed leads to higher cost of transport in salps. We hypothesize that colonial
28
29 36 architecture drives differences in swimming performance between salps due to differences in how
30
31 37 frontal drag scales with the number of propeller zooids in the colony. Moreover, we hypothesize
32
33 38 that faster swimming taxa are more energetically efficient in their locomotion since less energy
34
35 39 would be devoted to overcoming drag forces. We (1) compare swimming speed across salp
36
37 40 species and architectures, (2) evaluate how swimming speed scales with the number of zooids in
38
39 41 the colony in architectures with a constant constant and scaling motion-orthogonal frontal cross-
40
41 42 sectional-area as well as in those where this area increases with the number of zooids, and (3)
42
43 43 compare the metabolic cost of transport across different species and how it scales with swimming
44
45 44 speed. To measure their swimming speeds, we recorded swimming salp colonies using in situ
46
47 45 videography while SCUBA diving in the open ocean. To estimate the cost of transport, we
48
49 46 measured the respiration rates of swimming and anesthetized salps collected in situ using jars
50
51 47 equipped with non-invasive oxygen sensors. We found that linear colonies generally swim faster
52
53 48 and with a lower cost of transport due to their differential advantage in frontal drag area scaling
54
55 49 with an increasing number of zooids. While cost of transport generally did not differ significantly
56
57 50 between architectures, we did find that higher swimming speeds predict lower costs of transport
58
59 51 in salps. These findings underscore the importance of considering propeller arrangement to
60
61
62
63
64
65

Commented [KS1]: I streamlined this part of the abstract a bit.

Formatted: Not Highlight

1
2
3
4
5
6
7
8
9
10
11 52 optimize speed and energy efficiency in bioinspired underwater vehicle design, leveraging
12 53 lessons learned from the diverse natural laboratory provided by salp diversity.
13
14 54
15
16 55 **Keywords:** salps, colonial architecture, multi-jet propulsion, swimming, cost of transport
17
18 56
19
20 57
21 58
22
23 59
24
25 60 **Introduction**
26 61 Salps (Tunicata: Thaliacea: Salpida) are planktonic invertebrates that have a two-phase
27
28 62 life cycle comprised of a solitary oozooid that asexually buds colonies of sexually reproducing
29
30 63 blastozooids. Salp colonies are composed of up to hundreds of genetically identical, physically
31 64 and neurophysiologically integrated pulsatile zooids (Bone et al. 1980, Mackie 1986). Zooids in
32
33 65 the colony feed and propel themselves by inhaling water through the oral siphon, using muscle
34
35 66 contraction to compress their pharyngeal chamber, and exhaling a jet of water from their atrial
36 67 siphon (Bone & Trueman 1983). While solitary oozooids move using single-jet propulsion, salp
37
38 68 blastozooid colonies integrate multiple propelling jets, which increases their thrust and reduces
39
40 69 the drag that results from periodical acceleration and deceleration via asynchronous swimming
41
42 70 (Sutherland & Weihs 2017).

43 71 Currently, there are 48 described species of salps (WoRMS, 2024) and differences
44
45 72 between species have mainly been compared from a taxonomic lens, focused on zooid-level
46
47 73 diagnostic morphological characters. While salps are widely distributed, most salp species are
48
49 74 restricted to open ocean environments, far from the coast with extremely deep bottom depths,
50
51 75 which poses unique challenges to accessing them for direct study in their environment (Hamner
52
53 76 et al 1975, Haddock 2004). Moreover, salps cannot be maintained alive in containers beyond a
54
55 few hours since they are extremely fragile and sensitive to the presence of solid walls. Therefore,
56
57
58
59
60
61
62
63
64
65

1
2
3
4
5
6
7
8
9
10

11 78 many morphological, ecological, and functional aspects of salp diversity, such as swimming
12 79 speeds and metabolic demands, have remained unexplored. One such aspect is colonial
13 80 architecture or the way that the zooids are arranged relative to each other in the colony. Salp
14 81 colonies develop into species-specific architectures with distinct zooid orientations, including
15 82 transversal, oblique, linear, helical, and bipinnate chains; as well as whorls, and clusters (Damian-
16 83 Serrano & Sutherland, 2023). These architectures present distinct orientations of the propeller
17 84 zooids and their thrusting jets to the axes of colony elongation and locomotion hypothesized to
18 85 have an impact on their swimming performance (Madin 1990, Damian-Serrano et al. 2023).

24 86 Linear salp chains have been hypothesized to be more efficient swimmers due to the
25 87 reduction of drag associated with a more streamlined form (Bone & Trueman 1983). We expect
26 88 frontal (pressure and form) drag scaling to be one of the relevant factors to the hydrodynamics of
27 89 swimming salp colonies given that their intermediate Reynolds numbers are estimated to be
31 90 between ~100 (Sutherland & Madin 2010) for solitary salps and ~5000 for linear chains
32 91 (Sutherland & Weihs 2017). In animals swimming at high Reynolds numbers, such as colonial
34 92 salps, the pressure drag experienced during swimming ~~depends-is expected to~~ largely depend on
35 93 the frontal (motion-orthogonal) projected area (Alexander 1968, Vogel 1981). In a multi-jet
38 94 system, hHaving a larger number of propellers is expected to improve the hydrodynamic and
40 95 inertial benefits granted by asynchronous multijet propulsion, in addition to providing additional
41 96 thrust to the colony (Madin 1990, Sutherland & Weihs 2017). The effect of varying numbers of
43 97 propeller zooids on swimming speed has never been investigated in salps, nor how this
44 98 relationship may vary across their diverse colonial architectures. While relative (per propeller unit)
46 99 frontal ~~drag-area~~ is greatly reduced in linear chains when compared to the sum of each separate
48 100 blastozooid (Mackie 1986, Sutherland & Weihs 2017), we hypothesize that this advantage will be
49 101 lower in species with non-linear colonial architectures, and thus we predict finding differences in
51 102 swimming speed between colonial architectures. Salp colonial architectures differ in how the
53 103 number of zooids in the colony scales with their frontal area relative to motion (Madin 1990). Some
54
55

1
 2
 3
 4
 5
 6
 7
 8
 9
 10
 1104 architectures (linear, bipinnate, and helical) have a constant frontal area relative to their motion,
 12
 1305 regardless of zooid number. We expect these architectures to benefit from increased thrust
 14
 1306 delivered by larger numbers of zooids while maintaining a constant frontal drag resistance area.
 15
 1407 However, the rest of the architectures (oblique, transversal, whorl, and cluster) have an increasing
 16
 1408 (directly proportional) frontal area as the number of zooids increases (Fig. 1). Therefore, we
 17
 1409 expect the latter architectures to not only obtain more thrust, but to also experience more frontal
 18
 2110 water drag resistance as a result of bearing a greater number of propeller zooids. As a result, we
 22
 2311 also predict that swimming speed will be greater in colonies that bear a larger number of zooids,
 24
 2312 but only (or more so) for species with architectures that have a constant frontal area.
 25
 2613
 27

| | Transversal | Whorl | Cluster | Helical | Oblique | Linear | Bipinnate |
|-----------------------|-------------|-------|---------|---------|---------|--------|-----------|
| Architecture | | | | | | | |
| | | | | | | | |
| Frontal area 4 zooids | | | | | | | |
| Frontal area 8 zooids | | | | | | | |
| Scaling | 2 | 2 | 2 | 1 | 1<x<2 | 1 | 1 |

41
 42115 Figure 1. Salp colonial architectures with representative species photos (*Pegea* sp. For
 43 transversal, *Cyclosalpa affinis* for whorl, *Cyclosalpa sewelli* for cluster, *Helicosalpa virgula* for
 44
 45117 helical, *Thalia cicatricosa* for oblique, *Soestia zonaria* for linear, and *Ritteriella retracta* for bipinnate)
 46
 47 and diagrams showing the distinct zooid orientations. The subsequent rows show the frontal view
 48
 49 of colonies with four and eight zooids, with the final row indicating the expected frontal area
 50 increase factor between the four and the eight zooid colonies. Full black circles in the diagrams,
 51
 52represent viscerae while the open circle represent siphons. Black straight lines inside the zooids,
 53
 54indicate gill bars while gray straight lines represent endostyles.

Formatted: Font color: Auto

1
2
3
4
5
6
7
8
9
10
1123 Among the architectures with constant frontal area, we expect linear chains to be the
1124 fastest due to having the most streamlined arrangement of zooids parallel or near parallel to the
1125 axis of motion (Damian-Serrano & Sutherland, 2023), followed by the helical and bipinnate chains
1126 in which the zooids are angled relative to the axis of motion. Among the architectures with
1127 increasing frontal area with the number of zooids, we expect oblique chains to be the fastest,
1128 while still slower than those with constant frontal area, since their arrangement is partially aligned
1129 (angled dorsoventrally) with the axis of motion (Damian-Serrano & Sutherland 2023). Since both
1130 whorls and transversal chains have zooids rigidly attached at 90-degree angles to the axis of
1131 motion, we expect them both to have similar swimming speeds (slower than oblique) and scaling
1132 rates with the number of zooids in the colony. In cluster colonies the zooids are attached to a
1133 center point solely by their long flexible peduncle, which allows them to bend their orientation and
1134 pivot back and forth as a result of their jet propulsion. This may shunt thrust from propulsion into
1135 zooid pivoting torque, thus we expect these colonies to be the slowest swimmers. Salp zooids
1136 pump water as a means of filter feeding as well as to move in the water column. The latter function
1137 is particularly relevant for species that undergo diel vertical migration, which not all species do
1138 (Madin et al. 1996). Therefore, the eco-evolutionary relevance of swimming speed and the
1139 hydrodynamic efficiency may vary between species (Damian-Serrano et al. 2023).

1140 The degree of linearity in a colony can be expressed as the degree of parallelism between
1141 the zooids and the elongation axis of the chain colony (Fig. S10). This angle is determined by the
1142 degree of developmental dorsoventral zooid rotation, which can span from 90°, in transversal
1143 chains with no rotation, to 0° (perfect linearity), in some linear chains such as those from the
1144 species *Soestia zonaria* (Damian-Serrano & Sutherland, 2023). Strong reductions in the
1145 dorsoventral zooid rotation angle toward linear forms have evolved multiple times independently
1146 (Damian-Serrano et al. 2023), possibly due to adaptive advantages related to their swimming
1147 efficiency. Therefore, based on the same rationale as for the abovementioned hypotheses, we

Commented [AD2]: could delete this if we don't formally test for architecture-by-architecture differences

1
2
3
4
5
6
7
8
9
10

1148 further hypothesize that swimming speed is faster in species with lower dorsoventral zooid
12
1349 rotation angle.

1450 Madin (1990) found a linear relationship between swimming effort (pulsation rate) and
15 swimming velocity in solitary zooids. We hypothesize this relationship to also be present in
1651 colonial zooids. While body size predicts swimming velocity in many animals (Vogel 2008), Madin
17
1852 (1990) did not find such a relationship in salp blastozooids or oozoids. Since asynchronous-
19
2053 pulsating cruising salp colonies overcome many of the acceleration issues that limit single-jetters
2154 (Sutherland & Weihs 2017), we hypothesize that in salp colonies, zooid (propeller) size will be
22
2355 predictive of swimming speed across species. Salp zooids pump water as a means of filter feeding
24
2556 as well as to move in the water column. The latter function is particularly relevant for species that
26
2757 undergo diel vertical migration, which not all species do (Madin et al. 1996). Therefore, we expect
28
2958 the eco-evolutionary relevance of swimming speed, and the hydrodynamic efficiency may vary
30
3159 between species (Damian-Serrano et al. 2023).

32
3361 The energetic costs of salp locomotion have been previously estimated using
34 mechanically estimated propulsive efficiency as a proxy in three species (Sutherland & Madin
35
3662 2010, Gemmell et al. 2021) and with a direct comparison between swimming and anesthetized
37 respiration rates in *Salpa fusiformis* (Trueman et al. 1984). The metabolic demands of salp
38
3963 colonies have been estimated for a few species of salps in context with other gelatinous
40
4164 zooplankton (Biggs 1977, Schneider 1992, Mayzaud et al. 2005, Trueblood 2019), showing that
42
4365 salps have a relatively higher respiration rate than other gelatinous taxa. Cetta et al. (1986)
44
4566 compared the respiration rates across salp species to their pulsation rate and swimming speeds,
46
4767 revealing that more active species had higher respiration rates. However, the specific costs
48
4968 incurred by their swimming activity and their relationship to swimming speed have never been
50
5170 examined across the diversity of salp species. We hypothesize that species with a higher overall
52
5372 pulsation rate invest more of their metabolic demands in swimming.

54
55
56
57
58
59
60
61
62
63
64
65

1
2
3
4
5
6
7
8
9
10
11 73 In some single-jetters, swimming speed can be directly proportional to the cost of transport
12
13 74 (Bi & Zhu 2019) due to a highly inefficient refill phase in the jetting cycle which requires costly
14
15 75 acceleration forces to reach high swimming speeds. Since salps are also jet-propelled swimmers,
16
17 76 we hypothesize that faster-swimming salps will incur higher costs of transport than their slower
18
19 77 counterparts. If faster swimming salp species are faster due to experiencing less frontal drag force
20
21 78 as a result of their colonial architecture, we hypothesize that their swimming should also be less
22
23 79 costly, since they would spend less energy in overcoming the forces opposing their forward
24
25 80 motion. Under this hypothesis, we would predict that faster species will present lower costs of
26
27 81 transport (energetic costs of displacement per unit of distance).

28 82 In this study, we compare the swimming speeds across 17 salp species and the energetic
29
30 83 costs of swimming across 15 species ~~of salps~~, encompassing all six different salp colony
31
32 84 architectures (Table S3). In addition, we investigate how swimming speed varies with the number
33
34 85 of propeller zooids and evaluate whether differences in frontal area scaling drive disparities
35
36 86 between colonial architectures. Finally, we assess how the cost of transport of salp colony
37
38 87 swimming varies between species, as well as how ~~their swimming efficiency~~ it scales with
39
40 88 swimming speed and pulsation effort.

38 89 Materials and Methods

40 90 *Fieldwork* – We observed salps via bluewater SCUBA diving (Haddock & Heine, 2005)
41
42 91 from a small vessel off the coast of Kailua-Kona (Hawai'i Big Island, 19°42'38.7" N 156°06'15.8"
43
44 92 W), over 2000 m of offshore water. Some dives were diurnal, where we collected most of the
45
46 93 specimens of *Iasis cylindrica*, *Cyclosalpa affinis*, *Cyclosalpa sewelli*, and *Brooksia rostrata*. We
47
48 94 observed and collected most specimens of other species during night dives (blackwater diving).
49
50 95 We recorded in situ underwater videos of salp colonies swimming using a variety of cameras
51
52 96 including primarily a dark field stereovideography system (Sutherland et al. in review2024), as
53
54 97 well as a lightweight dual GoPro stereo system, a brightfield single-camera system (Colin et al.
55
56 98 2022), and a darkfield single-camera system. The primary stereovideography system was
57
58
59
60
61
62
63
64
65

1
2
3
4
5
6
7
8
9
10
1199 comprised of two synchronized high-resolution cameras (Z Cam E2 and Sync Cable; 4K at 60 or
1200 120 fps) with 17mm f/1.8 lenses (Olympus M.Zuiko Digital) housed in custom aluminum housings
13 (Sexton Company). Each field of view was 23 x 42 mm and in-focus depth were 20-25 mm. The
14 image from the right-hand camera was viewed using an external monitor (Aquatica Digital), and
15 illumination was provided with two 10,000-lumen lights (Keldan). An L-shaped plastic framer
16 helped the videographer position colonies in the field of view of both cameras. Before diving, the
17 stereo system was calibrated in a swimming pool using a cube with reflective landmarks.
18 Calibration images were processed using the CAL software package (SeaGIS measurement
19 science).
20
21
22

23 Measuring salp colony swimming speed — For most species, we collected and analyzed
24 footage from multiple specimens (Table S1 and S3). We analyzed the swimming behavior of salp
25 colonies arranged in linear (six species, 64 specimens), bipinnate (three species, 17 specimens),
26 whorl (three species, 10 specimens), cluster (two species, eight specimens), and transversal (one
27 species, two specimens) architectures, with oblique and helical architectures represented by a
28 single specimen. We used a combination of spatially calibrated stereo video and 2D videos with
29 a reference scale in the frame. From the stereo videos, we manually selected and measured the
30 relative XYZ positions of salp colonies—colony zooids in EventMeasure (SeaGIS). We
31 implemented a cutoff in the RMS (root mean squared) point error estimate of < 2 mm.
32
33

34 We complemented gaps in taxon sampling with archived 2D videos in the lab from
35 previous expeditions to West Palm Beach (FL, USA) and the Pacific coast of Panama. These two-
36 dimensional single-camera videos were collected using a Sony FDR-AX700 4K Camcorder
37 (3840x2160 pixels, 60-120 fps) with a Gates Underwater Housing using brightfield illumination
38 (Colin et al 2022) or darkfield illumination. For these 2D videos, we used the FFmpeg plugin in
39 ImageJ to manually select and measure the relative XY positions of salp zooids in sequences
40 where the colony was swimming horizontally within the focal plane. The colonies were assumed
41
42

1
2
3
4
5
6
7
8
9
10
11 225 to be in the same plane as the scale bar so at same distance from the camera. However, in videos
12 226 with a broad focal depth, this may not always had been the case, thus potentially introducing
13 227 some measurement error. In addition, when loading the 2D videos in ImageJ, the virtual stack
14 228 rendered a higher number of frames than those expected from the inherent frame rate. To address
15 229 this, we calculated an operational frame rate for those videos dividing the number of ImageJ slices
16 230 by the total duration.
17 231

18 231 We tracked and manually selected the position of the first zooid's viscera (using a contrast-
19 232 based centering macro to mark the center point) as well as the position of a reference particle in
20 233 the water (methods described in Sutherland et al. in review) in 10-30 frames across 50-500 frame
21 234 windows spanning 2-4s of swimming on the synchronized left and right videos in EventMeasure.
22 235 The reference particle was a non-swimming organism (such as a foraminiferan or radiolarian) or
23 236 a non-living particle. In addition, we recorded the pulsation rates of the specimens measured by
24 237 counting the number of times the atrial siphon contracted in a known period. For each analyzed
25 238 frame, we calculated the horizontal x, vertical y, and depth z (in the case of the stereo video
26 239 measurement files) components of the relative positions of the frontal zooid to the reference
27 240 particle as shown in Eq. 1.4-1.3.
28 241

$$\begin{aligned}x &= x_{\text{animal}} - x_{\text{particle}} \\y &= y_{\text{animal}} - y_{\text{particle}} \quad \text{Eq. 1}\end{aligned}$$

$$z = z_{\text{animal}} - z_{\text{particle}}$$

47 246 Then we calculated the instantaneous relative speeds of the frontal zooid using Eq. 2
48 247 (without the z component in the case of the 2D videos) given the known frame rate of each video.
49 248

$$U = \frac{\sqrt{(x_2-x_1)^2 + (y_2-y_1)^2 + (z_2-z_1)^2}}{t_2-t_1} \quad \text{Eq. 2}$$

1
2
3
4
5
6
7
8
9
10
11
12
13
14
15
16
17
18
19
20
21
22
23
24
25
26
27
28
29
30
31
32
33
34
35
36
37
38
39
40
41
42
43
44
45
46
47
48
49
50
51
52
53
54
55
56
57
58
59
60
61
62
63
64
65

1250
1251 *Salp colonial architecture* – To examine the relationships between locomotory efficiency
1252 variables and colonial architecture, we adopted the species-specific architecture
1253 characterizations and dorsoventral zooid rotation angle measurements for each species from
1254 Damian-Serrano et al. (2023). Using stills from the underwater videos, we measured zooid length,
1255 zooid width, and number of zooids in ImageJ manually selecting the point coordinates. These
1256 measurements were repeated in at least three locations from each colony. When a distinct zooid
1257 size gradient was observed, we measured zooids in locations from the proximal, middle, and
1258 distal regions to capture the full range of variation in the specimen.

1259 *Respiration measurements* – We collected healthy, adult blastozooid (aggregate stage)
1260 colonies across 18 salp species (Table S2) during blue- and black-water SCUBA dives off the
1261 coast of Kona (Hawaii, USA) between September 2021 and May 2023. We analyzed the
1262 respiration rates of salp colonies arranged in linear (seven species, 46 specimens), bipinnate
1263 (three species, 29 specimens), whorl (three species, 23 specimens), cluster (two species, 18
1264 specimens), and transversal (one species, 13 specimens) architectures, oblique chains (*Thalia*
1265 sp., seven specimens), and helical architectures represented by *Helicosalpa virgula* (two
1266 specimens). Specimens were sealed *in situ* with their surrounding water in plastic jars equipped
1267 with a Presens (Germany) oxygen sensor spot and a self-healing rubber port to allow for the
1268 injection of solutions without the introduction of air bubbles. We removed as many symbiotic
1269 animals from the salps as possible before closing the lid without damaging the colony. The same
1270 method was applied to one or more seawater controls to account for the oxygen demand of the
1271 local seawater's microbiome. Several collection events occurred during each 20-60 min long
1272 SCUBA dive. Jars with larger animals were opened during the safety stop to allow them to re-
1273 oxygenate. Upon the divers' return to the boat, we measured the initial oxygen concentration
1274 (mg/l) and temperature, and then repeated the measurements at intervals between 15min and
1275 3h, for total periods ranging between 2h and 5h, depending on logistic constraints in the field and

Formatted: Font: Italic

Formatted: Font: Italic

1
2
3
4
5
6
7
8
9
10

1 276 the rate of oxygen depletion. The exact interval time for each measurement was variable but
2 277 recorded (Table S2).

3 278 To estimate the energetic expenditure of different salp species while actively swimming,
4 279 we recorded the oxygen consumption of intact specimens while swimming inside the jar. To obtain
5 280 a baseline of basal respiration rate (while not swimming), we anesthetized some specimens
6 281 before the start of the first oxygen measurement time. A few specimens were used for paired
7 282 experiments, where their swimming respiration was recorded for a few hours, then inoculated with
8 283 the anesthetic, and recorded anesthetized for another set of hours. To anesthetize salps, we
9 284 injected their jars with small volumes of concentrated (50 g/l) bicarbonate-buffered MS-222
10 285 through the rubber ports on the lids. We tailored the injection volume to the jar size aiming for a
11 286 final concentration of 0.2g/l, following the methods in Trueman et al. (1984). We also injected
12 287 some seawater control jars to evaluate the effect of MS-222 on oxygen concentration in seawater
13 288 and found no effect.

14 289 When multiple seawater controls were collected using jars of different sizes, we paired
15 290 each jar with the control that had the most similar volume. If among multiple controls only some
16 291 were jars injected with anesthetic, we paired the anesthetized specimen jars with the injected
17 292 controls and the intact specimen jars with the intact controls. In experiment 26 (see Table S2 for
18 293 experiment numbers), the control jar was lost due to an encounter with an oceanic white tip shark,
19 294 thus we paired those measurements with the nearest relative time points from the control jar in
20 295 experiment 25, collected the same day hours earlier. At the end of each experiment, we identified
21 296 the salp specimens used in the experiments to the species level, counted the number of zooids,
22 297 and measured the zooid length (total length including projections), and measured the biovolume
23 298 of the colony using a graduated cylinder. For those specimens where colony or zooid volume was
24 299 not measured directly, we estimated the colony volume from their zooid length and the number of
25 300 zooids using a Generalized Additive Model with the measured specimens.

26
27
28
29
30
31
32
33
34
35
36
37
38
39
40
41
42
43
44
45
46
47
48
49
50
51
52
53
54
55
56
57
58
59
60
61
62
63
64
65

1
2
3
4
5
6
7
8
9
10
11 301 We estimated the oxygen consumption rate for each specimen by fitting a linear
12 302 regression of consumed oxygen mass (concentration by container volume) against the duration
13 303 of the measurement series. We subtracted the slope calculated for the relevant control jar to the
14 304 estimated slope of the animal jar. Since our seawater controls were not filtered, some experiments
15 305 had abnormally high estimated background respiration rates, leading to negative values. We
16 306 removed these data points before the analysis. To estimate biovolume-specific rates, we divided
17 307 the rates by the colony volumes. We then compared the biovolume-specific respiration rates of
18 308 active (swimming) and anesthetized specimens within each species, calculating the difference as
19 309 a measure of biovolume-specific swimming cost respiration rate. We also calculated the relative
20 310 investment in swimming as the proportion of biovolume-specific respiration rate comprised by the
21 311 swimming-specific rate. To capture variability within species, we calculated the mean respiration
22 312 rate of anesthetized specimens for each species and subtracted it from each intact specimen's
23 313 swimming-specific total respiration rate to get multiple swimming-specific rate values within each
24 314 species. We noticed that some species had higher average respiration rates among the
25 315 anesthetized specimens than among the swimming specimens, leading to negative swimming-
26 316 specific respiration estimates. We interpreted this anomaly as a systematic error due to the
27 317 extremely low respiration rates of some species that fall within the effective detection limit of our
28 318 experimental setup given the random variation range of respiration rates in seawater both in
29 319 experimental jars and in control jars. Small absolute negative values get amplified into large
30 320 relative values, especially in small animals with a minuscule biovolume denominator. Therefore,
31 321 we removed the swimming specimens that had lower respiration rates than the mean
32 322 anesthetized respiration rate for their species. We also removed two respirometry outliers of
33 323 *Thalia* sp. which had extremely high swimming respiration rates (>7500 pgO₂/ml/min, whereas
34 324 all other measurements across species including other *Thalia* sp. were limited to 0-1700
35 325 pgO₂/ml/min), which were likely due to amplification of experimental error (presence of organic
36
37
38
39
40
41
42
43
44
45
46
47
48
49
50
51
52
53
54
55
56
57
58
59
60
61
62
63
64
65

1
2
3
4
5
6
7
8
9
10
11 326 matter or symbionts, underestimation of colony volume due to loss of tiny zooids in the sieves)
12 327 with the small biovolume denominators in this species.
13
14 328 *Estimating costs of transport* – We define the cost of transport (COT) as the amount of
15
16 329 oxygen consumed per tissue volume per distance traveled by the colony. To estimate the COT,
17
18 330 we divided the swimming-specific respiration rates by the mean swimming speed for each species
19
20 331 measured from the stereo and 2D video data. Since the specimens used for speed measurements
21
22 332 in the videos and those used in the respirometry experiments had different zooid sizes, we used
23
24 333 the mean zooid-lengths per second speeds from the video measurements and then multiplied
25
26 334 them by the actual zooid lengths of the respirometry specimens to estimate their absolute (mm/s)
27
28 335 speeds. Pulsation rate estimates were taken from species averages from the video specimens.
29
30 336 We also calculated the size-specific COT by transforming the swimming distances into zooid
31
32 337 lengths measured from the respirometry specimens.
33
34 338 *Statistical Analyses* – All data wrangling and statistics were carried out in R 3.6.3 (R Core
35
36 339 Team 2021). To test for differences between architectures, we used ~~two-sided t-tests~~^{ANOVAs}
37
38 340 with Tukey's post-hoc pairwise contrasts, reporting the difference magnitude and the adjusted p-
39
40 341 value in supplementary tables S3 and S4. To test the relationships between pairs of continuous
41
42 342 variables, we used linear models (as well as exponential models when comparing swimming
43
44 343 speed to COT) and evaluated the significance of the slope parameter when compared against a
45
46 344 flat slope, (one-tailed t-test). To evaluate the relative contribution of zooid size, pulsation rate,
47
48 345 zooid number, and architecture type on swimming speed, we fitted a generalized linear model
49
50 346 and evaluated the significance and proportion of variance explained by each factor using their
51
52 347 partial R².

Formatted: Not Highlight

48 348 Results

49
50 349 Salp colony swimming speeds, pulsation rates, and respiration rates varied within and
51
52 350 across species and colony architectures. Speeds measured with 2D methods were slightly slower
53
54 351 than those measured with 3D methods within the species in which they overlapped. This is to be
55
56
57
58
59
60
61
62
63
64
65

1
2
3
4
5
6
7
8
9
10
11 352 expected since 2D methods cannot account for the z (depth) component of the speed vector.
12 353 When considering speed in terms of mm/s, we found no relationship between pulsation rate
13 (effort) and absolute speed (Speed mm/s ~ Pulsation rate, adjusted R² = 0.003, p = 0.68, Fig.
14 354 **Formatted: Superscript**
15 355 S1A), but a significant positive relationship with zooid-size corrected speed (Speed zooids/s ~
16 356 Pulsation rate, adjusted R² = 0.18, p < 0.0001, Fig. S1B). Moreover, zooid length was positively
17 357 correlated with speed, whether it is expressed as mm/s (Speed mm/s ~ Zooid length, adjusted R²
18 358 = 0.06, p < 0.0001, Fig. S2A) or mm/pulse (Speed mm/pulse ~ Zooid length, adjusted R² = 0.42,
19 359 p < 0.0001, Fig. S2B), in agreement with our initial hypotheses). Normalized swimming speeds
20 360 (zooid lengths per pulse) allow for a more direct comparison of swimming speed across colonial
21 361 architectures.
22
23 362 ~~Salp species vary widely in their mean absolute colonial swimming speeds (Fig. 2A), with the~~
24 363 ~~slowest being under 6 mm/s in an oblique chain of Thalia sp., closely followed by the transversal~~
25 364 ~~chains of Pegea confoederata with 7.38 mm/s, and the fastest mean speed reaching 114 mm/s~~
26 365 ~~in the linear chains of Salpa aspera, closely followed by the linear chains of Metcalfina hexagona~~
27 366 ~~(107 mm/s) and Soestia zonaria (106 mm/s). The fastest individual specimen however, belonged~~
28 367 ~~to the linear chain species Lasis cylindrica with a speed of 176 mm/s. When correcting by zooid~~
29 368 ~~size and pulsation rate (Fig. 2B), Soestia zonaria was fastest with a mean velocity of 7.09 zooid~~
30 369 ~~lengths/pulse, followed by Lasis cylindrica (2.09 zooids/pulse) and Salpa aspera (2.03~~
31 370 ~~zooids/pulse), whereas the oblique chains of Thalia sp. (0.37 zooids/pulse) were slowest, closely~~
32 371 ~~followed by the transversal chains of Pegea sp. with 0.43 zooids/pulse.~~
33
34
35 372
36 373
37 374
38
39
40
41
42
43
44
45
46
47
48
49
50
51
52
53
54
55
56
57
58
59
60
61
62
63
64
65

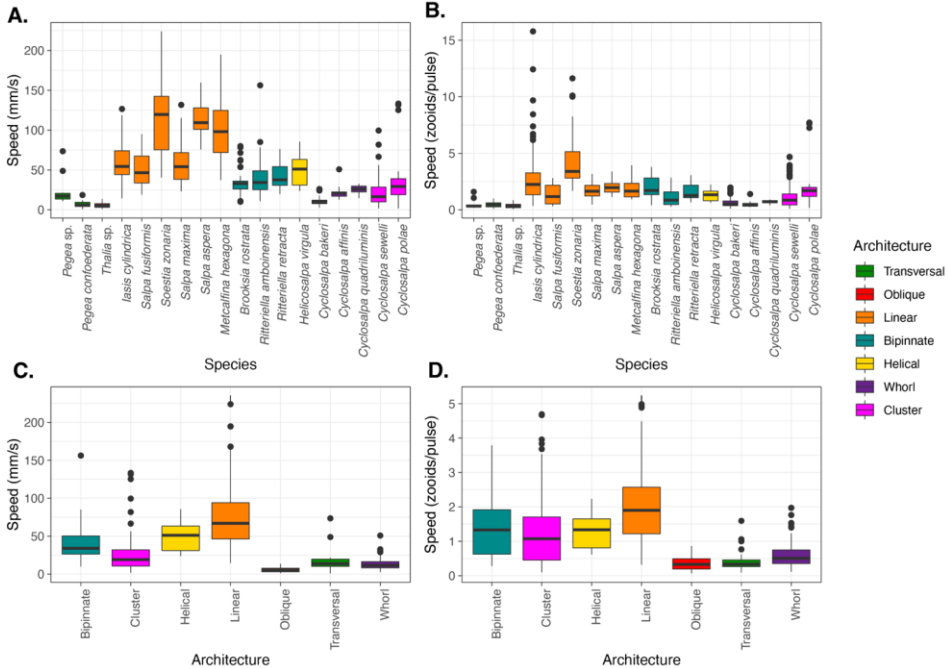


Figure 2. Boxplots showing the absolute (A) and corrected for body size and pulsation rate (B) swimming speeds recorded for each salf species and architecture (C, D) respectively. Colors correspond to colonial architecture types.

We find that swimming speed varies significantly (ANOVA $p < 0.001$) between colonial architecture types (Fig. 2C, D, Table S4). Measurements of helical and oblique chains were limited to a single specimen, so this result should be interpreted with care. Linear salf colonies are the faster than the rest ($p < 0.001$) with a mean speed of 73 mm/s (2.31 zooids/pulse), followed by helical chains (49.9 mm/s, 1.3 zooids/pulse), bipinnate colonies (39 mm/s, 1.41 zooids/pulse), and clusters (26.1 mm/s, 1.5 zooids/pulse). Among the slower architectures, we find whorls (13.4 mm/s, 0.64 zooids/pulse), transversal chains (16.7 mm/s, 0.44 zooids/pulse), and oblique chains (5.8 mm/s, 0.37 zooids/pulse). In terms of absolute speed (mm/s), linear architectures were significantly faster than every other architecture except helical (Tukey's $p < 0.001$). While

Commented [AD3]: add ANOVA results

Commented [AD4R3]: remove anecdotal comparisons.

Formatted: Not Highlight

1
2
3
4
5
6
7
8
9
10
11 388 bipinnate chains were significantly slower than linear ones and on par to clusters, they were
12
13 389 significantly faster than transversal chains, oblique chains, and whorls (Tukey's p < 0.02). Clusters
14
15 390 were significantly faster than transversal chains, whorls, and oblique chains (Tukey's p < 0.01).
16
17 391 Transversal chains were on par to whorls and oblique chains, with no significant differences
18
19 392 between them.

20
21 393 In terms of relative speed (zooid lengths/pulse), linear architectures were significantly
22
23 394 faster than every other architecture except helical (Tukey's p < 0.001). Bipinnate chains were
24
25 395 significantly faster than clusters, whorls, transversal chains, and oblique chains (Tukey's p <
26
27 396 0.008). Helical chains were significantly faster than whorls and oblique chains (Tukey's p < 0.03).
28
29 397 Clusters were on par with helical chains for relative speed and were also significantly faster than
30
31 398 whorls and oblique chains. Whorls, transversal chains, and oblique chains presented similar
32
33 399 relative swimming speeds with no significant differences. Our measurements of helical and oblique
34
35 400 chains are limited to a single specimen, so this result should be interpreted with care.

36
37 401 Since linear architectures had faster mean swimming speeds (Fig. 2C, D), we investigated
38
39 the relationship between swimming speeds with the dorsoventral zooid rotation angle, which
40
41 402 represents the degree of linearity of the colony (Fig. 3). As hypothesized, species with more
42
43 403 parallel (lower angles) dorsoventral zooid rotation present faster absolute speeds (Speed mm/s
44
45 404 ~ DV Zoid angle, adjusted R² = 0.33,-0.78, p < 0.0001) as well as somewhat faster size-and-
46
47 405 effort corrected swimming speeds (Speed zooids/pulse ~ DV Zoid angle, adjusted R² = 0.09,-
48
49 406 0.046 p < 0.0001). However, the latter relationship appears to be driven primarily by the distinctly
50
51 407 fast relative speed of the perfectly linear (0° zooid rotation angle) *Scolezia zonaria*.
52
53
54
55
56
57
58
59
60
61
62
63
64
65

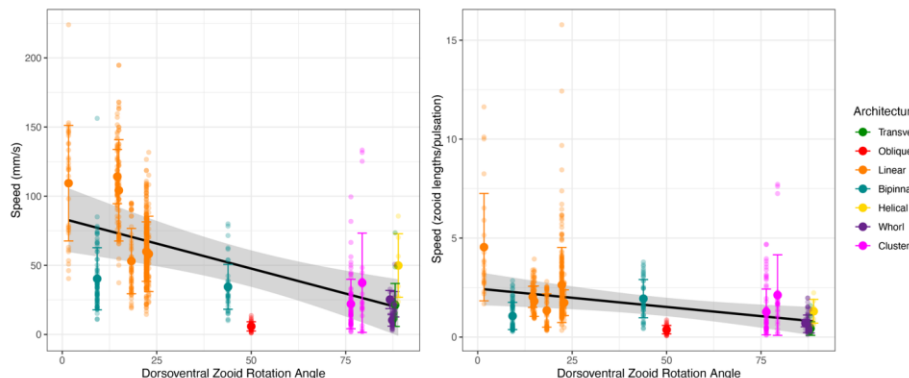
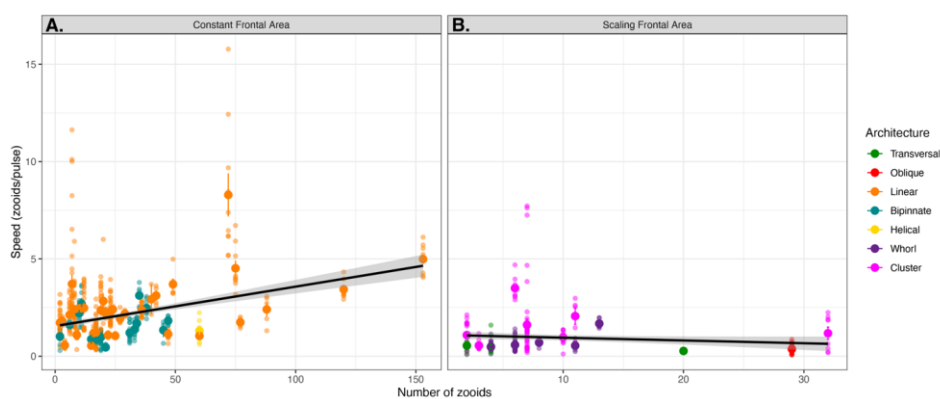


Figure 3. Absolute (A) and relative (B) colony swimming speed (specimen mean with standard errors) for each salp species across their degree of dorsoventral zooid rotation. Error bars indicate standard error. The color indicates colonial architecture. Gray areas indicate the 95% confidence interval of the linear regression (black line).

We compared how swimming speeds scale with the number of zooids in the colony (by species, see Fig. S3), and found differences between colonial architectures (Fig. S4). Swimming speed in whorls increased with number of zooids (Speed mm/s ~ Zoid number, adjusted R² = 0.3, p < 0.0001), which is incongruent with our frontal area hypothesis, but though the data for this architecture was limited to small numbers of zooids (4 to 13) and relatively slow speeds. As expected, linear chain architectures did increase in relative speed with the number of zooids (adjusted R² = 0.14, p < 0.001), as did bipinnate chains (adjusted R² = 0.04, p < 0.02)—congruent with our frontal area hypothesis. This relationship was not significant for any of the other architectures.

To further test our frontal area scaling hypothesis, we pooled the data from multiple architectures into scaling modes. We could then evaluate the overall relationship in colonies with a constant frontal area (linear, bipinnate, and helical species) and in colonies with scaling frontal area (transversal, whorl, cluster, and oblique species) with linear regressions. This

1
 2
 3
 4
 5
 6
 7
 8
 9
 10
 11 aggregation allowed the inclusion of data from architectures for which we only have one specimen
 12 (helical and oblique). When pooled by scaling mode (Fig. 4), the regression on colonies with a
 13 constant frontal area had a higher intercept on the swimming speed axis than in those with a
 14 scaling frontal area (1.54 and 1.09 zooids/pulse, respectively), reflecting the generally higher
 15 swimming speed of the former. Moreover, the regression on colonies with constant frontal area
 16 had a significant positive slope (Speed mm/s ~ Zoid number, slope = 0.02, adjusted R² = 0.12,
 17 p < 0.001), while the regression on those with scaling frontal area was not significant (p = 0.073).
 18
 19
 20
 21
 22



35
 36
 37 Figure 4. Linear relationships between relative swimming speed (zooid lengths per pulsation,
 38 specimen mean with standard errors) and number of zooids in the colony for constant (A) and
 39 scaling (B) frontal motion-orthogonal frontal area scaling modes. Gray areas represent the 95%
 40 confidence intervals of the regressions.
 41
 42
 43

43 Putting together all the different organismal factors that we analyzed in this study, we
 44 calculated a generalized linear regression model to predict absolute sarp swimming speed (U)
 45 from zooid length (L), pulsation rate (P), number of zooids (N), and colonial architecture
 46 represented as frontal area scaling mode (A) as expressed in Eq. 3. While our results suggest
 47 that the effect of N depends on A , we favored this simpler regression formula because it had a
 48 significantly lower ($\Delta > 70$) AIC score than those with interaction terms between N and A .
 49
 50
 51
 52
 53
 54
 55
 56
 57
 58
 59
 60
 61
 62
 63
 64

1
2
3
4
5
6
7
8
9
10

11445 $U \sim L + P + N + A$ Eq. 3

12
13 In this global model, we find found significant effects on swimming speed (pseudo-R² =
14 0.37, p < 0.001) from for L, N, and A. We find found that our global regression explains 36.76%
15
16 of the variance in our swimming speed data: 5.78% is explained by zooid size, 3.52% by pulsation
17
18 rate, 0.81% from zooid number, and 26.64% by the frontal scaling mode.

Formatted: Superscript

19
20 In addition to investigating the determinants of swimming speed in salp colonies, we also
21 compared their respiratory physiology and the energetic efficiency of their swimming. The
22
23 respiration rates of swimming and anesthetized salps in sealed jars at ambient temperature
24
25 revealed broad differences between species (Fig. S5). After estimating COT, we found a few
26
27 significant differences between architectures (ANOVA p < 0.05). In terms of absolute COT per
28
29 mm traveled, linear chains, helical chains, bipinnate chains, whorls, and clusters had similar high
30
31 transport efficiencies under 13 $\mu\text{gO}_2/\text{ml}$. Every one of these architectures was significantly more
32
33 efficient per mm traveled than oblique architectures (Tukey's p < 0.001). In terms of relative COT
34
35 per zooid length traveled, linear chains and whorls had similar transport efficiencies that are
36
37 significantly faster than transversal and oblique chains (Tukey's p < 0.04). Clusters are also
38
39 significantly faster than oblique chains (Tukey's p < 0.01). Bipinnate and helical chains show
40
41 similar values linear chains, clusters, and whorls, but are not significantly more efficient than
42
43 transversal or oblique chains, perhaps due to insufficient sample sizes. Among swimming

Formatted: Subscript

44
45 specimens (*Thalia* sp. high outliers removed), the highest mean swimming respiration rate was
46
47 for *Ihlea punctata*, with an average of 1560.9 $\mu\text{gO}_2/\text{min}/\text{ml}$. This species had also the largest
48
49 difference between swimming and anesthetized respiration rates. The lowest mean swimming
50
51 respiration rate (negative values removed) was for *Ritterella amboinensis* with 33 $\mu\text{gO}_2/\text{min}/\text{ml}$.
52
53 The highest mean anesthetized respiration rate per ml of biovolume we recorded was for *Thalia*
54
55 sp. with 715 $\mu\text{gO}_2/\text{min}/\text{ml}$, while the lowest was for *Cyclosaphe bakeri* (28 $\mu\text{gO}_2/\text{min}/\text{ml}$).
56

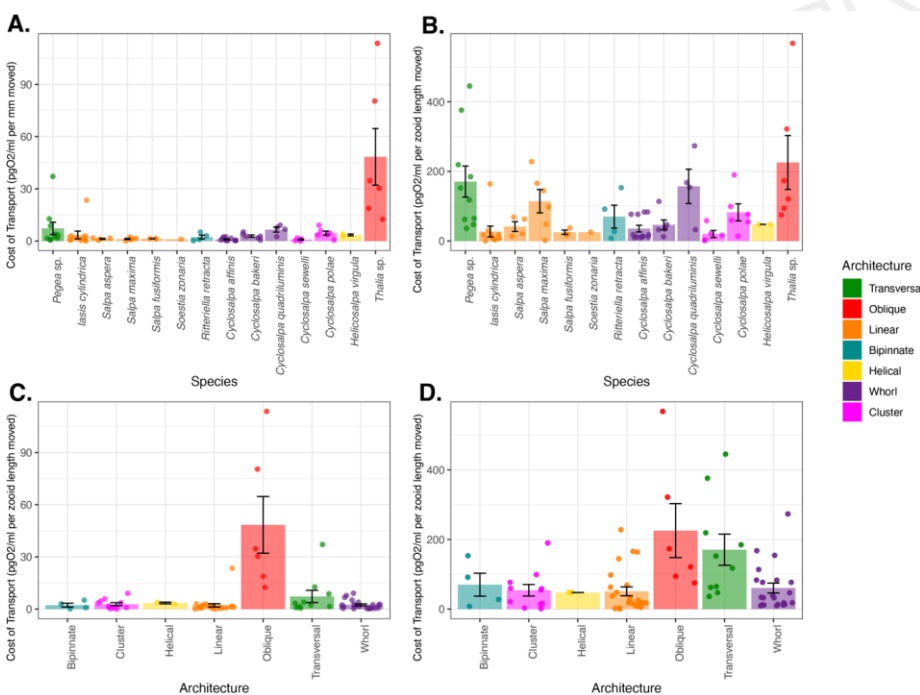
Formatted: Highlight

57
58 We estimated the cost of transport (COT) as the biovolume-normalized metabolic cost of
59
60 locomotion per unit of distance, as the mass of oxygen consumed both per mm traveled as well
61
62

Formatted: Indent: First line: 0"

1
 2
 3
 4
 5
 6
 7
 8
 9
 10
 11471 as normalized per body (zooid) length traveled. The species with the costliest locomotion was
 12 Thalia sp. (oblique architecture), followed by Pegea sp. (transversal architecture). We find that S.
 13 zonaria and C. sewelli have the lowest (most efficient) COT (Fig. 5A, B). Some of the differences
 14 between COT per mm and COT per zooid length are likely due to scaling with body size, as can
 15 be observed with the relative shift in the minuscule *Thalia* sp. (5.2 mm zooids) and the massive
 16 *Salpa maxima* (93.4 mm zooids). While linear architectures have the lowest mean COT values,
 17 these are not significantly lower than helical, bipinnate, whorls, or clusters (Fig. 5C, D). All these
 18 architectures have similar mean COT values that are much lower than those found in transversal
 19 and oblique architectures. These results do not support the hypothesis that more streamlined
 20 architectures have more energetically efficient locomotion.

Formatted: Highlight



1
2
3
4
5
6
7
8
9
10
11
12
13
14
15
16
17
18
19
20
21
22
23
24
25
26
27
28
29
30
31
32
33
34
35
36
37
38
39
40
41
42
43
44
45
46
47
48
49
50
51
52
53
54
55
56
57
58
59
60
61
62
63
64
65

1482 Figure 5. Mean cost-of-transport per mm (A) and per zooid length (B) moved for each salp
1483 species, and for each colonial architecture (C, D) with standard errors. Bar colors indicate colonial
1484 architecture.

1485 When comparing the proportion of investment of metabolic costs into swimming
1486 (compared to the species mean baseline) across salp species (Fig. S6), eight species had
1487 locomotion budgets under 50%, and the other seven have budgets above 50%. ~~The species with~~
1488 ~~the highest relative investment in locomotion are *I. punctata* (94.5%) and *H. virgula* (83.1%), while~~
1489 ~~the lowest investments were found in *C. affinis* (19.8%) and *Thalia* sp. (30.6%). Upon noticing~~
1490 ~~this variation, we~~ examined whether observed effort (pulsation rate) scales with the measured
1491 proportion of energetic investment in swimming across species (Fig. S7) and found no significant
1492 relationship (Swimming % ~ Pulsation rate, $p = 0.47$) between them, ~~and thus no support for the~~
1493 ~~hypothesis that higher swimming effort incurs a higher metabolic effort.~~

1494 We then compared the proportion of energetic investment in swimming to the COT values
1495 across species (Fig. S8) and found no relationship with absolute COT (Swimming % ~ COT per
1496 mm, $p = 0.24$) but found a positive relationship with zooid-length scaled COT (Swimming % ~
1497 COT per zooid length, adjusted $R^2 = 0.22, p < 0.001$), indicating that species with more costly
1498 locomotion per zooid length invest a larger proportion of their energy budget in swimming. Finally,
1499 we compared the proportion of energetic investment in swimming with speed (Swimming % ~
1500 Speed, Fig. S9). We found no relationship (neither in mm/s nor in zooids/s), indicating that faster
1501 swimmers do not invest more ~~or less proportion~~ of their energy budget into their locomotion efforts.
1502 We found that regardless of whether we consider transport in terms of absolute distances (Fig.
1503 6A, linear regression COT per mm ~ Speed mm/s, adjusted $R^2 = 0.09, p < 0.005$, exponential
1504 regression logCOT per mm ~ Speed mm/s, adjusted $R^2 = 0.14, p < 0.001$) or relative to body
1505 lengths (Fig. 6B, linear regression COT per zooid length ~ Speed zooids/s, adjusted $R^2 = 0.07, p$
1506 < 0.01 , exponential regression logCOT per zooid length ~ Speed zooids/s, adjusted $R^2 = 0.14, p$
1507 < 0.001), the COT decreases in species with faster swimming speeds.

Formatted: Superscript

Formatted: Superscript

Formatted: Superscript

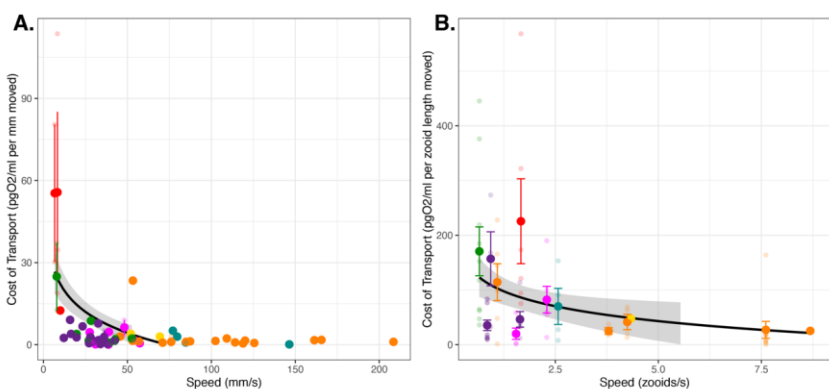


Figure 6. COT (specimen mean with standard error) per mm (A) and zooid length (B) moved across the specimen mean absolute (A) or relative (B) swimming speeds. The dot color indicates colonial architecture. Gray areas represent the 95% confidence intervals of the exponential regressions (black lines).

Discussion

We compared the swimming speeds and costs of transport of salp colonies across the most comprehensive representation of salp species diversity. Our results show a wide range of colonial swimming speeds across salp species and architectures. Moreover, this study shows for the first time how salp colonial swimming speed scales with the number of zooids in the colony, suggesting that incremental propulsive power from additional zooids does not always produce higher swimming speeds.

Architectural determinants of salp swimming speed

Colonial architecture was the strongest predictor of swimming speed, ~~and~~ though there is a large amount of unexplained variation which may relate to species-specific differences, behavioral, or environmental factors (see global GLM results). ~~When ranking the different architectures by their swimming speed, our results are partially in agreement with our~~

Formatted: Highlight

1
2
3
4
5
6
7
8
9
10
11 526 hypothesized ordination insofar as linear, bipinnate, and helical chains are the fastest, with
12 transversal chains and whorls ranking lower. However, cluster architectures were faster than we
13
14 528 anticipated, and oblique chains much slower than we expected.

Commented [AD5]: no stats behind this, remove?

15
16 529 We expected that swimming speed in colonial salps would be predicted by pulsation rate
17 as a measure of swimming effort. Our results indicate that this relationship only exists when
18 530 accounting for zooid size, suggesting an underlying relationship between pulsation rate and zooid
19 531 size that may be masking its predictive power over absolute speeds. This is consistent with the
20
21 532 distribution of our data and our observations in the field where larger salps pulsate at a slower
22 rate than smaller ones. While Madin (1990) found no relationship between zooid size and speed
23 533 in single zooids, we do find a significant increase in speed with larger zooid sizes, indicating that
24 534 multi-jet propelled animals follow more similar scaling rules to vertebrate swimmers (Vogel 2008)
25
26 535 than to single-jet propellers.

27
28 538 The relationship between the number of zooids and speed in linear chains is weaker than
29
30 539 we would expect complicated by shifts in zooid orientation during development. This may be partly
31 540 explained by the phenomenology behind more and less populous colonies. Salp colonies start
32
33 541 their free-living phase when the developing buds detach from the solitary oozoid. This is when
34
35 542 the colony is expected to have the maximum number of zooids since the zooid number only gets
36
37 543 reduced as the colony splits or loses zooids to turbulence, disease, or predation. Therefore,
38
39 544 colonies with higher numbers of zooids are typically composed of smaller, younger zooids. In
40
41 545 linear architectures, these younger colonies could still be developing their dorsoventral rotation
42
43 546 (Damian-Serrano & Sutherland 2023), thus effectively being more similar to like oblique
44
45 547 architecture. A less acute dorsoventral rotation angle would explain why these more numerous
46
47 548 linear chains are not as fast as we would expect, given that our results support a significant
48
49 549 relationship between this angle and swimming speed (Fig. 3). Finding a strong relationship
50
51 550 between zooid number and speed in whorls was surprising given their less hydrodynamic
52
53 551 configuration. This could be due to the smaller range of slow speeds and few zooids in the data

1
2
3
4
5
6
7
8
9
10
11 552 we obtained for these species. Our regression results on pooled architectures, as well as finding
12 553 a significant relationship between number of zooids and speed for linear and bipinnate chains but
13 554 not for clusters nor transversal chains, support our primary hypothesis that the different frontal
14 555 area scaling relationships across architectures has an impact on swimming speed.
15
16 556

Linear chains swam faster than all other architectures, including those that share a constant frontal area feature like helical and bipinnate chains. One potential explanation for this difference could come from the relative thrust provided by the jets. Linear chains eject their jet plumes at very small angles (near parallel) to the axis of locomotion (Sutherland et al., in review 2024, just wide enough to avoid interaction between jet plumes (Sutherland & Weihs 2017). Bipinnate and helical chains (both with constant frontal area) have the atrial siphons (point of jet ejection) of their constituent blastozooids oriented at a wider angle (Madin 1990), which may lead to wider angles of their jets relative to the axis of locomotion. This in turn would result in a larger proportion of the force exerted by the jet to be applied as torque rather than thrust onto the colony. This hypothesis could be tested by measuring the 3D angles of the actual jets instead of the angles of the zooids since salps can use their atrial muscles and siphon morphology to direct the angle of their jets.

Finding that clusters can swim at speeds comparable to those of bipinnate and helical chains, even faster than whorls, defies our intuitive understanding of the mechanical properties of these colonies and thus warrants further investigation into how these species coordinate their jets to produce forward thrust. While oblique chains are architectural intermediates between transversal and linear chains, our results-data indicates that oblique chains are-may be the slowest swimmers among salps. This incongruence may be explained by the fact that we only had speed data from one oblique specimen (of *Thalia* sp.) with very small zooid sizes. Small salps might operate at notably lower Reynolds numbers than large ones, which may require a non-linear size correction for meaningful speed comparisons. Swimming speed data from the much larger oblique

1
2
3
4
5
6
7
8
9
10
11
12
13
14
15
16
17
18
19
20
21
22
23
24
25
26
27
28
29
30
31
32
33
34
35
36
37
38
39
40
41
42
43
44
45
46
47
48
49
50
51
52
53
54
55
56
57
58
59
60
61
62
63
64
65

1577 chains of *Thetys vagina* may provide a more comparable example of the locomotory performance
1578 of this oblique colonial configuration.

Formatted: Font: Italic

1579 The questions addressed in this study focus on the effect of frontal area of colonial
1580 architectures on swimming speed. This effect may be associated with form and pressure drag
1581 differences between more and less streamlined colony shapes. To test whether these are the
1582 forces responsible for differences in swimming speed, drag would have to be measured or
1583 calculated, which is beyond the scope of this study. Other unaccounted forces may be significant
1584 energetic contributors to the system that explain the remainder of the observed variation. Chain
1585 length for the streamlined forms (helical, linear, and bipinnate chains) could have negative effects
1586 on swimming speeds that may partially counteract the positive effect of increased propeller thrust.
1587 For example, skin drag increases proportionally to the surface area of the system, and the
1588 smoothness of the chain may increase pressure drag through vortex shredding (Vogel 1981).
1589 While added (virtual) mass could also be an issue, asynchronously swimming colonies do not
1590 suffer as much from these acceleration-related costs, since their speed is maintained near
1591 constant while cruising. Chain length could also lead to reduced stability and efficiency, though
1592 some linear species capitalize on this by swimming in corkscrew orbital spirals (Sutherland et al.
1593 2024). However, if friction drag, chain stability, or vortex shredding were indeed more important
1594 contributors than frontal form drag, we would predict that linear chains would appear slower than
1595 other more stable and compact architectures. Future studies may unravel these potential
1596 confounding effects on the biomechanics of colonial salp swimming.

4597 Salp swimming speed and diel vertical migration

4598 Salps are important players in the oceanic carbon cycle, grazing upon both
4599 phytoplankton and bacteria (Henschke et al. 2016). Their carcasses and fecal pellets export large
4600 quantities of fixed carbon into the deep sea, accelerating carbon sequestration in the biological
4601 carbon pump (Wiebe et al. 1979, Décima et al. 2023). Part of this process is enhanced by the diel
4602 vertical migrations by some salp species though the distribution of this behavior across species

1
2
3
4
5
6
7
8
9
10

11603 diversity is poorly known. Off Bermuda, Madin et al. (1996) reported *Pegea* spp., *B. rostrata*, and
12
13604 *C. polae* as non-migratory, all of which we found to have slow swimming speeds. Other slow-
14
15605 swimmer species like *C. affinis* were found to only migrate a few meters through the diel cycle.
16
17606 The species *S. aspera*, *S. fusiformis*, *S. zonaria*, *I. punctata*, and *R. retracta* have been observed
18
19607 vertically migrating off Bermuda (Madin et al 1996, Stone & Steinberg 2014), which is congruent
20
21608 with our observations during fieldwork. These species all have constant frontal area and fast
22
23609 swimming speeds.

24
25610 Vertical migrants need to be fast enough to follow the dark isolines as they shift during
26
27611 dawn and dusk in time to maximize their exploitation of the food resources near the surface ~~while~~
28
29612 ~~avoiding exposure to daylight~~. Thus, absolute speed is important to the autoecology of these
30
31613 animals. Other *Salpa* species have also been reported as strong vertical migrants throughout the
32
33614 literature (Henschke et al. 2021, Madin et al. 2006, Pascual et al. 2017). A species that does not
34
35615 fit this pattern is *I. cylindrica*, a fast-swimming non-migratory species that spends night and day
36
37616 near the surface (Madin et al 1996; and pers. obs.). However, other studies do report moderate
38
39617 diel vertical migration for this species (Stone & Steinberg 2014), so it may be adapted for
40
41618 facultative vertical migration under specific oceanographic conditions. Some migratory species,
42
43619 such as *S. aspera*, are known to travel distances of over 800m at dawn and dusk, at rates
44
45620 predicted to require 5-10 m/min (83-166 mm/s) based on MOCNESS trawl intervals (Wiebe et al.
46
47621 1979). These predictions are consistent with the speeds we recorded for this species (88-145
48
49622 mm/s) and similar congeners.

45623 *Ecophysiological implications*

46
47624 While the importance of a few well-studied linear chain salp species in the biological
48
49625 carbon pump has been delineated, the question of whether this ecological role is generalizable to
50
51626 other salp species remains unanswered. In addition to vertical migration behavior, another likely
52
53627 important factor in their carbon flow is their respiration rate. The higher their respiration rate, the
54
55628 larger the proportion of assimilated carbon that will be released back into the water as dissolved

1
2
3
4
5
6
7
8
9
10

1629 carbon dioxide. This study provides the broadest taxonomic perspective on respiration rates (18
1630 species, Fig. S5) and swimming cost of transport (14 species), finding 17-fold differences in their
1631 respiration rates and over 77-fold differences in their mean COT. Except for a few species with
1632 extremely high and low values, most respiration rates are centered between 0.2 and 1
1633 $\mu\text{mol/g/hour}$, assuming a salp tissue density of 1.025 g/ml. In general, the respiration rates we
1634 estimated for salps are within the range of those reported in the literature (Trueblood 2019, Iguchi
1635 and Ikeda 2004). Compared to the metabolic rates estimated for the broader diversity of marine
1636 pelagic animals (Seibel & Drazen 2007), the rates that we measured for salps are in a similar
1637 range to those measured for *Salpa thompsoni* (Iguchi and Ikeda 2004). Our values are also similar
1638 to those measured- by Seibel & Drazen (2007) in nemerteans, chaetognaths, and most fishes
1639 ($0.1\text{-}1 \mu\text{molO}_2/\text{g/h}$), which are generally higher than other gelatinous animals like ctenophores or
1640 scyphomedusae ($0.01\text{-}0.1 \mu\text{molO}_2/\text{g/h}$), but generally lower than those of cephalopods,
1641 crustaceans, or large fish ($1\text{-}10 \mu\text{molO}_2/\text{g/h}$). Salp species known to have strong vertical migration
1642 behaviors (*Salpa* spp., *S. zonaria*, *I. punctata*, and *R. retracta*) have low basal metabolic rates
1643 (Fig. S5) and low costs of transport. These results indicate that many non-migratory species, while
1644 likely still being important players in the biological carbon pump via their fecal pellet production,
1645 are releasing more of the consumed carbon as carbon dioxide near the surface than their more
1646 metabolically efficient relatives. The ultimate ecological outcome of each species needs to be
1647 assessed holistically, considering their microbial filtration and pellet deposition rate as well as
1648 their relative abundance in the water column.

44
4549 Our metabolically calculated costs of transport range between 5-50 J/kg/m when
46650 converting the mg of oxygen to J via aerobic respiration free energy equations at 23°C. Our values
47651 are higher than the highly efficient 1-2 J/kg/m reported for salps in the literature (Bone & Trueman
48652 1983, Gemmell et al. 2021), rather approaching the less-efficient values found in single jet-
49653 propelled invertebrates like scallops or squids. We suspect that COT calculated from mechanical
50654 parameters such as the displacement of water mass is not directly comparable to the COT

55
56
57
58
59
60
61
62
63
64
65

1
2
3
4
5
6
7
8
9
10
11 655 calculated from respiration rates. Furthermore, ~~we hypothesize that~~ the standard aerobic
12 respiration free-energy equation based on glucose ~~is not an exact representation~~~~may not fully~~
13
14 656 ~~represent of~~ the metabolic energy-conversion processes in salps, which may rely on a
15 combination of sugars and fatty acids derived from their microscopic prey.
16
17

18 659 ~~While other studies on jet-propelled systems have shown that COT increases with~~
19 ~~swimming speed (Bi & Zhu 2019), we did not find support for this hypothesis. This may be due to~~
20
21 660 ~~salps being unique among jet-propelled animals since their incurrent flow is separate, parallel,~~
22 ~~and thus synergistic with the excurrent flow on the opposite end of their bodies, avoiding the~~
23 ~~deceleration forces typically associated with the refill phase (Bone and Trueman, 1983).~~ Our
24 results show that faster swimming species have lower COT (Fig. 6), which suggests that faster
25 speeds and higher locomotory efficiency have a common cause, ~~congruent with the hypothesis~~
26
27 663 ~~that where both speed and efficiency depend on frontal drag area which may partly drive form and~~
28 ~~pressure drag forces. However, this hypothesis is not supported by the distribution of COT across~~
29
30 666 ~~architectures (Fig 5C, D), where except for oblique and transversal chains, all architectures~~
31 ~~present similarly efficient COT values. These results may be explained by the fact that swimming~~
32 ~~speed is an inversely proportional factor in the calculation of COT from respiration rates.~~
33
34 669 ~~Therefore, where we found surprisingly high and low speeds for clusters and oblique chains, we~~
35 ~~found surprisingly low and high COT values respectively.~~ Perhaps there are other underlying
36 explanatory factors linking swimming speed and swimming efficiency, such as shared ancestry,
37 muscle content, jet coordination, or jetting angles (thrust-to-torque ratios).
38
39 672 *Evolutionary implications*
40
41 675 Across the evolutionary history of salps, linear chains have evolved multiple times
42 independently from oblique ancestors (Damian-Serrano et al. 2023), suggesting the adaptive role
43 of this architecture as a functional trait. Linear chain architectures evolved independently in *M.*
44 *hexagona*, *S. zonaria*, *I. punctata*, and before the common ancestor of *Jasis* and *Salpa*. Our results
45 show that going from an oblique form to a linear one may confer significant advantages in
46
47

48 678 Formatted: Font: Italic

49 679 Formatted: Font: Italic

50 680 Formatted: Font: Italic

1
2
3
4
5
6
7
8
9
10
11
12
13
14
15
16
17
18
19
20
21
22
23
24
25
26
27
28
29
30
31
32
33
34
35
36
37
38
39
40
41
42
43
44
45
46
47
48
49
50
51
52
53
54
55
56
57
58
59
60
61
62
63
64
65

1681 locomotory speed and energetic efficiency. However, multiple colonial architectures, which we
1682 find to be slower swimmers (such as transversal chains, helical chains, whorls, and clusters in
1683 the genus *Pegea* and the Cyclosalpidae family) had also evolved from linear-oblique and oblique
1684 linear formsancestors. This is incongruent with a scenario where natural selection strongly favors
1685 locomotion efficiency across all ecological niches of salps. Therefore, we hypothesize that in
1686 somethese lineages, the evolution of colonial architecture may be driven by ecological trade-offs
1687 with other non-locomotory functions. Alternatively, we hypothesize that, in some of these lineages,
1688 locomotion at the colonial stage may not be important enough for selection to maintain these
1689 highly hydrodynamic forms, allowing for neutral evolutionary processes to produce a diversity of
1690 non-adaptive forms. We do not expect the relationships between speed, architecture, and
1691 energetic efficiency to be a result of them co-evolving with one another, but rather a result of
1692 present mechanical relationships derived from colonial form. Therefore, it would not be
1693 appropriate to analyze these relationships using phylogenetic comparative methods. However,
1694 there may be unaccounted factors explaining the residual variation in our analyses that may bear
1695 phylogenetic signal. For example, tunic stiffness, tunic smoothness, muscle band number, muscle
1696 fiber density, swimming behavior, as well as metabolic and physiological baselines may be more
1697 similar between more closely related species, potentially erasing some of the architecture-specific
1698 signal. Future studies may address the role of phylogeny and heritable factors in salp swimming
1699 speed and cost of transport. These factors may have co-evolved with each other and/or with
1700 respiration rate or colonial architecture.

Formatted: Font: Italic

4701 Insights for bioinspired underwater vehicle design

4702 Pulsatile jet propulsion is a promising avenue for bioinspired aquatic vehicles and robots
4703 (Mohensi 2006, Gohardini 2014, Yue et al. 2015). Multijet propulsion systems with multiple
4704 propellers akin to salp colonies are starting to be explored in an engineering context (Chao et al.
4705 2017, Costello et al. 2015) with direct inspiration from gelatinous animals (Marut 2014, Krummel
4706 2019, Bi et al 2022, Du Clos et al. 2022). Salp diversity provides a natural laboratory to explore

1
2
3
4
5
6
7
8
9
10

11 707 the hydrodynamic implications of different multijet arrangement designs. Our findings underscore
12 708 the importance of considering the scaling hydrodynamic properties of propeller arrangements to
13 709 optimize speed and energy efficiency in bioinspired underwater vehicle design. While linear chain
14 710 arrangements were the fastest and among the most energy efficient, robot (or vehicle)
15 711 configurations such as a cluster form may confer unique object manipulation or maneuverability
16 712 advantages. Our results show that these seemingly inefficient propeller configurations do not
17 713 impose large disadvantages in terms of speed and fuel efficiency.
18
19

20 23 14 **Acknowledgments:**

21 24 715 We are grateful to the crew of Aquatic Life Divers, Kona Honu Divers for their assistance
22 25 and support in hosting our offshore diving operations. We also wish to thank Marc Hughes, Jeff
23 26 716 Milisen, Rebecca Gordon, Matt Connelly, Clint Collins, Paul Richardson, and Anne Thompson for
24 27 717 their assistance during diving, collections, and filming operations in the field. Finally, we would
25 28 718 like to thank Tiffany Bachtel for her valuable advice on the respirometry experiment design.
26 29 719
27 30 720

31 33 20 **Funding**

32 34 35 721 This research was supported by the Gordon and Betty Moore Foundation [grant number
33 36 722 8835] and the Office of Naval Research [grant number N00014-23-1-2171].
34 37

38 23 **Literature cited**

- 39 40 724 Alexander, A. J. (1968). Forward Speed Effects on Annular Jet Cushions. *The Aeronautical
41 725 Journal*, 72(689), 438-441.
- 42 43 726 Bi, X., & Zhu, Q. (2019). Dynamics of a squid-inspired swimmer in free swimming. *Bioinspiration
44 727 & Biomimetics*, 15(1), 016005.
- 45 728 Bi, X., Tang, H., & Zhu, Q., 2022. Feasibility of hydrodynamically activated valves for 416 salp-
46 729 like propulsion. *Physics of Fluids*, 34(10), 101903.
- 47 50 730 Biggs, D. C. (1977). Respiration and ammonium excretion by open ocean gelatinous zooplankton
51 731 1. *Limnology and Oceanography*, 22(1), 108-117.
- 52
53
54
55
56
57
58
59
60
61
62
63
64
65

Formatted: Font: 11 pt
Formatted: Font: 11 pt, Not Italic
Formatted: Font: 11 pt
Formatted: Font: 11 pt, Not Italic
Formatted: Font: 11 pt

1
2
3
4
5
6
7
8
9
10

- 11 732 Bone, Q., Anderson, P. A. V., & Pulsford, A. (1980). Morphology of salp chain communication.
12
13 733 *Proceedings of the Royal Society of London. Series B. Biological Sciences*, 210(1181),
14 734 549-558.
15
16 735 Bone, Q., & Trueman, E. R. (1983). Jet propulsion in salps (Tunicata: Thaliacea). *Journal of*
17
18 736 *Zoology*, 201(4), 481-506.
19 737 Cetta, C. M., Madin, L. P., & Kremer, P. (1986). Respiration and excretion by oceanic salps.
20
21 738 *Marine Biology*, 91, 529-537.
22
23 739 Chao, S., Guan, G., & Hong, G. S., 2017, September. Design of a finless torpedo-shaped micro
24 740 AUV with high maneuverability. In OCEANS 2017-Anchorage (pp. 425 1-6). IEEE.
25
26 741 Colin, S. P., Gemmell, B. J., Costello, J. H., & Sutherland, K. R. (2022). In situ high-speed
27
28 742 brightfield imaging for studies of aquatic organisms. Protocols.io.
29
30 743 Costello, J. H., Colin, S. P., Gemmell, B. J., Dabiri, J. O., & Sutherland, K. R., 2015. 429 Multi-jet
31 744 propulsion organized by clonal development in a colonial siphonophore. 430 *Nature*
32
33 745 *communications*, 6(1), 8158.
34
35 746 Damian-Serrano, A., & Sutherland, K. R. (2023). A developmental ontology for the colonial
36 747 architecture of salps. [The BioRxiv Biological Bulletin](#), 245(1), 9-18, 2023-09.
37
38 748 Damian-Serrano, A., Hughes, M., & Sutherland, K. R. (2023). A new molecular phylogeny of salps
39
40 749 (Tunicata: thalicea: salpida) and the evolutionary history of their colonial architecture.
41 750 Integrative Organismal Biology, 5(1), obad037.
42
43 751 Décima, M., Stukel, M. R., Nodder, S. D., Gutiérrez-Rodríguez, A., Selph, K. E., Dos Santos, A.
44
45 752 L., ... & Pinkerton, M. (2023). Salp blooms drive strong increases in passive carbon export
46
47 753 in the Southern Ocean. *Nature communications*, 14(1), 425.
48 754 Du Clos, K. T., Gemmell, B. J., Colin, S. P., Costello, J. H., Dabiri, J. O., and Sutherland, K. R.
49
50 755 2022. Distributed propulsion enables fast and efficient swimming modes in physonect
51
52 756 siphonophores. *Proceedings of the National Academy of Sciences*. 119:e2202494119.

Formatted: Font: 11 pt, Not Italic

Formatted: Font: 11 pt

- 1
2
3
4
5
6
7
8
9
10
11 757 Gemmell, B. J., Dabiri, J. O., Colin, S. P., Costello, J. H., Townsend, J. P., & Sutherland, K. R.
12
13 758 (2021). Cool your jets: biological jet propulsion in marine invertebrates. *Journal of*
14 759 *Experimental Biology*, 224(12), jeb222083.
15
16 760 Gohardani, A. S. Distributed Propulsion Technology Nova Science Publishers (2014).
17
18 761 Haddock, S. H. (2004). A golden age of gelata: past and future research on planktonic
19 762 ctenophores and cnidarians. *Hydrobiologia*, 530, 549-556.
20
21 763 Haddock, S. H., & Heine, J. N. (2005). Scientific blue-water diving.
22
23 764 Hamner, W. M., Madin, L. P., Allredge, A. L., Gilmer, R. W., & Hamner, P. P. (1975). Underwater
24 765 observations of gelatinous zooplankton: Sampling problems, feeding biology, and
25
26 766 behavior 1. *Limnology and Oceanography*, 20(6), 907-917.
27
28 767 Henschke, N., Cherel, Y., Cotté, C., Espinasse, B., Hunt, B.P. and Pakhomov, E.A., 2021. Size
29
30 768 and stage specific patterns in *Salpa thompsoni* vertical migration. *Journal of Marine*
31 769 *Systems*, 222, p.103587.
32
33 770 Krummel, G. M. (2019). Locomotion and Control of Cnidarian-Inspired Robots (Doctoral
34
35 771 dissertation, Virginia Tech).
36 772 Mackie, G. O. (1986). From aggregates to integrates: physiological aspects of modularity in
37
38 773 colonial animals. *Philosophical Transactions of the Royal Society of London. B, Biological*
39
40 774 *Sciences*, 313(1159), 175-196.
41 775 Madin, L. P. (1990). Aspects of jet propulsion in salps. *Canadian Journal of Zoology*, 68(4), 765-
42
43 776 777.
44
45 777 Madin, L. P., & Deibel, D. (1998). Feeding and energetics of Thaliacea. *The biology of pelagic*
46
47 778 *tunicates*, 81-104.
48 779 Madin, L. P., Kremer, P., & Hacker, S. (1996). Distribution and vertical migration of salps
49
50 780 (Tunicata, Thaliacea) near Bermuda. *Journal of Plankton Research*, 18(5), 747-755.
51
52 781 Madin, L.P., Kremer, P., Wiebe, P.H., Purcell, J.E., Horgan, E.H. and Nemazie, D.A., 2006.
53 782 Periodic swarms of the salp *Salpa aspera* in the Slope Water off the NE United States:
54
55
56
57
58
59
60
61
62
63
64
65

1
2
3
4
5
6
7
8
9
10
11 783 Biovolume, vertical migration, grazing, and vertical flux. Deep Sea Research Part I:
12
13 784 Oceanographic Research Papers, 53(5), pp.804-819.
14 785 Marut, K. J. (2014). Underwater Robotic Propulsors Inspired by Jetting Jellyfish (Doctoral
15 dissertation, Virginia Tech).
16 786
17 787 Mayzaud, P., Boutoute, M., Gasparini, S., Mousseau, L., & Lefevre, D. (2005). Respiration in
18 marine zooplankton—the other side of the coin: CO₂ production. *Limnology and*
19
20 788 *Oceanography*, 50(1), 291-298.
21 789
22 790 Mohensi, K., 2006. Pulsatile vortex generators for low-speed maneuvering of small 482
23 underwater vehicles. *Ocean Eng.* 33, 2209–2223.
24 791
25
26 792 Pascual, M., Acuña, J.L., Sabatés, A., Raya, V. and Fuentes, V., 2017. Contrasting diel vertical
27 migration patterns in *Salpa fusiformis* populations. *Journal of Plankton Research*, 39(5),
28
29 793 pp.836-842.
30 794
31 795 R Core Team, R. (2021). R: A language and environment for statistical computing.
32
33 796 Schneider, G. (1992). A comparison of carbon-specific respiration rates in gelatinous and non-
34
35 797 gelatinous zooplankton: a search for general rules in zooplankton metabolism.
36 798 *Helgoländer Meeresuntersuchungen*, 46, 377-388.
37
38 799 Seibel, B. A., & Drazen, J. C. (2007). The rate of metabolism in marine animals: environmental
39 constraints, ecological demands and energetic opportunities. *Philosophical Transactions*
40
41 800 *of the Royal Society B: Biological Sciences*, 362(1487), 2061-2078.
42
43 801 Stone, J. P., & Steinberg, D. K. (2014). Long-term time-series study of sulp population dynamics
44
45 802 in the Sargasso Sea. *Marine Ecology Progress Series*, 510, 111-127.
46 803
47 804 Sutherland, K. R., & Weihs, D. (2017). Hydrodynamic advantages of swimming by sulp chains.
48 805 Journal of The Royal Society Interface, 14(133), 20170298.
49
50 806 Sutherland, K. R., Damian-Serrano, A., Du Clos, K. T., Gemmell, B. J., Colin, S. P., Costello, J.
51
52 807 H. (in-review2024). Spinning and corkscrewing of oceanic macroplankton revealed
53
54 808 through in situ imaging. *Science Advances*, 10(20).
55
56
57
58
59
60
61
62
63
64
65

Formatted: Font: Not Italic

1
2
3
4
5
6
7
8
9
10
11
12
13
14
15
16
17
18
19
20
21
22
23
24
25
26
27
28
29
30
31
32
33
34
35
36
37
38
39
40
41
42
43
44
45
46
47
48
49
50
51
52
53
54
55
56
57
58
59
60
61
62
63
64
65

- 1809 Sutherland, K. R., & Madin, L. P. (2010). Comparative jet wake structure and swimming
1810 performance of salps. *Journal of Experimental Biology*, 213(17), 2967-2975.
- 1811 Trueblood, L. A. (2019). Salp metabolism: temperature and oxygen partial pressure effect on the
1812 physiology of *Salpa fusiformis* from the California Current. *Journal of Plankton Research*,
1813 41(3), 281-291.
- 1814 Trueman, E. R., Bone, Q., & Braconnat, J. C. (1984). Oxygen consumption in swimming salps
1815 (Tunicata: Thaliacea). *Journal of Experimental Biology*, 110(1), 323-327.
- 1816 Vogel, S. (1981). Life in moving fluids. *Princeton University Press*, Princeton, NJ.
- 1817 Vogel, S. (2008). Modes and scaling in aquatic locomotion. *Integrative and Comparative Biology*,
1818 48(6), 702-712.
- 1819 Wiebe, P. H., Madin, L. P., Haury, L. R., Harbison, G. R., & Philbin, L. M. (1979). Diel vertical
1820 migration by *Salpa aspera* and its potential for large-scale particulate organic matter
1821 transport to the deep-sea. *Marine Biology*, 53, 249-255.
- 1822 World Register of Marine Species (WoRMS). (2024). WoRMS Editorial Board. Accessed January
1823 30, 2024. Available online at <http://www.marinespecies.org>
- 1824 Yue, C. et al., 2015. Mechantronic system and experiments of a spherical underwater 510 robot:
1825 SUR-II. *J. Intell. Robot Syst.* Doi:10.1007/s10846-015-0177-3.

Figure 1

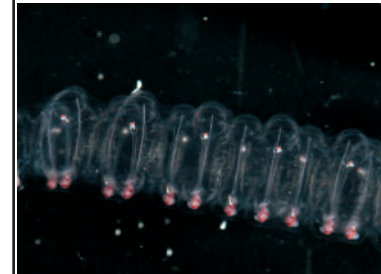
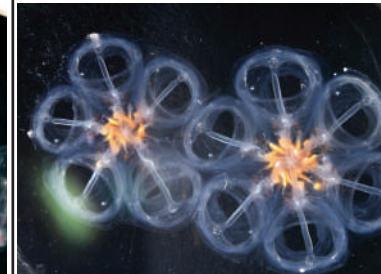
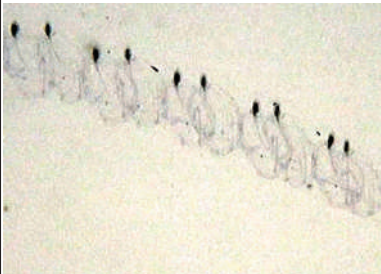
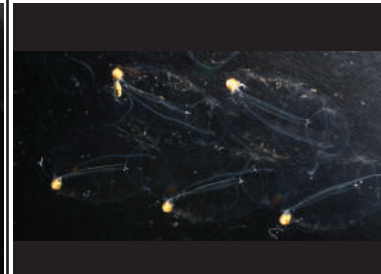
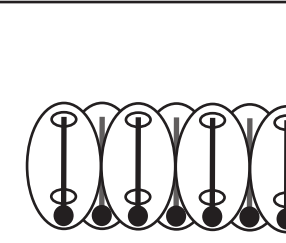
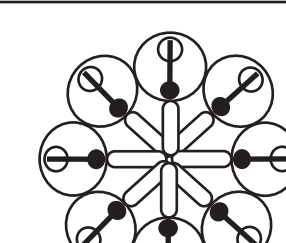
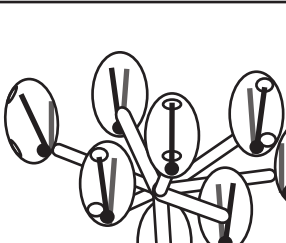
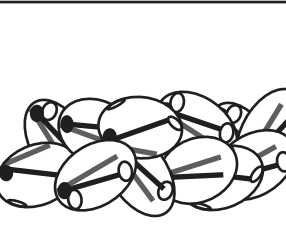
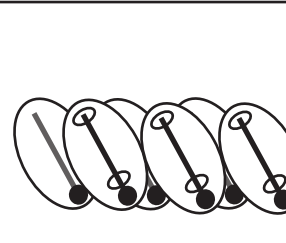
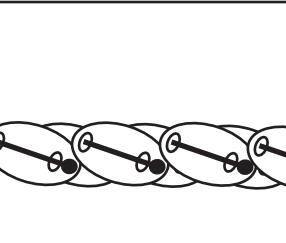
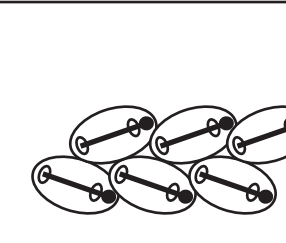
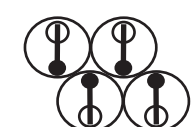
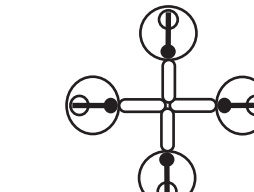
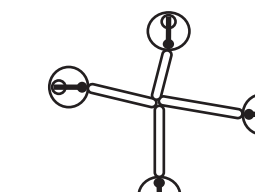
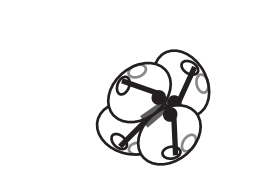
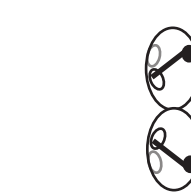
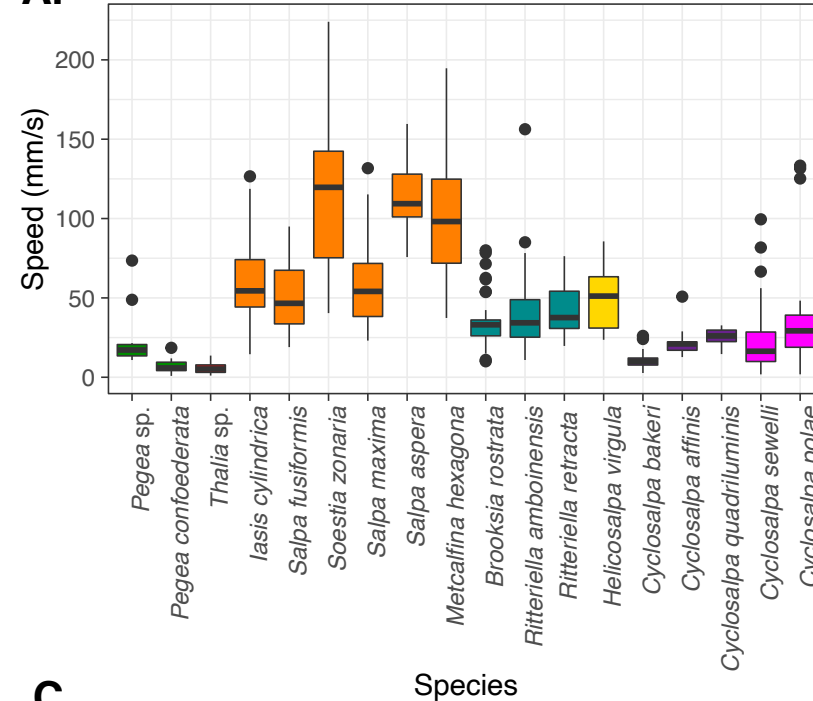
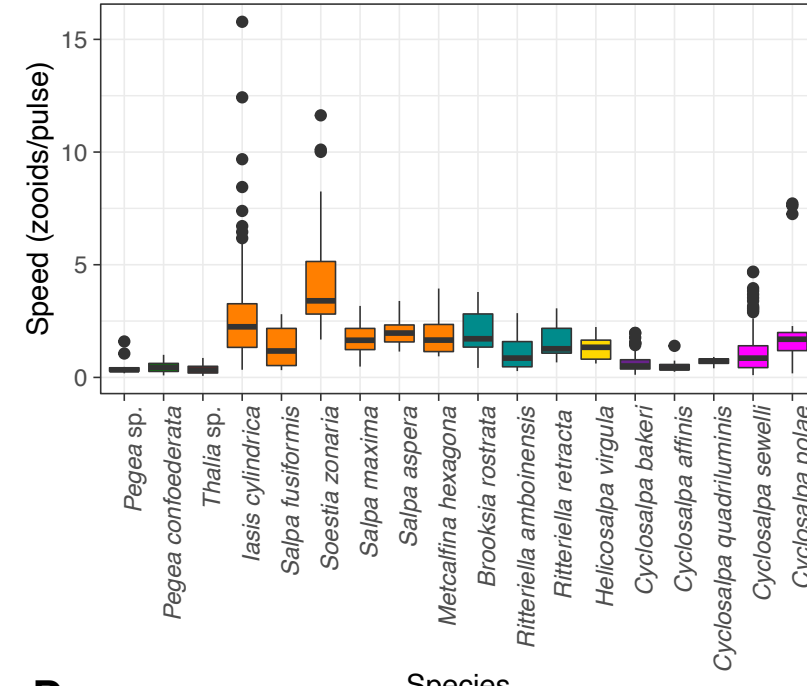
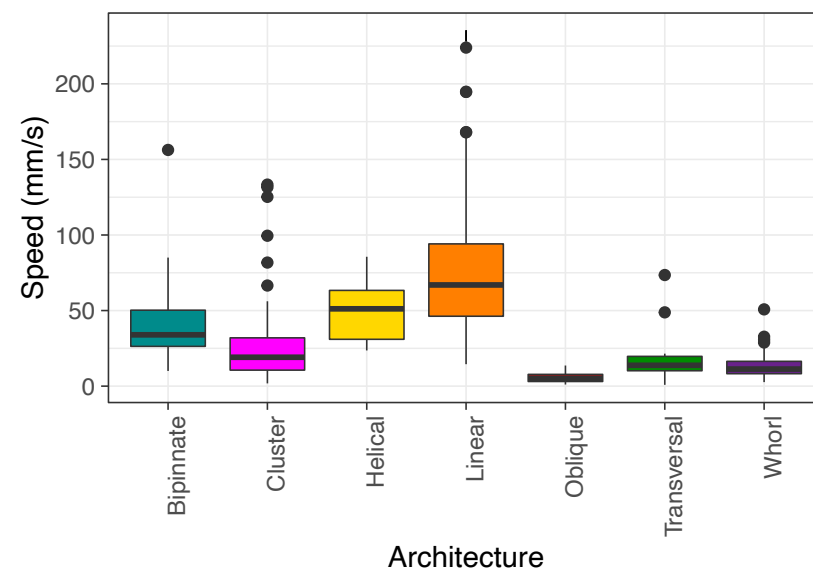
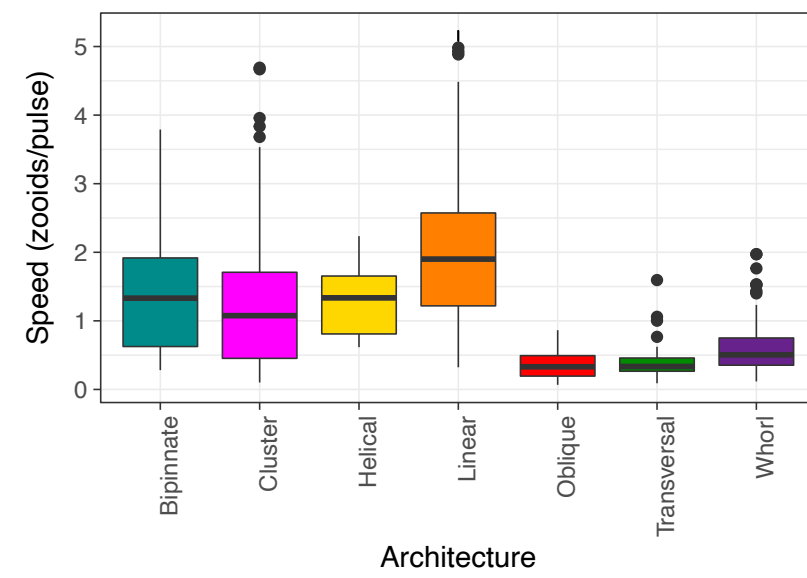
| | Transversal | Whorl | Cluster | Helical | Oblique | Linear | Bipinnate |
|----------------------------------|--|---|--|--|--|--|--|
| Architecture |  |  |  |  |  |  |  |
| |  |  |  |  |  |  |  |
| Frontal area 4 zooids |  |  |  |  |  |  |  |
| Frontal area 8 zooids |  |  |  |  |  |  |  |
| Scaling | 2 | 2 | 2 | 1 | $1 < x < 2$ | 1 | 1 |

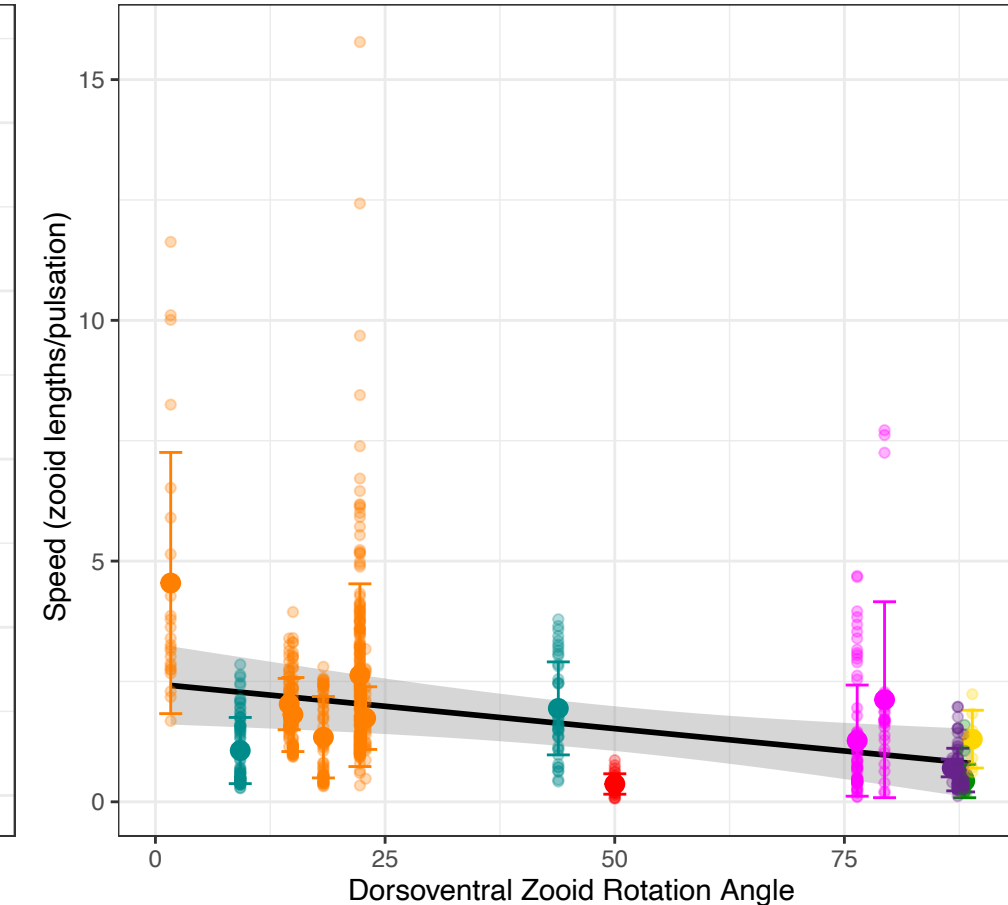
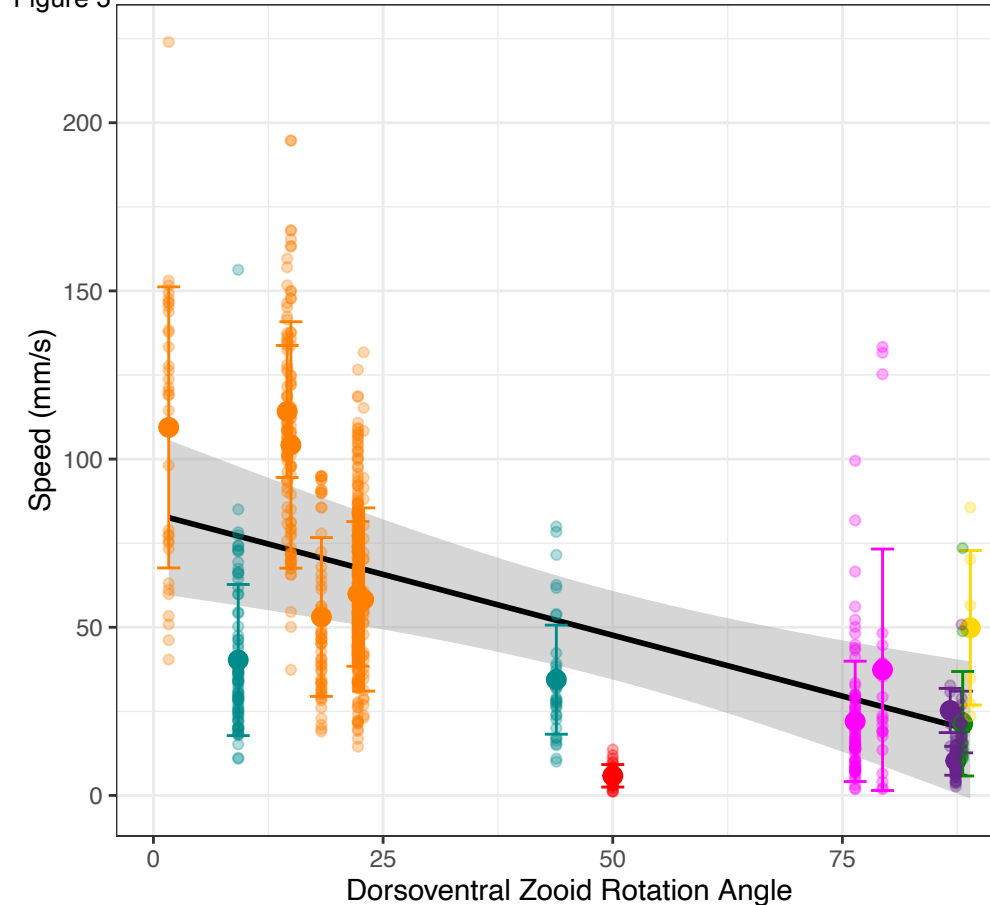
Figure 2

A.**B.****C.****D.**

Architecture

- Transversal
- Oblique
- Linear
- Bipinnate
- Helical
- Whorl
- Cluster

Figure 3



Architecture

- Transversal
- Oblique
- Linear
- Bipinnate
- Helical
- Whorl
- Cluster

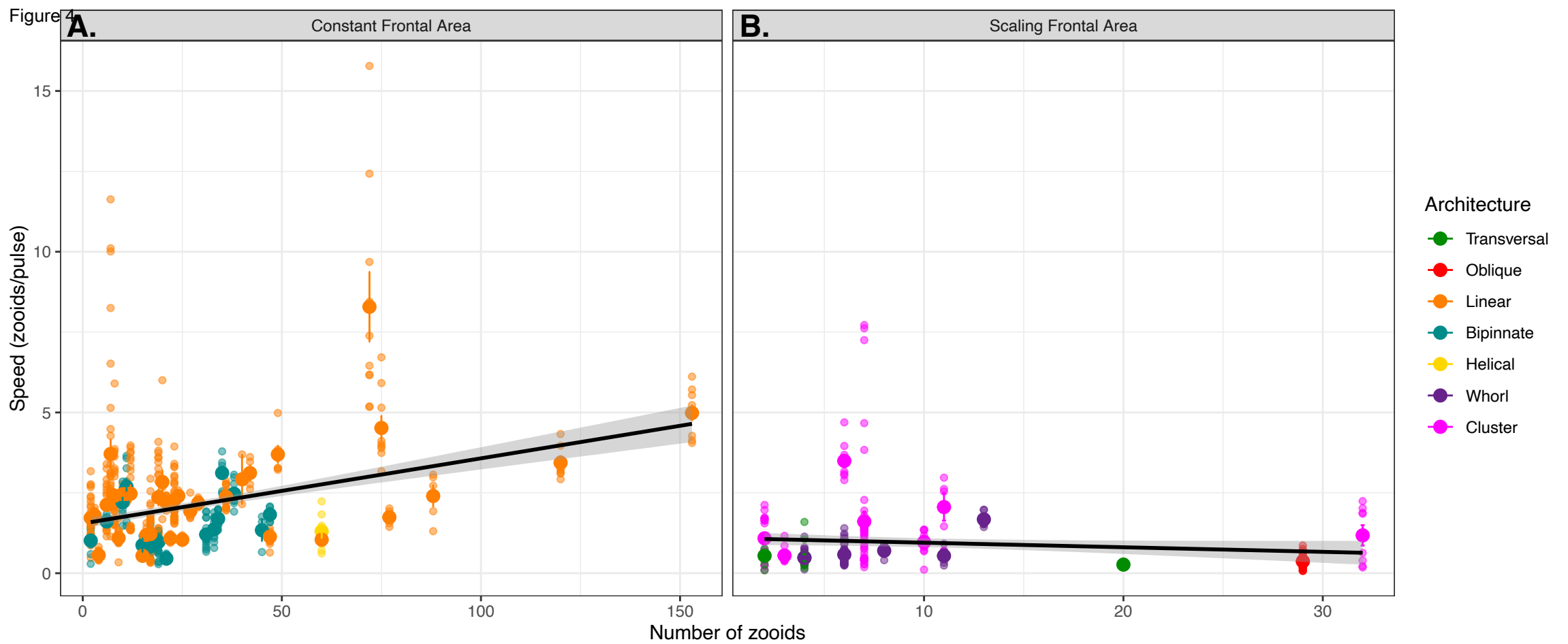


Figure 5

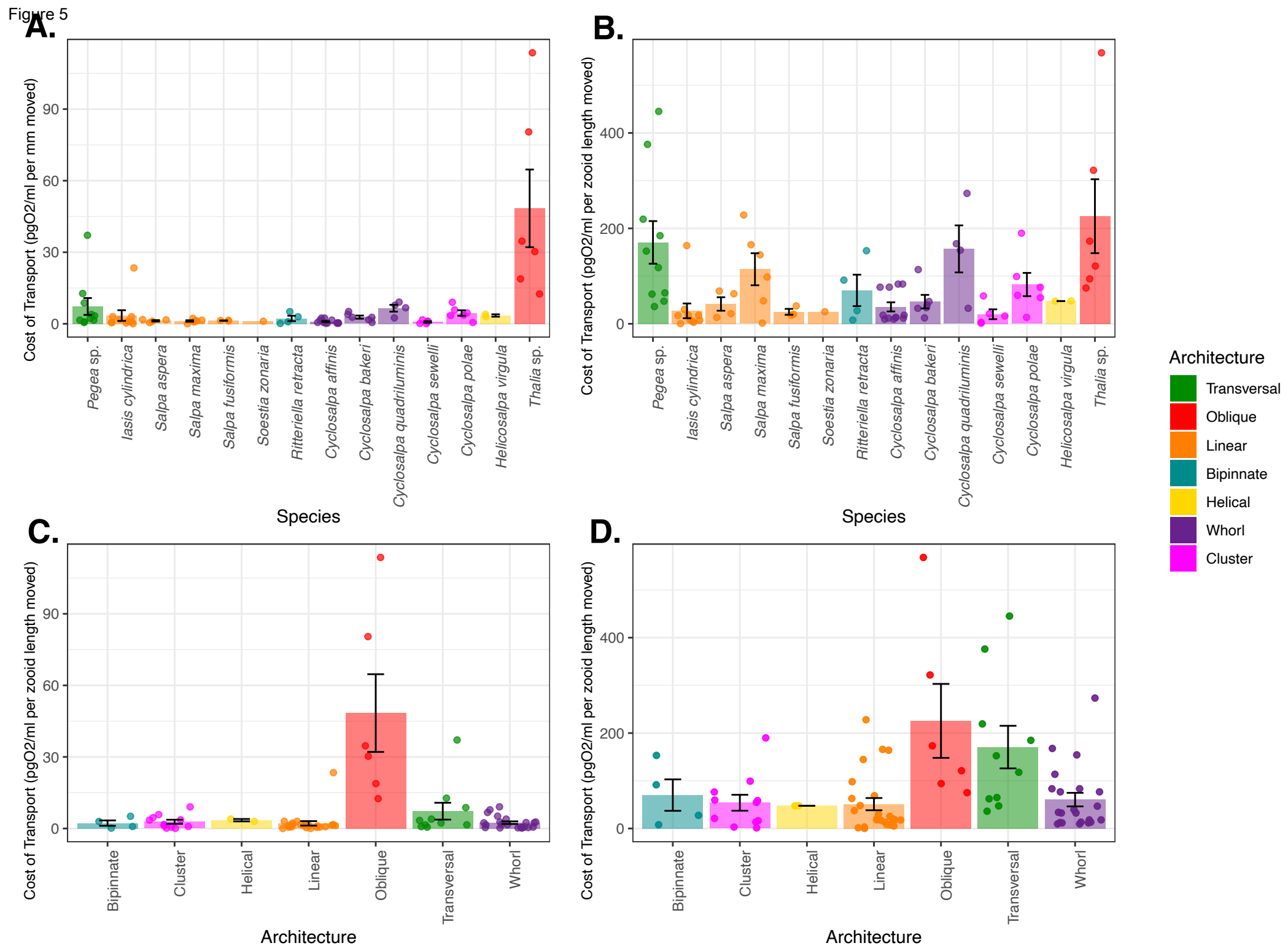
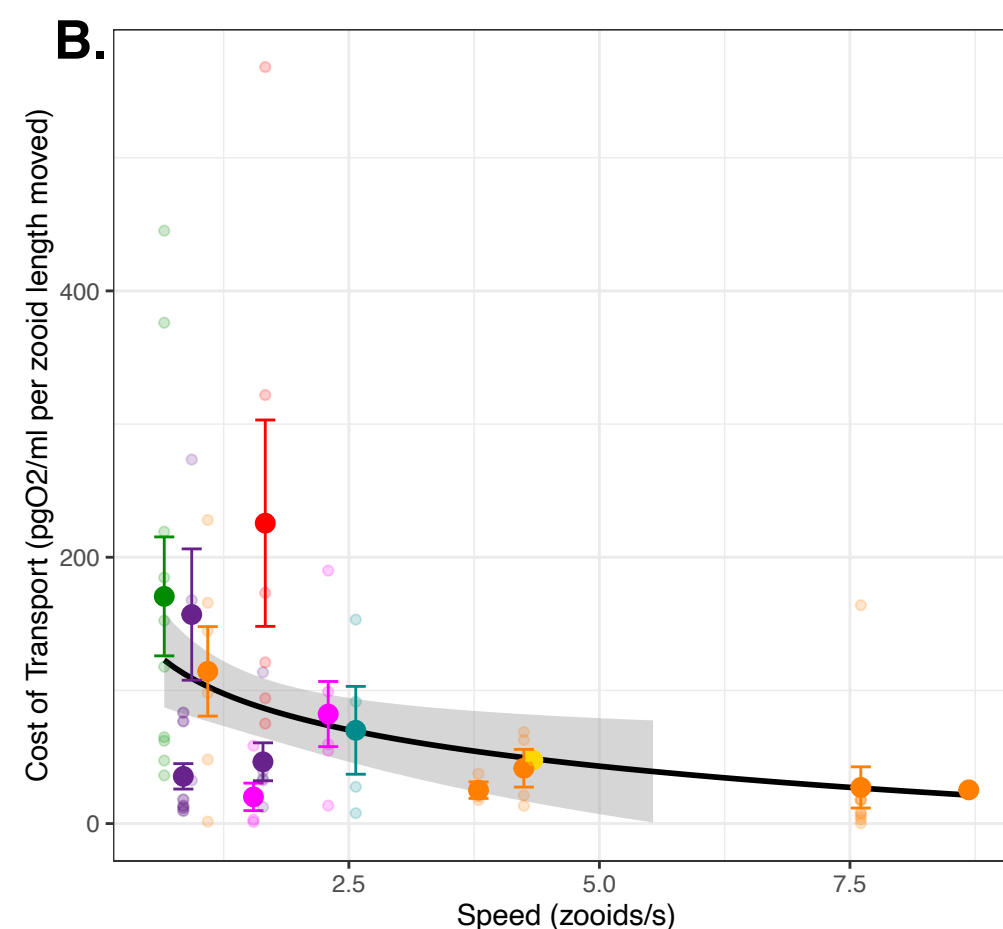
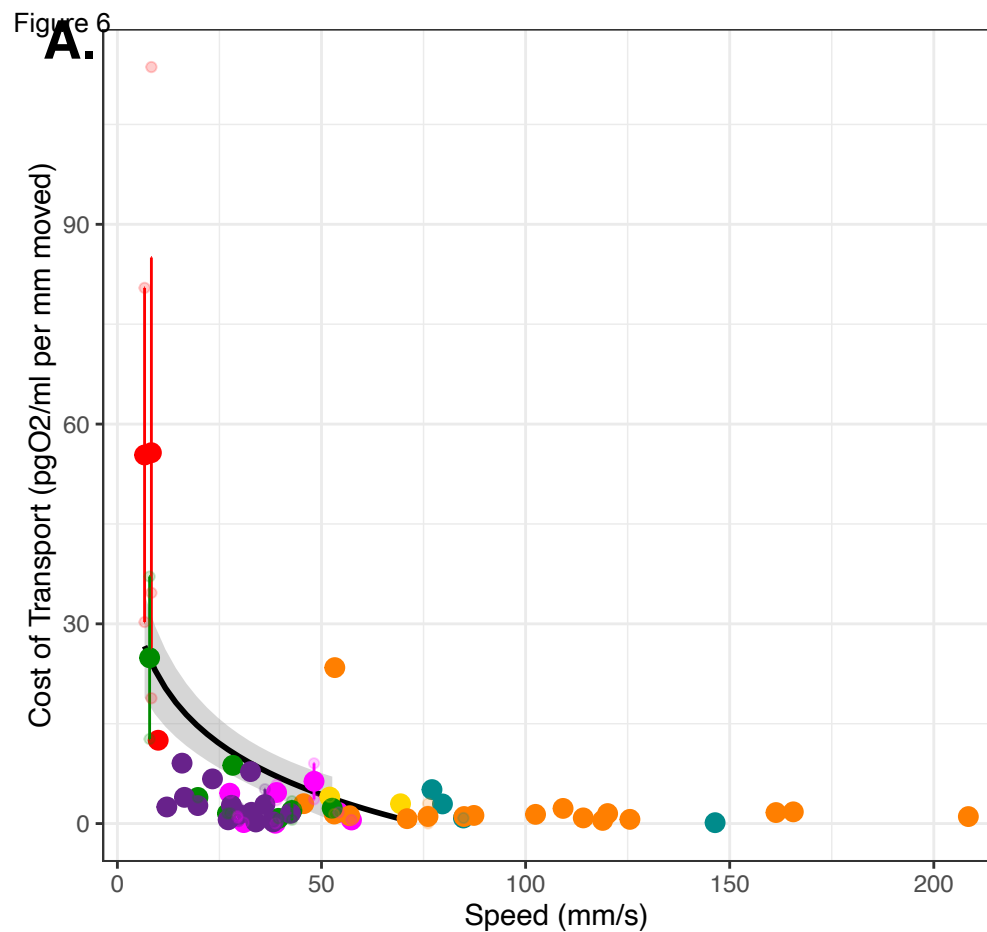


Figure 6



Supplementary Material

Table S1. Salp video specimens analyzed with video specifications, as well as mean morphological and kinematic attributes.

| Video file | Type | FPS | Species | Architecture | Number of measurements | Timespan of measurements (s) | Number of zooids | Mean zooid length (mm) | Mean zooid width (mm) | Pulsation rate (pulses/s) | Mean swimming speed (mm/s) |
|---------------------------------|------|-----|--------------------------------|--------------|------------------------|------------------------------|------------------|------------------------|-----------------------|---------------------------|----------------------------|
| A001C0113_20210709170400_0001 | 3D | 120 | <i>Brooksia rostrata</i> | Bipinnate | 9 | 1.51 | 34 | 7.144 | 2.693 | 2.5 | 30.25 |
| A001C0114_20210709170545_0001 | 3D | 120 | <i>Brooksia rostrata</i> | Bipinnate | 9 | 1.50 | 33 | 6.902 | 3.4 | 3 | 28.32 |
| A001C0143_20210709181838_0001_1 | 3D | 120 | <i>Brooksia rostrata</i> | Bipinnate | 9 | 1.50 | 11 | 7.963 | 4.026 | 2.75 | 58.79 |
| A001C0223_20210917230616_0001 | 3D | 120 | <i>Brooksia rostrata</i> | Bipinnate | 9 | 1.51 | 35 | 4.363 | 2.306 | 2.56 | 34.83 |
| A001C0294_20210920202610_0001 | 3D | 120 | <i>Brooksia rostrata</i> | Bipinnate | 9 | 1.51 | 17 | 10.592 | 4.322 | 2.25 | 19.94 |
| A001C0284_20210919222752_0001 | 3D | 120 | <i>Ritteriella amboinensis</i> | Bipinnate | 7 | 1.17 | 47 | 13.449 | 7.488 | 2.8 | 68.65 |
| A001C0288_20210919223646_0001 | 3D | 120 | <i>Ritteriella amboinensis</i> | Bipinnate | 9 | 1.51 | 6 | 13.729 | 6.186 | 1.73 | 38.26 |
| A001C0321_20210921220020_0001 | 3D | 120 | <i>Ritteriella amboinensis</i> | Bipinnate | 7 | 1.17 | 2 | 69.473 | 33.031 | 0.75 | 52.90 |
| A001C0322_20210921220127_0001 | 3D | 120 | <i>Ritteriella amboinensis</i> | Bipinnate | 14 | 2.33 | 21 | 26.047 | 9.561 | 2.75 | 33.12 |
| A001C0323_20210921220235_0001 | 3D | 120 | <i>Ritteriella amboinensis</i> | Bipinnate | 15 | 2.50 | 21 | 22.705 | 10.298 | 2.2 | 22.47 |
| A001C0331_20210921221849_0001 | 3D | 120 | <i>Ritteriella amboinensis</i> | Bipinnate | 9 | 1.50 | 19 | 21.485 | 12.129 | 3 | 55.50 |
| A001C0332_20210921222049_0001_2 | 3D | 120 | <i>Ritteriella amboinensis</i> | Bipinnate | 7 | 1.17 | 19 | 20.047 | 13.747 | 1.5 | 35.01 |
| A001C0332_20210921222049_0001_1 | 3D | 120 | <i>Ritteriella amboinensis</i> | Bipinnate | 1 | 0.17 | 19 | 21.48 | 12.695 | 1.5 | 20.09 |
| A002C0018_20220420225725_0001 | 3D | 60 | <i>Ritteriella amboinensis</i> | Bipinnate | 8 | 2.67 | 10 | 22.403 | 11.767 | 1.14 | 56.31 |
| A001C0348_20210922220852_0001 | 3D | 120 | <i>Ritteriella</i> sp. | Bipinnate | 9 | 1.50 | 38 | 16.593 | 7.375 | 1.5 | 61.56 |
| A001C0349_20210922220958_0001 | 3D | 120 | <i>Ritteriella</i> sp. | Bipinnate | 20 | 3.34 | 31 | 23.682 | 16.25 | 1.25 | 33.81 |
| A001C0349_20210922220958_0001 | 3D | 120 | <i>Ritteriella</i> sp. | Bipinnate | 20 | 3.34 | 31 | 23.682 | 16.25 | 1.13 | 33.81 |
| A001C0344_20210922220308_0001 | 3D | 120 | <i>Cyclosalpa polae</i> | Cluster | 10 | 2.51 | 7 | 17.275 | 12.861 | 1 | 55.48 |
| A002C0047_20220421225032_0001 | 3D | 60 | <i>Cyclosalpa polae</i> | Cluster | 9 | 4.51 | 2 | 17.091 | 33.996 | 1.33 | 39.73 |
| A001C0247_20210918223147_0001_1 | 3D | 120 | <i>Cyclosalpa sewelli</i> | Cluster | 7 | 1.17 | 7 | 17.764 | 8.919 | 1.2 | 46.27 |
| A001C0262_20210919202019_0001 | 3D | 120 | <i>Cyclosalpa sewelli</i> | Cluster | 9 | 1.50 | 7 | 12.584 | 3.675 | 1.33 | 21.10 |
| A001C0274_20210919203457_0001 | 3D | 120 | <i>Cyclosalpa sewelli</i> | Cluster | 9 | 1.50 | 7 | 17.705 | 13.97 | 2 | 14.06 |
| A001C0283_20210919222440_0001 | 3D | 120 | <i>Cyclosalpa sewelli</i> | Cluster | 9 | 1.51 | 6 | 9.458 | 5.528 | 1.5 | 49.58 |
| A001C0326_20210921220800_0001 | 3D | 120 | <i>Cyclosalpa sewelli</i> | Cluster | 9 | 1.51 | 2 | 17.069 | 7.959 | 1.25 | 8.99 |
| A001C0358_20210922222944_0001 | 3D | 120 | <i>Cyclosalpa sewelli</i> | Cluster | 9 | 1.50 | 10 | 15.668 | 10.298 | 1.25 | 20.66 |
| GX010177_Helicosalpa_Trim | 2D | 60 | <i>Helicosalpa virgula</i> | Helical | 7 | 1.20 | 60 | 11.5 | 6.4 | 3.33 | 49.86 |
| A001C0093_20210708143858_0001 | 3D | 60 | <i>Iasis cylindrica</i> | Linear | 9 | 3.01 | 75 | 4.011 | 2.27 | 2.75 | 49.83 |
| A001C0143_20210709181838_0001_2 | 3D | 120 | <i>Iasis cylindrica</i> | Linear | 6 | 1.00 | 49 | 4.399 | 3.081 | 3 | 48.77 |
| A001C0147_20210709182345_0001 | 3D | 120 | <i>Iasis cylindrica</i> | Linear | 9 | 1.50 | 30 | NA | NA | 2.17 | 43.20 |
| A001C0164_20210709183900_0001_1 | 3D | 120 | <i>Iasis cylindrica</i> | Linear | 13 | 2.21 | 44 | NA | NA | 3 | 51.55 |
| A001C0164_20210709183900_0001_2 | 3D | 120 | <i>Iasis cylindrica</i> | Linear | 9 | 1.50 | 9 | NA | NA | 5 | 36.22 |

| | | | | | | | | | | | |
|---------------------------------|----|-----|----------------------------|--------|----|------|-----|--------|--------|------|--------|
| A001C0165_20210709184012_0001_1 | 3D | 120 | <i>Iasis cylindrica</i> | Linear | 9 | 1.50 | 24 | NA | NA | 2.75 | 48.29 |
| A001C0165_20210709184012_0001_2 | 3D | 120 | <i>Iasis cylindrica</i> | Linear | 9 | 1.50 | 89 | NA | NA | 2.75 | 59.70 |
| A001C0166_20210709184051_0001_1 | 3D | 120 | <i>Iasis cylindrica</i> | Linear | 9 | 1.50 | 94 | NA | NA | 3 | 38.18 |
| A001C0167_20210709184129_0001 | 3D | 120 | <i>Iasis cylindrica</i> | Linear | 9 | 1.50 | 19 | 12.936 | 6.246 | 3.25 | 52.55 |
| A001C0169_20210709184226_0001 | 3D | 120 | <i>Iasis cylindrica</i> | Linear | 8 | 1.33 | 13 | NA | NA | 3 | 101.65 |
| A001C0170_20210709184247_0001_2 | 3D | 120 | <i>Iasis cylindrica</i> | Linear | 9 | 1.50 | 46 | NA | NA | 5.78 | 58.74 |
| A001C0171_20210709184313_0001_2 | 3D | 120 | <i>Iasis cylindrica</i> | Linear | 9 | 1.58 | 153 | 4.387 | 3.277 | 1.83 | 40.03 |
| A001C0171_20210709184313_0001_3 | 3D | 120 | <i>Iasis cylindrica</i> | Linear | 10 | 1.67 | 72 | 4.384 | 2.968 | 1.83 | 66.49 |
| A001C0172_20210709184345_0001_2 | 3D | 120 | <i>Iasis cylindrica</i> | Linear | 9 | 1.50 | 10 | 8.295 | 4.276 | 4 | 81.51 |
| A001C0173_20210709184408_0001 | 3D | 120 | <i>Iasis cylindrica</i> | Linear | 10 | 1.67 | 25 | 12.964 | 6.301 | 5.5 | 74.50 |
| A001C0173_20210709184408_0001 | 3D | 120 | <i>Iasis cylindrica</i> | Linear | 10 | 1.67 | 9 | 12.964 | 6.301 | 5.5 | 74.50 |
| A001C0178_20210709184853_0001 | 3D | 120 | <i>Iasis cylindrica</i> | Linear | 9 | 1.50 | 47 | 11.129 | 3.892 | 3.88 | 49.01 |
| A001C0179_20210709184957_0001 | 3D | 120 | <i>Iasis cylindrica</i> | Linear | 9 | 1.51 | 11 | 12.45 | 5.628 | 2.33 | 71.53 |
| A001C0192_20210710135057_0001 | 3D | 120 | <i>Iasis cylindrica</i> | Linear | 9 | 1.50 | 3 | 8.197 | 3.8 | 5 | 73.47 |
| A001C0279_20210919221855_0001 | 3D | 120 | <i>Iasis cylindrica</i> | Linear | 9 | 1.50 | 12 | 7.079 | 2.363 | 4.67 | 45.89 |
| A001C0336_20210921222915_0001 | 3D | 120 | <i>Iasis cylindrica</i> | Linear | 9 | 1.50 | 17 | 11.806 | 5.368 | 4 | 58.15 |
| A001C0339_20210921223812_0001 | 3D | 120 | <i>Iasis cylindrica</i> | Linear | 9 | 1.50 | 12 | 10.575 | 5.944 | 2.57 | 96.65 |
| A001C0346_20210922220601_0001 | 3D | 120 | <i>Iasis cylindrica</i> | Linear | 18 | 3.00 | 36 | 7.753 | 5.053 | 4.8 | 79.08 |
| A001C0346_20210922220601_0001 | 3D | 120 | <i>Iasis cylindrica</i> | Linear | 18 | 3.00 | 36 | 7.753 | 5.053 | 3.89 | 79.08 |
| A001C0354_20210922222311_0001 | 3D | 120 | <i>Iasis cylindrica</i> | Linear | 9 | 1.54 | 19 | 10.264 | 6.371 | 2.83 | 102.18 |
| A001C0355_20210922222503_0001 | 3D | 120 | <i>Iasis cylindrica</i> | Linear | 7 | 1.18 | 77 | 7.307 | 4.041 | 4.17 | 53.07 |
| A002C0044_20220421224612_0001_1 | 3D | 60 | <i>Iasis cylindrica</i> | Linear | 9 | 3.01 | 120 | 6.143 | 2.546 | 2.67 | 56.34 |
| A002C0044_20220421224612_0001_2 | 3D | 60 | <i>Iasis cylindrica</i> | Linear | 14 | 2.33 | 17 | 12.401 | 5.106 | 3.25 | 69.39 |
| A002C0045_20220421224748_0001 | 3D | 60 | <i>Iasis cylindrica</i> | Linear | 5 | 1.67 | 88 | 9.587 | 5.544 | 2.67 | 61.48 |
| A002C0078_20220422224659_0001 | 3D | 60 | <i>Iasis cylindrica</i> | Linear | 9 | 3.01 | 60 | 7.767 | 4.856 | 5.4 | 43.76 |
| A002C0079_20220422224739_0001 | 3D | 60 | <i>Iasis cylindrica</i> | Linear | 9 | 3.00 | 51 | NA | NA | NA | 35.00 |
| A002C0089_20220422230510_0001 | 3D | 60 | <i>Iasis cylindrica</i> | Linear | 9 | 3.00 | 9 | 9.326 | 5.86 | 5.33 | 54.97 |
| A001C0353_20210922221657_0001 | 3D | 120 | <i>Metcalfina hexagona</i> | Linear | 9 | 1.50 | 7 | 10.879 | 6.975 | 3 | 71.25 |
| A002C0035_20220421223821_0001 | 3D | 60 | <i>Metcalfina hexagona</i> | Linear | 6 | 2.00 | 22 | 30.057 | 12.198 | 3 | 97.43 |
| A002C0071_20220422223546_0001 | 3D | 60 | <i>Metcalfina hexagona</i> | Linear | 18 | 6.00 | 9 | 28.887 | 17.127 | 2.1 | 71.69 |
| A002C0071_20220422223546_0001 | 3D | 60 | <i>Metcalfina hexagona</i> | Linear | 18 | 6.00 | 9 | 28.887 | 17.127 | 2.43 | 71.69 |
| A002C0075_20220422224136_0001_1 | 3D | 60 | <i>Metcalfina hexagona</i> | Linear | 6 | 2.00 | 23 | 28.519 | 12.844 | 2.46 | 131.25 |
| A002C0075_20220422224136_0001_2 | 3D | 60 | <i>Metcalfina hexagona</i> | Linear | 12 | 4.00 | 23 | 26.693 | 14.766 | 1.85 | 160.22 |
| A002C0075_20220422224136_0001_2 | 3D | 60 | <i>Metcalfina hexagona</i> | Linear | 12 | 4.00 | 23 | 26.693 | 14.766 | 2.2 | 160.22 |
| A002C0076_20220422224245_0001 | 3D | 60 | <i>Metcalfina hexagona</i> | Linear | 12 | 4.01 | 23 | 30.239 | 17.388 | 2.08 | 111.52 |
| A002C0076_20220422224245_0001 | 3D | 60 | <i>Metcalfina hexagona</i> | Linear | 12 | 4.01 | 23 | 30.239 | 17.388 | 2.1 | 111.52 |
| A001C0334_20210921222327_0001 | 3D | 120 | <i>Salpa aspera</i> | Linear | 9 | 1.50 | 8 | 27.926 | 14.631 | 2.5 | 145.45 |
| A001C0335_20210921222656_0001 | 3D | 120 | <i>Salpa aspera</i> | Linear | 9 | 1.50 | 8 | 30.132 | 15.661 | 2.33 | 110.41 |
| A002C0042_20220421224445_0001 | 3D | 60 | <i>Salpa aspera</i> | Linear | 6 | 2.00 | 7 | 24.502 | 18.494 | 1.78 | 118.80 |
| A002C0053_20220421225858_0001 | 3D | 60 | <i>Salpa aspera</i> | Linear | 8 | 2.75 | 29 | 19.568 | 11 | 2.4 | 102.55 |
| A002C0062_20220421231037_0001 | 3D | 60 | <i>Salpa aspera</i> | Linear | 9 | 3.01 | 2 | 41.084 | 15.521 | 1.29 | 88.33 |
| A002C0080_20220422224908_0001 | 3D | 60 | <i>Salpa aspera</i> | Linear | 8 | 2.66 | 6 | 28.543 | 10.405 | 2.86 | 117.07 |
| A002C0081_20220422224921_0001 | 3D | 60 | <i>Salpa aspera</i> | Linear | 8 | 2.67 | 6 | 26.068 | 8.932 | 1.6 | 117.48 |

| | | | | | | | | | | | |
|---------------------------------|----|-----|---------------------------------|-------------|----|-------|----|--------|--------|-------------|--------|
| A001C0205_20210710141212_0001_1 | 3D | 120 | <i>Salpa fusiformis</i> | Linear | 9 | 1.50 | 15 | 10.685 | 5.114 | 5.43 | 31.44 |
| A001C0225_20210917231024_0001 | 3D | 120 | <i>Salpa fusiformis</i> | Linear | 9 | 1.50 | 7 | 9.448 | 4.298 | 2 | 47.47 |
| A001C0230_20210918220927_0001 | 3D | 120 | <i>Salpa fusiformis</i> | Linear | 5 | 0.83 | 27 | 8.428 | 4.307 | 4.25 | 69.08 |
| A001C0350_20210922221154_0001 | 3D | 120 | <i>Salpa fusiformis</i> | Linear | 9 | 1.50 | 16 | 21.126 | 7.991 | 2.2 | 55.35 |
| A002C0059_20220421230521_0001 | 3D | 60 | <i>Salpa fusiformis</i> | Linear | 12 | 4.01 | 21 | 18.078 | 7.499 | 2.44 | 91.67 |
| A002C0059_20220421230521_0001 | 3D | 60 | <i>Salpa fusiformis</i> | Linear | 12 | 4.01 | 21 | 18.078 | 7.499 | 2.17 | 91.67 |
| A002C0072_20220422223646_0001 | 3D | 60 | <i>Salpa fusiformis</i> | Linear | 9 | 3.00 | 17 | 27.564 | 14.766 | 3.75 | 43.57 |
| A002C0095_20220422231109_0001 | 3D | 60 | <i>Salpa fusiformis</i> | Linear | 9 | 3.01 | 4 | 24.133 | 10.177 | 2 | 27.09 |
| A001C0320_20210921215927_0001 | 3D | 120 | <i>Salpa maxima</i> | Linear | 8 | 1.33 | 2 | 48.129 | 30.804 | 1 | 71.99 |
| A002C0019_20220420225823_0001_1 | 3D | 60 | <i>Salpa maxima</i> | Linear | 11 | 3.67 | 2 | 68.311 | 34.78 | 0.5 | 74.01 |
| A002C0019_20220420225823_0001_2 | 3D | 60 | <i>Salpa maxima</i> | Linear | 8 | 2.67 | 2 | 68.311 | 34.78 | 0.5 | 47.55 |
| C0164 | 2D | 120 | <i>Salpa maxima</i> | Linear | 7 | 0.87 | 2 | NA | NA | NA | 30.03 |
| A001C0247_20210918223147_0001_2 | 3D | 120 | <i>Soestia zonaria</i> | Linear | 8 | 1.34 | 8 | 25.304 | 12.515 | 1.5 | 141.34 |
| A001C0252_20210918223920_0001 | 3D | 120 | <i>Soestia zonaria</i> | Linear | 9 | 1.50 | 8 | NA | NA | 1.14 | 142.34 |
| A001C0357_2021092222753_0001 | 3D | 120 | <i>Soestia zonaria</i> | Linear | 9 | 1.50 | 7 | 6.499 | 4.37 | 1.83 | 84.33 |
| GX010104 | 2D | 240 | <i>Soestia zonaria</i> | Linear | 8 | 0.50 | 20 | 9.162 | 3.417 | 3 | 68.68 |
| C0123_b | 2D | 30 | <i>Thalia</i> sp. | Oblique | 28 | 13.13 | 29 | 3.508 | 2.281 | 4.5 | 5.84 |
| A001C0341_20210921224426_0001 | 3D | 120 | <i>Pegea</i> sp. | Transversal | 7 | 1.75 | 20 | 31.186 | 11.264 | 1.9 | 15.88 |
| A001C0352_20210922221526_0001 | 3D | 120 | <i>Pegea</i> sp. | Transversal | 11 | 2.75 | 4 | 30.728 | 16.412 | 1.5 | 24.78 |
| C0066 | 2D | 30 | <i>Cyclosalpa affinis</i> | Whorl | 11 | 5.50 | 4 | 41.74 | 17.384 | 1.219512195 | 18.82 |
| c0165_b | 2D | 30 | <i>Cyclosalpa affinis</i> | Whorl | 4 | 2.00 | 6 | 24.178 | 8.754 | 1.5 | 30.11 |
| A001C0207_20210710141533_0001 | 3D | 120 | <i>Cyclosalpa bakeri</i> | Whorl | 9 | 2.50 | 4 | 8.44 | 4.664 | 2.38 | 11.86 |
| A001C0209_20210710141857_0001 | 3D | 120 | <i>Cyclosalpa bakeri</i> | Whorl | 9 | 1.50 | 4 | 8.702 | 3.699 | 2.63 | 11.49 |
| A001C0210_20210710142059_0001_1 | 3D | 120 | <i>Cyclosalpa bakeri</i> | Whorl | 9 | 1.50 | 6 | 4.519 | 2.036 | 4.33 | 10.46 |
| A001C0211_20210710142218_0001 | 3D | 120 | <i>Cyclosalpa bakeri</i> | Whorl | 9 | 1.50 | 6 | 4.297 | 2.552 | 2 | 6.83 |
| A001C0214_20210710142543_0001 | 3D | 120 | <i>Cyclosalpa bakeri</i> | Whorl | 9 | 1.50 | 6 | 10.659 | 4.358 | 3.45 | 11.08 |
| A001C0330_20210921221301_0001 | 3D | 120 | <i>Cyclosalpa bakeri</i> | Whorl | 11 | 1.84 | 11 | 8.057 | 3.892 | 2 | 8.73 |
| A002C0073_20220422223852_0001 | 3D | 60 | <i>Cyclosalpa bakeri</i> | Whorl | 7 | 3.50 | 13 | 4.545 | 2.311 | 1.64 | 12.49 |
| C0070 | 2D | 30 | <i>Cyclosalpa quadriluminis</i> | Whorl | 6 | 3.00 | 8 | 27.104 | 12.105 | 1.33 | 25.26 |

Table S2. Salp specimens used in the respirometry experiments with mean physiological attributes.

| Specimen | Species | Architecture | Experiment | Date | Activity level | Zoid length (mm) | Number of zooids | Colony volume (ml) | Container volume (ml) | Treatment | Timespan (min) | Temperature range (°C) | Gross respiration rate (mgO2/min) | Control rate (mgO2/min) | Net respiration rate (mgO2/min) | Biovolume-corrected gross respiration rate (pgCO2/min/ml) | Biovolume-corrected net respiration rate (pgCO2/min/ml) |
|--------------|---------------------------|--------------|------------|-----------|----------------|------------------|------------------|--------------------|-----------------------|--------------|----------------|------------------------|-----------------------------------|-------------------------|---------------------------------|---|---|
| 028-Bros-B-1 | <i>Brookzia rostrata</i> | Bipinnate | 15 | 6/27/2022 | Anesthetized | 8 | 9 | 0.5 | 208 | Anesthetized | 150 | 1.7 | 0.00012 | 0.00008 | 0.00005 | 277.12 | 104.02 |
| 035-Bros-B-1 | <i>Brookzia rostrata</i> | Bipinnate | 21 | 9/12/2022 | Anesthetized | 4 | 22 | 0.2 | 208 | Anesthetized | 200 | 5.1 | 0.00007 | 0.00012 | -0.00005 | 364.00 | -245.14 |
| 039-Bros-B-2 | <i>Brookzia rostrata</i> | Bipinnate | 23 | 9/14/2022 | Anesthetized | 4 | 12 | 0.2 | 208 | Anesthetized | 240 | 0.8 | 0.00020 | 0.00009 | 0.00011 | 1005.12 | 556.50 |
| 041-Bros-B-1 | <i>Brookzia rostrata</i> | Bipinnate | 24 | 9/15/2022 | Anesthetized | 11 | 37 | 11.5 | 208 | Anesthetized | 270 | 0.5 | -0.00011 | 0.00000 | -0.00011 | -9.52 | -9.65 |
| 011-BR-B-1 | <i>Brookzia rostrata</i> | Bipinnate | 6 | 9/22/2021 | Moderate | 10 | 14 | 7.4 | 208 | Intact | 295 | 2.3 | -0.00023 | -0.00002 | -0.00021 | -31.60 | -28.89 |
| 011-BR-B-2 | <i>Brookzia rostrata</i> | Bipinnate | 6 | 9/22/2021 | Moderate | 7.5 | 32 | 8.9 | 208 | Intact | 295 | 2.3 | -0.00029 | -0.00002 | -0.00027 | -31.98 | -29.73 |
| 015-BR-B-1 | <i>Brookzia rostrata</i> | Bipinnate | 8 | 4/19/2022 | Moderate | 10 | 8 | 0.8 | 208 | Intact | 123 | 1.5 | 0.00024 | 0.00010 | 0.00014 | 299.86 | 172.37 |
| 015-BR-B-2 | <i>Brookzia rostrata</i> | Bipinnate | 8 | 4/19/2022 | Moderate | 3 | 14 | 3.8 | 208 | Intact | 123 | 1.5 | 0.00040 | 0.00010 | 0.00030 | 106.39 | 79.28 |
| 021-BR-B-1 | <i>Brookzia rostrata</i> | Bipinnate | 11 | 4/22/2022 | Moderate | 4 | 14 | 0.2 | 208 | Intact | 150 | 1.2 | 0.00017 | 0.00006 | 0.00012 | 855.52 | 579.73 |
| 025-BR-B-1 | <i>Brookzia rostrata</i> | Bipinnate | 13 | 4/25/2022 | Moderate | 4 | 60 | 1.0 | 208 | Intact | 126 | 1.2 | 0.00019 | 0.00025 | -0.00007 | 187.34 | -67.12 |
| 031-Bros-B-1 | <i>Brookzia rostrata</i> | Bipinnate | 18 | 6/30/2022 | Moderate | 3 | 7 | 0.1 | 208 | Intact | 180 | 3.0 | 0.00005 | -0.00003 | 0.00008 | 520.00 | 802.86 |
| 07-BR-B-1 | <i>Brookzia rostrata</i> | Bipinnate | 4 | 9/20/2021 | Very active | 7 | 28 | 8.0 | 208 | Intact | 300 | NA | -0.00040 | -0.00009 | -0.00031 | -49.29 | -38.27 |
| 07-BR-B-2 | <i>Brookzia rostrata</i> | Bipinnate | 4 | 9/20/2021 | Very active | 8 | 24 | 7.9 | 208 | Intact | 300 | NA | -0.00047 | -0.00009 | -0.00038 | -59.17 | -48.00 |
| 07-BR-B-3 | <i>Brookzia rostrata</i> | Bipinnate | 4 | 9/20/2021 | Very active | 8 | 19 | 7.1 | 208 | Intact | 300 | NA | -0.00038 | -0.00009 | -0.00029 | -53.27 | -40.87 |
| 029-Bros-B-1 | <i>Brookzia rostrata</i> | Bipinnate | 16 | 6/28/2022 | Active | 6 | 8 | 0.2 | 208 | Paired | 120 | 2.2 | 0.00008 | 0.00006 | 0.00001 | 331.59 | 60.29 |
| 029-Bros-B-1 | <i>Brookzia rostrata</i> | Bipinnate | 16 | 6/28/2022 | Active | 6 | 8 | 0.2 | 208 | Paired | 90 | 0.2 | -0.00017 | -0.00002 | -0.00015 | -723.48 | -640.00 |
| 029-Bros-B-2 | <i>Brookzia rostrata</i> | Bipinnate | 16 | 6/28/2022 | Active | 7 | 17 | 1.1 | 208 | Paired | 120 | 2.2 | 0.00011 | 0.00006 | 0.00005 | 100.85 | 44.12 |
| 029-Bros-B-2 | <i>Brookzia rostrata</i> | Bipinnate | 16 | 6/28/2022 | Active | 7 | 17 | 1.1 | 208 | Paired | 90 | 0.2 | -0.00021 | -0.00002 | -0.00020 | -195.39 | -177.94 |
| 031-Caff-B-1 | <i>Cyclosalpa affinis</i> | Whorl | 18 | 6/30/2022 | Anesthetized | 32 | 8 | 5.5 | 208 | Anesthetized | 180 | 3.0 | -0.00068 | -0.00003 | -0.00065 | -122.91 | -117.77 |
| 031-Caff-B-2 | <i>Cyclosalpa affinis</i> | Whorl | 18 | 6/30/2022 | Anesthetized | 32 | 6 | 8.0 | 208 | Anesthetized | 180 | 3.0 | -0.00073 | -0.00003 | -0.00070 | -90.69 | -87.15 |
| 011-CA-B-1 | <i>Cyclosalpa affinis</i> | Whorl | 6 | 9/22/2021 | Active | 45 | 6 | 24.3 | 208 | Intact | 295 | 2.3 | -0.00275 | -0.00002 | -0.00273 | -113.22 | -112.40 |
| 013-CA-B-1 | <i>Cyclosalpa affinis</i> | Whorl | 7 | 9/23/2021 | Active | 35 | 6 | 19.1 | 208 | Intact | 30 | 2.0 | -0.00208 | 0.00010 | -0.00218 | -108.78 | -113.80 |
| 013-CA-B-2 | <i>Cyclosalpa affinis</i> | Whorl | 7 | 9/23/2021 | Active | 35 | 6 | 19.1 | 208 | Intact | 105 | 0.8 | -0.00188 | -0.00025 | -0.00163 | -98.49 | -85.46 |
| 013-CA-B-3 | <i>Cyclosalpa affinis</i> | Whorl | 7 | 9/23/2021 | Active | 35 | 6 | 19.1 | 208 | Intact | 156 | 1.6 | -0.00137 | -0.00006 | -0.00131 | -71.51 | -68.28 |
| 015-Caff-B-1 | <i>Cyclosalpa affinis</i> | Whorl | 8 | 4/19/2022 | Active | 50 | 6 | 42.0 | 208 | Intact | 123 | 1.5 | -0.00694 | 0.00010 | -0.00704 | -165.15 | -167.58 |
| 017-Caff-B-1 | <i>Cyclosalpa affinis</i> | Whorl | 9 | 4/20/2022 | Moderate | 35 | 11 | 27.5 | 208 | Intact | 120 | 1.4 | -0.00467 | 0.00009 | -0.00476 | -169.74 | -173.09 |
| 017-Caff-B-2 | <i>Cyclosalpa affinis</i> | Whorl | 9 | 4/20/2022 | Active | 40 | 8 | 48.0 | 980 | Intact | 120 | 1.4 | -0.00379 | 0.00009 | -0.00389 | -79.06 | -80.98 |
| 07-CA-B-1 | <i>Cyclosalpa affinis</i> | Whorl | 4 | 9/20/2021 | Moderate | 40 | 4 | 21.4 | 208 | Intact | 300 | NA | -0.00246 | -0.00009 | -0.00237 | -114.72 | -110.57 |
| 032-Chak-B-1 | <i>Cyclosalpa bakeri</i> | Whorl | 19 | 7/1/2022 | Anesthetized | 12 | 5 | 1.3 | 208 | Anesthetized | 180 | 3.1 | 0.00020 | 0.00007 | 0.00013 | 150.48 | 97.73 |
| 039-Chak-B-1 | <i>Cyclosalpa bakeri</i> | Whorl | 23 | 9/14/2022 | Anesthetized | 9 | 4 | 0.2 | 208 | Anesthetized | 240 | 0.8 | 0.00019 | 0.00009 | 0.00010 | 968.82 | 520.20 |
| 019-Chak-B-1 | <i>Cyclosalpa bakeri</i> | Whorl | 10 | 4/21/2022 | Moderate | 12 | 6 | 3.6 | 208 | Intact | 120 | 1.2 | -0.00003 | 0.00026 | -0.00030 | -9.52 | -82.25 |

| | | | | | | | | | | | | | | | | | |
|--------------|---------------------------------|---------|----|------------|--------------|----|----|------|-----|--------------|-----|-----|----------|----------|----------|---------|---------|
| 037-Cbak-B-1 | <i>Cyclospala bakeri</i> | Whorl | 22 | 9/13/2022 | Low | 10 | 8 | 1.5 | 208 | Intact | 180 | 0.3 | -0.00014 | 0.00000 | -0.00014 | -91.02 | -93.65 |
| 044-Cbak-B-1 | <i>Cyclospala bakeri</i> | Whorl | 27 | 05/06/2023 | Moderate | 20 | 9 | 7.0 | 208 | Paired | 264 | 2.3 | -0.00063 | -0.00004 | -0.00059 | -90.69 | -84.52 |
| 044-Cbak-B-1 | <i>Cyclospala bakeri</i> | Whorl | 27 | 05/06/2023 | Moderate | 20 | 9 | 7.0 | 208 | Paired | 155 | 0.7 | -0.00004 | 0.00007 | -0.00011 | -5.80 | -15.69 |
| 044-Cbak-B-2 | <i>Cyclospala bakeri</i> | Whorl | 27 | 05/06/2023 | Moderate | 17 | 11 | 5.1 | 208 | Paired | 264 | 2.3 | -0.00058 | -0.00004 | -0.00054 | -114.15 | -105.68 |
| 044-Cbak-B-2 | <i>Cyclospala bakeri</i> | Whorl | 27 | 05/06/2023 | Moderate | 17 | 11 | 5.1 | 208 | Paired | 155 | 0.7 | -0.00004 | 0.00007 | -0.00011 | -8.22 | -21.80 |
| 044-Cbak-B-3 | <i>Cyclospala bakeri</i> | Whorl | 27 | 05/06/2023 | Moderate | 22 | 5 | 2.0 | 208 | Paired | 264 | 2.3 | -0.00047 | -0.00004 | -0.00043 | -237.16 | -215.58 |
| 044-Cbak-B-3 | <i>Cyclospala bakeri</i> | Whorl | 27 | 05/06/2023 | Moderate | 22 | 5 | 2.0 | 208 | Paired | 155 | 0.7 | -0.00003 | 0.00007 | -0.00010 | -14.67 | -49.30 |
| 044-Cpol-B-1 | <i>Cyclospala polae</i> | Cluster | 27 | 05/06/2023 | Anesthetized | 23 | 7 | 9.0 | 980 | Anesthetized | 352 | 2.3 | -0.00038 | -0.00003 | -0.00034 | -41.69 | -38.12 |
| 032-Cpol-B-1 | <i>Cyclospala polae</i> | Cluster | 19 | 7/1/2022 | Low | 28 | 13 | 6.0 | 980 | Intact | 180 | 3.1 | -0.00094 | 0.00007 | -0.00101 | -157.50 | -168.93 |
| 048-Cpol-B-1 | <i>Cyclospala polae</i> | Cluster | 29 | 05/08/2023 | Moderate | 21 | 1 | 1.0 | 208 | Paired | 147 | 2.1 | -0.00010 | 0.00057 | -0.00066 | -95.55 | -662.51 |
| 048-Cpol-B-1 | <i>Cyclospala polae</i> | Cluster | 29 | 05/08/2023 | Moderate | 21 | 1 | 1.0 | 208 | Paired | 103 | 0.6 | 0.00026 | 0.00067 | -0.00040 | 263.60 | -402.33 |
| 050-Cpol-B-1 | <i>Cyclospala polae</i> | Cluster | 30 | 05/09/2023 | Moderate | 17 | 4 | 2.3 | 208 | Paired | 200 | 1.6 | -0.00040 | 0.00064 | -0.00104 | -175.47 | -454.11 |
| 050-Cpol-B-1 | <i>Cyclospala polae</i> | Cluster | 30 | 05/09/2023 | Moderate | 17 | 4 | 2.3 | 208 | Paired | 97 | 0.6 | 0.00010 | 0.00094 | -0.00084 | 44.46 | -363.55 |
| 050-Cpol-B-2 | <i>Cyclospala polae</i> | Cluster | 30 | 05/09/2023 | Low | 25 | 6 | 7.6 | 490 | Paired | 200 | 1.6 | -0.00132 | 0.00064 | -0.00196 | -173.30 | -257.62 |
| 050-Cpol-B-2 | <i>Cyclospala polae</i> | Cluster | 30 | 05/09/2023 | Low | 25 | 6 | 7.6 | 490 | Paired | 97 | 0.6 | -0.00060 | 0.00094 | -0.00154 | -79.43 | -202.90 |
| 052-Cpol-B-1 | <i>Cyclospala polae</i> | Cluster | 31 | 05/10/2023 | Moderate | 12 | 8 | 2.1 | 208 | Paired | 157 | 1.5 | -0.00038 | 0.00036 | -0.00074 | -181.94 | -352.24 |
| 052-Cpol-B-1 | <i>Cyclospala polae</i> | Cluster | 31 | 05/10/2023 | Moderate | 12 | 8 | 2.1 | 208 | Paired | 137 | 0.7 | 0.00005 | 0.00052 | -0.00047 | 23.54 | -224.43 |
| 053-Cpol-B-1 | <i>Cyclospala polae</i> | Cluster | 31 | 05/10/2023 | Low | 14 | 10 | 1.8 | 208 | Paired | 138 | 1.9 | -0.00026 | 0.00009 | -0.00036 | -146.33 | -197.99 |
| 053-Cpol-B-1 | <i>Cyclospala polae</i> | Cluster | 31 | 05/10/2023 | Low | 14 | 10 | 1.8 | 208 | Paired | 122 | 0.6 | -0.00015 | 0.00008 | -0.00023 | -82.84 | -129.00 |
| 031-Cqua-B-1 | <i>Cyclospala quadriluminis</i> | Whorl | 18 | 6/30/2022 | Anesthetized | 13 | 16 | 2.8 | 208 | Anesthetized | 180 | 3.0 | -0.00027 | -0.00003 | -0.00024 | -96.39 | -86.29 |
| 042-Cqua-B-1 | <i>Cyclospala quadriluminis</i> | Whorl | 25 | 9/16/2022 | Anesthetized | 28 | 5 | 28.0 | 208 | Anesthetized | 424 | 1.0 | -0.00111 | -0.00005 | -0.00105 | -39.49 | -37.67 |
| 025-Cqua-B-1 | <i>Cyclospala quadriluminis</i> | Whorl | 13 | 4/25/2022 | Moderate | 25 | 4 | 4.0 | 208 | Intact | 126 | 1.2 | -0.00060 | 0.00025 | -0.00085 | -148.82 | -212.43 |
| 041-Cqua-B-1 | <i>Cyclospala quadriluminis</i> | Whorl | 24 | 9/15/2022 | Moderate | 17 | 11 | 5.5 | 208 | Intact | 270 | 0.5 | -0.00110 | 0.00000 | -0.00110 | -199.57 | -199.85 |
| 045-Cqua-B-1 | <i>Cyclospala quadriluminis</i> | Whorl | 27 | 05/06/2023 | Active | 35 | 6 | 15.0 | 490 | Intact | 228 | 1.4 | -0.00495 | -0.00029 | -0.00466 | -330.02 | -310.82 |
| 051-Cqua-B-1 | <i>Cyclospala quadriluminis</i> | Whorl | 30 | 05/09/2023 | Anesthetized | 29 | 8 | 21.0 | 490 | Paired | 187 | 1.2 | -0.00088 | 0.00005 | -0.00093 | -41.91 | -44.24 |
| 028-Csew-B-1 | <i>Cyclospala sewelli</i> | Cluster | 15 | 6/27/2022 | Anesthetized | 12 | 10 | 2.4 | 208 | Anesthetized | 150 | 1.7 | 0.00001 | 0.00008 | -0.00007 | 2.96 | -29.50 |
| 028-Csew-B-2 | <i>Cyclospala sewelli</i> | Cluster | 15 | 6/27/2022 | Anesthetized | 8 | 16 | 2.5 | 208 | Anesthetized | 150 | 1.7 | 0.00000 | 0.00008 | -0.00008 | 0.57 | -30.59 |
| 039-Csew-B-1 | <i>Cyclospala sewelli</i> | Cluster | 23 | 9/14/2022 | Anesthetized | 9 | 15 | 1.3 | 208 | Anesthetized | 240 | 0.8 | 0.00013 | 0.00009 | 0.00004 | 100.58 | 31.56 |
| 015-CPol-B-1 | <i>Cyclospala sewelli</i> | Cluster | 8 | 4/19/2022 | Moderate | 15 | 7 | 4.4 | 208 | Intact | 123 | 1.5 | -0.00004 | 0.00010 | -0.00014 | -9.75 | -32.93 |
| 023-Cpol-B-1 | <i>Cyclospala sewelli</i> | Cluster | 12 | 4/24/2022 | Moderate | 35 | 1 | 2.4 | 208 | Intact | 123 | 1.1 | -0.00025 | 0.00007 | -0.00032 | -102.22 | -133.20 |
| 04-Csew-B-1 | <i>Cyclospala sewelli</i> | Cluster | 2 | 9/19/2021 | Low | 20 | 1 | 10.5 | 208 | Intact | 60 | NA | -0.00001 | 0.00049 | -0.00050 | -1.32 | -47.35 |
| 09-Csew-B-1 | <i>Cyclospala sewelli</i> | Cluster | 5 | 9/21/2021 | Moderate | 25 | 4 | 13.6 | 208 | Intact | 360 | 1.6 | -0.00057 | -0.00006 | -0.00051 | -42.01 | -37.36 |

| | | | | | | | | | | | | | | | | | |
|---------------|-----------------------------|-------------|----|------------|--------------|----|----|------|-----|--------------|-----|-----|----------|----------|----------|----------|----------|
| 09-Cæw-B-2 | <i>Cyclospala sewelli</i> | Cluster | 5 | 9/21/2021 | Moderate | 25 | 6 | 13.9 | 208 | Intact | 360 | 1.6 | -0.00069 | -0.00006 | -0.00062 | -49.20 | -44.65 |
| 09-Cæw-B-3 | <i>Cyclospala sewelli</i> | Cluster | 5 | 9/21/2021 | Moderate | 20 | 2 | 10.7 | 208 | Intact | 360 | 1.6 | -0.00027 | -0.00006 | -0.00021 | -25.47 | -19.55 |
| 09-Cæw-B-4 | <i>Cyclospala sewelli</i> | Cluster | 5 | 9/21/2021 | Moderate | 25 | 1 | 13.1 | 208 | Intact | 360 | 1.6 | -0.00025 | -0.00006 | -0.00018 | -18.86 | -14.04 |
| 09-Cæw-B-1 | <i>Cyclospala sewelli</i> | Cluster | 16 | 6/28/2022 | Moderate | 19 | 5 | 4.5 | 208 | Paired | 120 | 2.2 | -0.00028 | 0.00006 | -0.00034 | -61.63 | -75.50 |
| 09-Cæw-B-1 | <i>Cyclospala sewelli</i> | Cluster | 16 | 6/28/2022 | Moderate | 19 | 5 | 4.5 | 208 | Paired | 90 | 0.2 | -0.00033 | -0.00002 | -0.00031 | -72.41 | -68.15 |
| 043-Hvir-B-1 | <i>Helicosalpa virgula</i> | Helical | 26 | 9/16/2022 | Moderate | 12 | 68 | 13.0 | 980 | Intact | 312 | 0.5 | -0.00328 | -0.00004 | -0.00324 | -252.24 | -249.06 |
| 054-Hvir-B-1 | <i>Helicosalpa virgula</i> | Helical | 31 | 05/10/2023 | Moderate | 16 | 64 | 16.5 | 980 | Paired | 138 | 1.9 | -0.00401 | 0.00009 | -0.00410 | -242.74 | -248.37 |
| 054-Hvir-B-1 | <i>Helicosalpa virgula</i> | Helical | 31 | 05/10/2023 | Moderate | 16 | 64 | 16.5 | 980 | Paired | 122 | 0.6 | -0.00061 | 0.00008 | -0.00069 | -36.93 | -41.97 |
| 030-Icyl-B-1 | <i>Iasis cylindrica</i> | Linear | 17 | 6/29/2022 | Anesthetized | 11 | 9 | 12.0 | 208 | Anesthetized | 142 | 0.9 | -0.00007 | 0.00002 | -0.00009 | -6.06 | -7.34 |
| 032-Icyl-B-1 | <i>Iasis cylindrica</i> | Linear | 19 | 7/1/2022 | Anesthetized | 6 | 26 | 0.1 | 208 | Anesthetized | 180 | 3.1 | 0.00013 | 0.00007 | 0.00006 | 1312.38 | 626.67 |
| 033-Icyl-B-1 | <i>Iasis cylindrica</i> | Linear | 20 | 9/11/2022 | Anesthetized | 6 | 11 | 0.3 | 208 | Anesthetized | 180 | 1.8 | 0.00016 | 0.00025 | -0.00009 | 533.71 | -303.83 |
| 011-WC-B-1 | <i>Iasis cylindrica</i> | Linear | 6 | 9/22/2021 | Very active | 15 | 12 | 9.7 | 208 | Intact | 295 | 2.3 | -0.00113 | -0.00002 | -0.00111 | -116.62 | -114.55 |
| 014-WC-B-1A | <i>Iasis cylindrica</i> | Linear | 7 | 9/23/2021 | Very active | 10 | 20 | 8.3 | 208 | Intact | 246 | 3.9 | -0.00141 | -0.00014 | -0.00127 | -168.66 | -152.14 |
| 014-WC-B-1B | <i>Iasis cylindrica</i> | Linear | 7 | 9/23/2021 | Very active | 10 | 28 | 9.6 | 208 | Intact | 246 | 3.9 | -0.00213 | -0.00014 | -0.00199 | -221.66 | -207.31 |
| 014-WC-B-2 | <i>Iasis cylindrica</i> | Linear | 7 | 9/23/2021 | Very active | 10 | 34 | 10.5 | 208 | Intact | 30 | 2.0 | -0.00312 | 0.00010 | -0.00322 | -295.85 | -304.95 |
| 014-WC-B-3 | <i>Iasis cylindrica</i> | Linear | 7 | 9/23/2021 | Very active | 10 | 34 | 10.5 | 208 | Intact | 105 | 0.8 | -0.00261 | -0.00025 | -0.00236 | -247.82 | -224.19 |
| 014-WC-B-4 | <i>Iasis cylindrica</i> | Linear | 7 | 9/23/2021 | Very active | 10 | 34 | 10.5 | 208 | Intact | 156 | 1.6 | -0.00184 | -0.00006 | -0.00178 | -174.65 | -168.79 |
| 021-Icyl-B-1 | <i>Iasis cylindrica</i> | Linear | 11 | 4/22/2022 | Moderate | 7 | 21 | 1.3 | 208 | Intact | 150 | 1.2 | -0.00016 | 0.00006 | -0.00021 | -121.33 | -163.75 |
| 021-Icyl-B-2A | <i>Iasis cylindrica</i> | Linear | 11 | 4/22/2022 | Very active | 15 | 28 | 6.0 | 980 | Intact | 150 | 1.2 | -0.00173 | 0.00006 | -0.00179 | -289.10 | -298.29 |
| 021-Icyl-B-2B | <i>Iasis cylindrica</i> | Linear | 11 | 4/22/2022 | Very active | 15 | 15 | 3.0 | 980 | Intact | 150 | 1.2 | -0.00011 | 0.00006 | -0.00016 | -36.30 | -54.68 |
| 023-Icyl-B-1 | <i>Iasis cylindrica</i> | Linear | 12 | 4/24/2022 | Active | 15 | 44 | 14.1 | 980 | Intact | 123 | 1.1 | -0.00318 | 0.00007 | -0.00326 | -225.69 | -230.96 |
| 032-Icyl-B-2 | <i>Iasis cylindrica</i> | Linear | 19 | 7/1/2022 | Active | 7 | 76 | 0.5 | 208 | Intact | 180 | 3.1 | -0.00064 | 0.00007 | -0.00071 | -1277.71 | -1414.86 |
| 041-Icyl-B-1 | <i>Iasis cylindrica</i> | Linear | 24 | 9/15/2022 | Active | 10 | 10 | 1.5 | 208 | Paired | 105 | 0.2 | -0.00055 | 0.00004 | -0.00059 | -367.28 | -395.82 |
| 041-Icyl-B-1 | <i>Iasis cylindrica</i> | Linear | 24 | 9/15/2022 | Active | 10 | 10 | 1.5 | 208 | Paired | 115 | 0.2 | -0.00030 | -0.00001 | -0.00029 | -199.35 | -190.74 |
| 048-Ipun-B-1 | <i>Ihlea punctata</i> | Linear | 29 | 05/08/2023 | Moderate | 12 | 68 | 3.7 | 980 | Paired | 147 | 2.1 | -0.00521 | 0.00057 | -0.00578 | -1407.69 | -1560.92 |
| 048-Ipun-B-1 | <i>Ihlea punctata</i> | Linear | 29 | 05/08/2023 | Moderate | 12 | 68 | 3.7 | 980 | Paired | 103 | 0.6 | 0.00035 | 0.00067 | -0.00032 | 94.70 | -85.28 |
| 039-Mhex-B-1 | <i>Metcalflina hexagona</i> | Linear | 23 | 9/14/2022 | Anesthetized | 28 | 16 | 22.0 | 980 | Anesthetized | 240 | 0.8 | -0.00104 | 0.00077 | -0.00180 | -47.07 | -81.93 |
| 027-Pcon-B-1 | <i>Pegea sp.</i> | Transversal | 14 | 6/26/2022 | Anesthetized | 28 | 2 | 3.5 | 208 | Anesthetized | 120 | 2.0 | -0.00006 | 0.00004 | -0.00010 | -18.15 | -28.70 |
| 030-Pco-B-1 | <i>Pegea sp.</i> | Transversal | 17 | 6/29/2022 | Anesthetized | 36 | 5 | 15.0 | 980 | Anesthetized | 142 | 0.9 | 0.00021 | 0.00002 | 0.00020 | 14.32 | 13.30 |
| 035-Pcon-B-1 | <i>Pegea sp.</i> | Transversal | 21 | 9/12/2022 | Anesthetized | 35 | 8 | 23.0 | 980 | Anesthetized | 200 | 5.1 | -0.00153 | 0.00012 | -0.00165 | -66.65 | -71.95 |
| 037-Pcon-B-1 | <i>Pegea sp.</i> | Transversal | 22 | 9/13/2022 | Anesthetized | 60 | 12 | 80.0 | 980 | Anesthetized | 180 | 0.3 | -0.00920 | 0.00003 | -0.00923 | -115.01 | -115.42 |
| 019-Pso-B-1 | <i>Pegea sp.</i> | Transversal | 10 | 4/21/2022 | Moderate | 80 | 5 | 65.0 | 980 | Intact | 120 | 1.2 | -0.01312 | 0.00026 | -0.01338 | -201.78 | -205.81 |
| 019-Pso-B-2 | <i>Pegea sp.</i> | Transversal | 10 | 4/21/2022 | Moderate | 65 | 5 | 50.0 | 980 | Intact | 120 | 1.2 | -0.01116 | 0.00026 | -0.01142 | -223.24 | -228.48 |
| 019-Pso-B-3 | <i>Pegea sp.</i> | Transversal | 10 | 4/21/2022 | Moderate | 65 | 1 | 18.0 | 208 | Intact | 120 | 1.2 | -0.00168 | 0.00026 | -0.00195 | -93.56 | -108.10 |
| 023-Pso-B-1 | <i>Pegea sp.</i> | Transversal | 12 | 4/24/2022 | Moderate | 30 | 22 | 44.0 | 980 | Intact | 123 | 1.1 | -0.00704 | 0.00007 | -0.00712 | -160.07 | -161.76 |

| 025-Pso-B-1 | <i>Pegea</i> sp. | Transversal | 13 | 4/25/2022 | Active | 42 | 7 | 35.0 | 980 | Intact | 126 | 1.2 | -0.00269 | 0.00176 | -0.00444 | -76.73 | -126.97 |
|--------------|--------------------------------|-------------|----|------------|--------------|----|----|------|-----|--------------|-----|-----|----------|----------|----------|---------|---------|
| 031-Pcon-B-2 | <i>Pegea</i> sp. | Transversal | 18 | 6/30/2022 | Moderate | 41 | 3 | 9.0 | 980 | Intact | 180 | 3.0 | -0.00115 | -0.00003 | -0.00113 | -128.33 | -125.19 |
| 05-PC-B-1 | <i>Pegea</i> sp. | Transversal | 3 | 9/19/2021 | Moderate | 25 | 5 | 13.8 | 208 | Intact | 259 | NA | -0.00042 | -0.00001 | -0.00042 | -30.76 | -30.39 |
| 046-Psp-B-1 | <i>Pegea</i> sp. | Transversal | 28 | 05/07/2023 | Moderate | 12 | 87 | 4.9 | 490 | Paired | 243 | 1.3 | -0.00170 | 0.00015 | -0.00185 | -347.02 | -377.14 |
| 046-Psp-B-1 | <i>Pegea</i> sp. | Transversal | 28 | 05/07/2023 | Moderate | 12 | 87 | 4.9 | 490 | Paired | 74 | 0.4 | -0.00073 | 0.00017 | -0.00090 | -149.42 | -184.55 |
| 052-Psp-B-1 | <i>Pegea</i> sp. | Transversal | 31 | 05/10/2023 | Low | 43 | 8 | 18.0 | 980 | Paired | 157 | 1.5 | -0.00561 | 0.00036 | -0.00597 | -311.81 | -331.67 |
| 052-Psp-B-1 | <i>Pegea</i> sp. | Transversal | 31 | 05/10/2023 | Low | 43 | 8 | 18.0 | 980 | Paired | 137 | 0.7 | 0.00015 | 0.00052 | -0.00037 | 8.11 | -20.82 |
| 030-Ramb-B-1 | <i>Ritteriella amboinensis</i> | Bipinnate | 17 | 6/29/2022 | Anesthetized | 18 | 3 | 1.5 | 208 | Anesthetized | 142 | 0.9 | 0.00010 | 0.00002 | 0.00008 | 66.31 | 56.09 |
| 030-Ramb-B-2 | <i>Ritteriella amboinensis</i> | Bipinnate | 17 | 6/29/2022 | Anesthetized | 15 | 5 | 0.8 | 208 | Anesthetized | 142 | 0.9 | 0.00010 | 0.00002 | 0.00008 | 124.46 | 105.29 |
| 030-Ramb-B-4 | <i>Ritteriella amboinensis</i> | Bipinnate | 17 | 6/29/2022 | Anesthetized | 22 | 38 | 6.3 | 980 | Anesthetized | 142 | 0.9 | -0.00036 | 0.00002 | -0.00037 | -56.69 | -59.13 |
| 023-Ramb-B-1 | <i>Ritteriella amboinensis</i> | Bipinnate | 12 | 4/24/2022 | Moderate | 40 | 23 | 40.0 | 208 | Intact | 123 | 1.1 | -0.00164 | 0.00007 | -0.00171 | -40.95 | -42.81 |
| 027-Ramb-B-1 | <i>Ritteriella amboinensis</i> | Bipinnate | 14 | 6/26/2022 | Moderate | 28 | 10 | 3.5 | 208 | Intact | 120 | 2.0 | -0.00009 | 0.00004 | -0.00012 | -24.44 | -34.99 |
| 027-Ramb-B-2 | <i>Ritteriella amboinensis</i> | Bipinnate | 14 | 6/26/2022 | Moderate | 15 | 5 | 2.5 | 208 | Intact | 120 | 2.0 | -0.00003 | 0.00004 | -0.00006 | -10.79 | -25.57 |
| 030-Ramb-B-3 | <i>Ritteriella amboinensis</i> | Bipinnate | 17 | 6/29/2022 | Moderate | 17 | 5 | 1.4 | 208 | Intact | 142 | 0.9 | -0.00002 | 0.00002 | -0.00004 | -17.68 | -28.64 |
| 047-Rret-B-1 | <i>Ritteriella retracta</i> | Bipinnate | 28 | 05/07/2023 | Moderate | 31 | 2 | 1.2 | 208 | Paired | 133 | 0.6 | -0.00095 | -0.00134 | 0.00039 | -789.91 | 323.08 |
| 047-Rret-B-1 | <i>Ritteriella retracta</i> | Bipinnate | 28 | 05/07/2023 | Moderate | 31 | 2 | 1.2 | 208 | Paired | 115 | 0.4 | -0.00012 | -0.00051 | 0.00039 | -95.94 | 328.64 |
| 050-Rret-B-1 | <i>Ritteriella retracta</i> | Bipinnate | 30 | 05/09/2023 | Low | 31 | 8 | 7.8 | 980 | Paired | 200 | 1.6 | -0.00161 | 0.00064 | -0.00225 | -205.81 | -287.97 |
| 050-Rret-B-1 | <i>Ritteriella retracta</i> | Bipinnate | 30 | 05/09/2023 | Low | 31 | 8 | 7.8 | 980 | Paired | 97 | 0.6 | 0.00063 | 0.00094 | -0.00030 | 81.28 | -39.03 |
| 022-Rsp-B-1 | <i>Ritteriella retracta</i> | Bipinnate | 20 | 9/11/2022 | Anesthetized | 25 | 25 | 11.0 | 980 | Anesthetized | 180 | 1.8 | -0.00026 | 0.00025 | -0.00051 | -23.75 | -46.59 |
| 037-Rsp-B-1 | <i>Ritteriella retracta</i> | Bipinnate | 22 | 9/13/2022 | Anesthetized | 57 | 8 | 63.0 | 980 | Anesthetized | 180 | 0.3 | -0.00456 | 0.00003 | -0.00460 | -72.43 | -72.95 |
| 025-Rsp-B-1 | <i>Ritteriella retracta</i> | Bipinnate | 21 | 9/12/2022 | Moderate | 33 | 14 | 18.2 | 980 | Intact | 200 | 5.1 | -0.00216 | 0.00010 | -0.00225 | -118.46 | -123.69 |
| 032-Rsp-B-1 | <i>Ritteriella retracta</i> | Bipinnate | 19 | 7/1/2022 | Moderate | 30 | 55 | 34.0 | 980 | Intact | 180 | 3.1 | -0.01511 | 0.00007 | -0.01518 | -444.36 | -446.38 |
| 028-Sasp-B-2 | <i>Salpa aspera</i> | Linear | 15 | 6/27/2022 | Anesthetized | 22 | 57 | 16.5 | 980 | Anesthetized | 150 | 1.7 | -0.00152 | 0.00008 | -0.00159 | -91.90 | -96.62 |
| 032-Sasp-B-1 | <i>Salpa aspera</i> | Linear | 19 | 7/1/2022 | Anesthetized | 28 | 9 | 6.0 | 208 | Anesthetized | 180 | 3.1 | -0.00104 | 0.00007 | -0.00111 | -174.16 | -185.59 |
| 027-Sasp-B-1 | <i>Salpa aspera</i> | Linear | 14 | 6/26/2022 | Active | 45 | 3 | 8.0 | 980 | Intact | 120 | 2.0 | 0.00100 | 0.00004 | 0.00097 | 125.43 | 120.82 |
| 027-Sasp-B-2 | <i>Salpa aspera</i> | Linear | 14 | 6/26/2022 | Active | 39 | 13 | 15.5 | 980 | Intact | 120 | 2.0 | -0.00648 | 0.00004 | -0.00652 | -418.10 | -420.48 |
| 028-Sasp-B-1 | <i>Salpa aspera</i> | Linear | 15 | 6/27/2022 | Active | 20 | 10 | 3.3 | 208 | Intact | 150 | 1.7 | -0.00064 | 0.00008 | -0.00072 | -195.33 | -218.93 |
| 049-Sasp-B-1 | <i>Salpa aspera</i> | Linear | 29 | 05/08/2023 | Moderate | 38 | 5 | 5.4 | 980 | Paired | 135 | 1.7 | -0.00179 | 0.00034 | -0.00214 | -332.12 | -395.96 |
| 049-Sasp-B-1 | <i>Salpa aspera</i> | Linear | 29 | 05/08/2023 | Moderate | 38 | 5 | 5.4 | 980 | Paired | 70 | 0.5 | -0.00042 | 0.00014 | -0.00056 | -78.48 | -104.23 |
| 033-Sfus-B-1 | <i>Salpa fusiformis</i> | Linear | 20 | 9/11/2022 | Anesthetized | 28 | 3 | 1.0 | 208 | Anesthetized | 180 | 1.8 | 0.00017 | 0.00025 | -0.00008 | 166.95 | -84.31 |
| 035-Sfus-B-1 | <i>Salpa fusiformis</i> | Linear | 21 | 9/12/2022 | Anesthetized | 15 | 13 | 1.6 | 208 | Anesthetized | 200 | 5.1 | -0.00013 | 0.00012 | -0.00026 | -83.57 | -159.71 |
| 039-Sfus-B-1 | <i>Salpa fusiformis</i> | Linear | 23 | 9/14/2022 | Anesthetized | 13 | 16 | 1.0 | 208 | Anesthetized | 240 | 0.8 | 0.00011 | 0.00009 | 0.00002 | 111.99 | 22.27 |
| 027-Sfus-B-1 | <i>Salpa fusiformis</i> | Linear | 14 | 6/26/2022 | Moderate | 15 | 5 | 1.6 | 208 | Intact | 120 | 2.0 | -0.00006 | 0.00004 | -0.00009 | -35.03 | -58.11 |
| 028-Sfus-B-1 | <i>Salpa fusiformis</i> | Linear | 15 | 6/27/2022 | Active | 12 | 19 | 1.8 | 980 | Intact | 150 | 1.7 | 0.00035 | 0.00008 | 0.00027 | 192.01 | 148.73 |
| 033-Sfus-B-2 | <i>Salpa fusiformis</i> | Linear | 20 | 9/11/2022 | Moderate | 27 | 11 | 5.5 | 208 | Intact | 180 | 1.8 | -0.00104 | 0.00025 | -0.00129 | -188.46 | -234.15 |
| 053-Sfus-B-1 | <i>Salpa fusiformis</i> | Linear | 31 | 05/10/2023 | Active | 14 | 24 | 2.0 | 980 | Paired | 138 | 1.9 | -0.00024 | 0.00009 | -0.00034 | -122.15 | -168.65 |
| 053-Sfus-B-1 | <i>Salpa fusiformis</i> | Linear | 31 | 05/10/2023 | Active | 14 | 24 | 2.0 | 980 | Paired | 122 | 0.6 | 0.00002 | 0.00008 | -0.00007 | 8.81 | -32.73 |

| | | | | | | | | | | | | | | | | | |
|---------------|------------------------|---------|----|------------|--------------|-----|----|------|-----|--------------|-----|-----|----------|----------|----------|----------|----------|
| 029-Smax-B-1a | <i>Salpa maxima</i> | Linear | 16 | 6/28/2022 | Anesthetized | 115 | 3 | 55.0 | 980 | Anesthetized | 120 | 2.2 | -0.00268 | 0.00006 | -0.00274 | -48.70 | -49.84 |
| 037-Smax-B-1 | <i>Salpa maxima</i> | Linear | 22 | 9/13/2022 | Anesthetized | 70 | 1 | 7.0 | 208 | Anesthetized | 180 | 0.3 | 0.00099 | 0.00003 | 0.00096 | 141.67 | 137.02 |
| 041-Smax-B-1 | <i>Salpa maxima</i> | Linear | 24 | 9/15/2022 | Anesthetized | 65 | 3 | 17.0 | 980 | Anesthetized | 270 | 0.5 | -0.00264 | 0.00000 | -0.00264 | -155.19 | -155.28 |
| 045-Smax-B-1 | <i>Salpa maxima</i> | Linear | 27 | 05/06/2023 | Anesthetized | 47 | 9 | 18.0 | 980 | Anesthetized | 228 | 1.4 | -0.00212 | -0.00029 | -0.00183 | -117.64 | -101.65 |
| 031-Smax-B-2 | <i>Salpa maxima</i> | Linear | 18 | 6/30/2022 | Moderate | 80 | 3 | 20.0 | 980 | Intact | 180 | 3.0 | -0.00422 | -0.00003 | -0.00420 | -211.17 | -209.75 |
| 033-Smax-B-1 | <i>Salpa maxima</i> | Linear | 20 | 9/11/2022 | Moderate | 100 | 5 | 32.5 | 980 | Intact | 180 | 1.8 | -0.01118 | 0.00025 | -0.01143 | -343.97 | -351.70 |
| 041-Smax-B-2 | <i>Salpa maxima</i> | Linear | 24 | 9/15/2022 | Moderate | 110 | 1 | 20.0 | 980 | Intact | 270 | 0.5 | -0.00567 | 0.00000 | -0.00568 | -283.73 | -283.81 |
| 029-Smax-B-1b | <i>Salpa maxima</i> | Linear | 16 | 6/28/2022 | Active | 115 | 4 | 53.0 | 980 | Paired | 120 | 2.2 | -0.01375 | 0.00006 | -0.01382 | -259.48 | -260.66 |
| 029-Smax-B-1b | <i>Salpa maxima</i> | Linear | 16 | 6/28/2022 | Active | 115 | 4 | 53.0 | 980 | Paired | 90 | 0.2 | -0.00555 | -0.00002 | -0.00553 | -104.78 | -104.42 |
| 037-Szon-B-1 | <i>Soestia zonaria</i> | Linear | 22 | 9/13/2022 | Active | 21 | 9 | 5.4 | 208 | Intact | 0 | 0.0 | NA | NA | NA | NA | NA |
| 037-Szon-B-2 | <i>Soestia zonaria</i> | Linear | 22 | 9/13/2022 | Active | 21 | 9 | 5.4 | 208 | Intact | 0 | 0.0 | NA | NA | NA | NA | NA |
| 037-Szon-B-3 | <i>Soestia zonaria</i> | Linear | 22 | 9/13/2022 | Active | 21 | 9 | 5.4 | 208 | Intact | 0 | 0.0 | NA | NA | NA | NA | NA |
| 037-Szon-B-4 | <i>Soestia zonaria</i> | Linear | 22 | 9/13/2022 | Active | 21 | 9 | 5.4 | 208 | Intact | 0 | 0.0 | NA | NA | NA | NA | NA |
| 037-Szon-B-5 | <i>Soestia zonaria</i> | Linear | 22 | 9/13/2022 | Active | 21 | 9 | 5.4 | 208 | Intact | 0 | 0.0 | NA | NA | NA | NA | NA |
| 037-Szon-B-6 | <i>Soestia zonaria</i> | Linear | 22 | 9/13/2022 | Active | 21 | 9 | 5.4 | 208 | Intact | 0 | 0.0 | NA | NA | NA | NA | NA |
| 029-Szon-B-1 | <i>Soestia zonaria</i> | Linear | 16 | 6/28/2022 | Active | 7 | 9 | 0.7 | 208 | Paired | 120 | 2.2 | -0.00003 | 0.00006 | -0.00010 | -49.52 | -138.67 |
| 029-Szon-B-1 | <i>Soestia zonaria</i> | Linear | 16 | 6/28/2022 | Active | 7 | 9 | 0.7 | 208 | Paired | 90 | 0.2 | -0.00012 | -0.00002 | -0.00010 | -168.38 | -140.95 |
| 047-Szon-B-1 | <i>Soestia zonaria</i> | Linear | 28 | 05/07/2023 | Active | 24 | 10 | 4.0 | 490 | Paired | 133 | 0.6 | -0.00278 | -0.00134 | -0.00144 | -694.72 | -360.83 |
| 047-Szon-B-1 | <i>Soestia zonaria</i> | Linear | 28 | 05/07/2023 | Active | 24 | 10 | 4.0 | 490 | Paired | 115 | 0.4 | -0.00041 | -0.00051 | 0.00010 | -101.81 | 25.56 |
| 050-Tcic-B-1 | <i>Thalia cicar</i> | Oblique | 30 | 05/09/2023 | Low | 6 | 12 | 0.1 | 208 | Paired | 200 | 1.6 | -0.00028 | 0.00064 | -0.00092 | -2771.86 | -9180.62 |
| 050-Tcic-B-1 | <i>Thalia cicar</i> | Oblique | 30 | 05/09/2023 | Low | 6 | 12 | 0.1 | 208 | Paired | 97 | 0.6 | 0.00009 | 0.00094 | -0.00085 | 887.68 | -8496.46 |
| 053-Tcic-B-1 | <i>Thalia cicar</i> | Oblique | 31 | 05/10/2023 | Low | 6 | 37 | 0.3 | 208 | Paired | 138 | 1.9 | -0.00012 | 0.00009 | -0.00021 | -388.90 | -698.90 |
| 053-Tcic-B-1 | <i>Thalia cicar</i> | Oblique | 31 | 05/10/2023 | Low | 6 | 37 | 0.3 | 208 | Paired | 122 | 0.6 | -0.00003 | 0.00008 | -0.00011 | -99.76 | -376.74 |
| 042-Tlon-B-1 | <i>Thalia sp.</i> | Oblique | 25 | 9/16/2022 | Low | 9 | 7 | 0.8 | 208 | Intact | 424 | 1.0 | -0.00005 | -0.00005 | 0.00000 | -59.23 | 4.47 |
| 046-Tlon-B-1 | <i>Thalia sp.</i> | Oblique | 28 | 05/07/2023 | Low | 5 | 20 | 0.3 | 208 | Paired | 243 | 1.3 | -0.00011 | 0.00015 | -0.00026 | -379.87 | -871.81 |
| 046-Tlon-B-1 | <i>Thalia sp.</i> | Oblique | 28 | 05/07/2023 | Low | 5 | 20 | 0.3 | 208 | Paired | 74 | 0.4 | -0.00000 | 0.00017 | -0.00017 | -0.00 | -573.79 |
| 046-Tlon-B-2 | <i>Thalia sp.</i> | Oblique | 28 | 05/07/2023 | Low | 4 | 20 | 0.2 | 208 | Paired | 243 | 1.3 | -0.00004 | 0.00015 | -0.00018 | -178.77 | -916.69 |
| 046-Tlon-B-2 | <i>Thalia sp.</i> | Oblique | 28 | 05/07/2023 | Low | 4 | 20 | 0.2 | 208 | Paired | 74 | 0.4 | -0.00008 | 0.00017 | -0.00025 | -390.38 | -1251.06 |
| 048-Tlon-B-1 | <i>Thalia sp.</i> | Oblique | 29 | 05/08/2023 | Low | 5 | 19 | 0.3 | 208 | Paired | 147 | 2.1 | 0.00007 | 0.00057 | -0.00050 | 228.56 | -1661.29 |
| 048-Tlon-B-1 | <i>Thalia sp.</i> | Oblique | 29 | 05/08/2023 | Low | 5 | 19 | 0.3 | 208 | Paired | 103 | 0.6 | 0.00036 | 0.00067 | -0.00030 | 1216.12 | -1003.64 |
| 049-Tlon-B-1 | <i>Thalia sp.</i> | Oblique | 29 | 05/08/2023 | Low | 6 | 15 | 0.3 | 208 | Paired | 135 | 1.7 | 0.00009 | 0.00034 | -0.00025 | 308.97 | -840.09 |
| 049-Tlon-B-1 | <i>Thalia sp.</i> | Oblique | 29 | 05/08/2023 | Low | 6 | 15 | 0.3 | 208 | Paired | 70 | 0.5 | 0.00003 | 0.00014 | -0.00011 | 93.69 | -369.82 |

Table S3. Summary of numbers of specimens, number of measurements, and descriptive variable averages per species including both the video speed data and the respiration experiments data.

| Species | Architecture | Speed Measurements from Videos | | | | | | Respiration Measurements from Experiments | | | | |
|---------------------------------|--------------|--------------------------------|-----------------------|--------------------------------|----------------------------|---------------------|------------------------|---|-----------------------|-------------------------|---------------------|------------------------|
| | | Mean Number of zooids | Mean zoid length (mm) | Mean Pulsation rate (pulses/s) | Mean swimming speed (mm/s) | Number of Specimens | Number of Measurements | Mean Number of zooids | Mean zoid length (mm) | Mean Colony volume (ml) | Number of Specimens | Number of Measurements |
| <i>Brookia rostrata</i> | Bipinnate | 26 | 7.4 | 2.6 | 34.4 | 5 | 45 | 20.3 | 6.5 | 3.7 | 16 | 130 |
| <i>Ritterellia amboinensis</i> | Bipinnate | 18 | 25.6 | 1.9 | 42.5 | 9 | 77 | 12.7 | 22.1 | 8.0 | 7 | 44 |
| <i>Ritterellia sp.</i> | Bipinnate | 33 | 21.3 | 1.3 | 43.1 | 3 | 49 | 18.7 | 34.5 | 22.5 | 6 | 42 |
| <i>Cyclosalpa polae</i> | Cluster | 5 | 17.2 | 1.2 | 47.6 | 2 | 19 | 7.0 | 20.0 | 4.3 | 7 | 55 |
| <i>Cyclosalpa sewelli</i> | Cluster | 7 | 15.0 | 1.4 | 26.8 | 6 | 52 | 6.2 | 19.4 | 7.2 | 11 | 88 |
| <i>Helicosalpa virgula</i> | Helical | 60 | 11.5 | 3.3 | 49.9 | 1 | 7 | 66.0 | 14.0 | 14.8 | 2 | 13 |
| <i>Iasis cylindrica</i> | Linear | 43 | 8.9 | 3.6 | 61.1 | 32 | 308 | 26.8 | 10.5 | 6.5 | 15 | 103 |
| <i>Iiles punctata</i> | Linear | NA | NA | NA | NA | 0 | 0 | 68 | 12 | 3.7 | 1 | 7 |
| <i>Metcalfina hexagona</i> | Linear | 18 | 26.8 | 2.4 | 109.6 | 9 | 105 | 16.0 | 28.0 | 22.0 | 1 | 7 |
| <i>Salpa aspera</i> | Linear | 9 | 28.3 | 2.1 | 114.3 | 7 | 57 | 16.2 | 32.0 | 9.1 | 6 | 42 |
| <i>Salpa fusiformis</i> | Linear | 16 | 17.2 | 3.0 | 57.2 | 8 | 74 | 13.0 | 17.7 | 2.1 | 7 | 47 |
| <i>Salpa maxima</i> | Linear | 2 | 61.6 | 0.7 | 55.9 | 4 | 34 | 3.6 | 87.8 | 27.8 | 8 | 52 |
| <i>Soestia zonaria</i> | Linear | 11 | 13.7 | 1.9 | 109.2 | 4 | 34 | 9.1 | 19.6 | 4.6 | 8 | 23 |
| <i>Thalia sp.</i> | Oblique | 29 | 3.5 | 4.5 | 5.8 | 1 | 28 | 18.6 | 5.9 | 0.3 | 7 | 53 |
| <i>Peges sp.</i> | Transversal | 12 | 31.0 | 1.7 | 20.3 | 2 | 18 | 13.1 | 43.2 | 29.2 | 13 | 91 |
| <i>Cyclosalpa affinis</i> | Whorl | 5 | 33.0 | 1.4 | 24.5 | 2 | 15 | 6.7 | 37.9 | 23.4 | 10 | 65 |
| <i>Cyclosalpa bakeri</i> | Whorl | 7 | 7.0 | 2.6 | 10.4 | 7 | 63 | 6.9 | 14.6 | 3.0 | 7 | 57 |
| <i>Cyclosalpa quadriluminis</i> | Whorl | 8 | 27.1 | 1.3 | 25.3 | 1 | 6 | 8.3 | 24.5 | 12.7 | 6 | 36 |

Table S4. Tukey's post-hoc pairwise comparisons from an ANOVA on swimming speed across different colonial architectures reporting magnitude of difference and adjusted p-values.

| | | Speed (mm/s) | | Speed (zooids/pulse) | |
|--------------|-------------|--------------|--------------|----------------------|--------------|
| Architecture | | Difference | p-value adj. | Difference | p-value adj. |
| Cluster | Bipinnate | 0.082 | 0.999 | -12.900 | 0.008 |
| Helical | Bipinnate | -0.112 | 1.000 | 10.870 | 0.959 |
| Helical | Cluster | -0.194 | 1.000 | 23.769 | 0.345 |
| Linear | Bipinnate | 0.896 | 0.000 | 33.971 | 0.000 |
| Linear | Cluster | 0.814 | 0.000 | 46.871 | 0.000 |
| Linear | Helical | 1.008 | 0.478 | 23.101 | 0.347 |
| Oblique | Bipinnate | -1.044 | 0.005 | -33.143 | 0.000 |
| Oblique | Cluster | -1.126 | 0.003 | -20.244 | 0.017 |
| Oblique | Helical | -0.932 | 0.691 | -44.013 | 0.006 |
| Oblique | Linear | -1.940 | 0.000 | -67.114 | 0.000 |
| Transversal | Bipinnate | -0.969 | 0.015 | -22.314 | 0.004 |
| Transversal | Cluster | -1.050 | 0.009 | -9.415 | 0.738 |
| Transversal | Helical | -0.856 | 0.772 | -33.184 | 0.095 |
| Transversal | Linear | -1.864 | 0.000 | -56.286 | 0.000 |
| Transversal | Oblique | 0.075 | 1.000 | 10.829 | 0.804 |
| Whorl | Bipinnate | -0.774 | 0.001 | -25.559 | 0.000 |
| Whorl | Cluster | -0.856 | 0.001 | -12.659 | 0.046 |
| Whorl | Helical | -0.662 | 0.890 | -36.429 | 0.023 |
| Whorl | Linear | -1.670 | 0.000 | -59.530 | 0.000 |
| Whorl | Oblique | 0.270 | 0.974 | 7.584 | 0.891 |
| Whorl | Transversal | 0.195 | 0.996 | -3.245 | 0.999 |

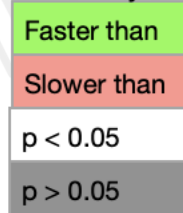
Color key:

 Faster than
 Slower than
 p < 0.05
 p > 0.05

Table S5. Tukey's post-hoc pairwise comparisons from an ANOVA on COT across different colonial architectures reporting magnitude of difference and adjusted p-values.

| | | COT per mm | | COT per zooid length | |
|--------------|-------------|------------|--------------|----------------------|--------------|
| Architecture | | Difference | p-value adj. | Difference | p-value adj. |
| Cluster | Bipinnate | 0.558 | 1.000 | -16.055 | 1.000 |
| Helical | Bipinnate | 1.220 | 1.000 | -22.338 | 1.000 |
| Helical | Cluster | 0.662 | 1.000 | -6.283 | 1.000 |
| Linear | Bipinnate | -0.109 | 1.000 | -19.013 | 1.000 |
| Linear | Cluster | -0.667 | 1.000 | -2.958 | 1.000 |
| Linear | Helical | -1.329 | 1.000 | 3.326 | 1.000 |
| Oblique | Bipinnate | 46.132 | 0.000 | 155.555 | 0.122 |
| Oblique | Cluster | 45.574 | 0.000 | 171.610 | 0.006 |
| Oblique | Helical | 44.912 | 0.000 | 177.893 | 0.209 |
| Oblique | Linear | 46.241 | 0.000 | 174.567 | 0.001 |
| Transversal | Bipinnate | 4.999 | 0.991 | 100.580 | 0.498 |
| Transversal | Cluster | 4.441 | 0.976 | 116.636 | 0.061 |
| Transversal | Helical | 3.778 | 1.000 | 122.919 | 0.581 |
| Transversal | Linear | 5.108 | 0.906 | 119.593 | 0.013 |
| Transversal | Oblique | -41.134 | 0.000 | -54.974 | 0.900 |
| Whorl | Bipinnate | 0.180 | 1.000 | -9.487 | 1.000 |
| Whorl | Cluster | -0.378 | 1.000 | 6.568 | 1.000 |
| Whorl | Helical | -1.041 | 1.000 | 12.851 | 1.000 |
| Whorl | Linear | 0.289 | 1.000 | 9.526 | 1.000 |
| Whorl | Oblique | -45.952 | 0.000 | -165.042 | 0.003 |
| Whorl | Transversal | -4.819 | 0.931 | -110.067 | 0.032 |

| Color key: |
|---------------------|
| More efficient than |
| Less efficient than |
| p < 0.05 |
| p > 0.05 |

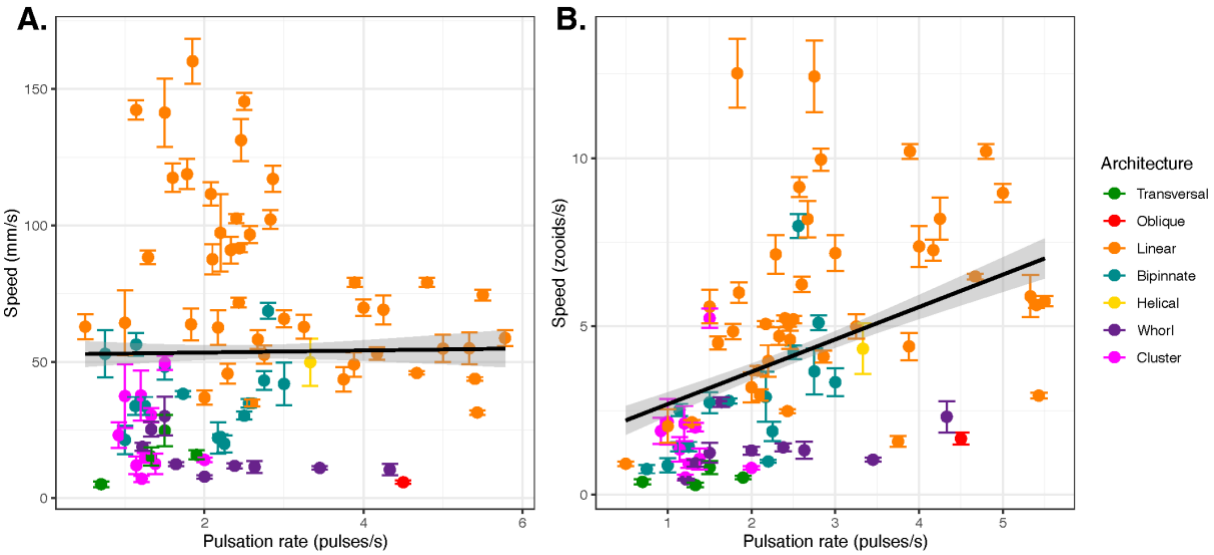


Figure S1. Distribution of salp colony absolute (A) and zooid size-corrected (B) swimming speed across pulsation rates. Lines represent linear regressions with a 95% confidence interval shaded in grey.

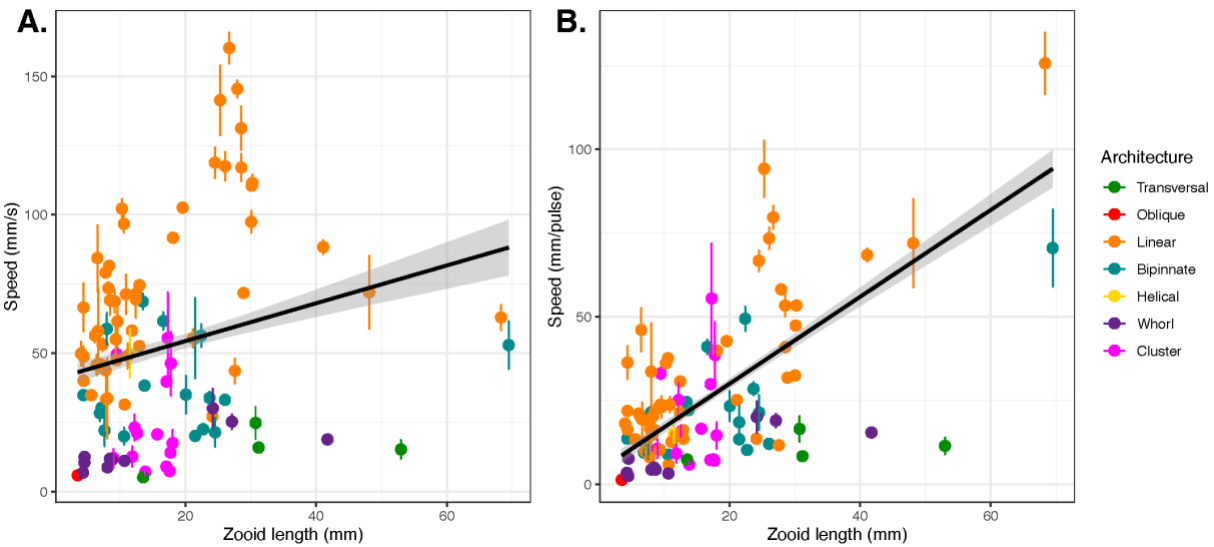


Figure S2. Distribution of salp colony absolute (A) and pulsation rate-corrected (B) swimming speed (specimen means with standard errors) across zooid sizes. Lines represent linear regressions with a 95% confidence interval shaded in grey.

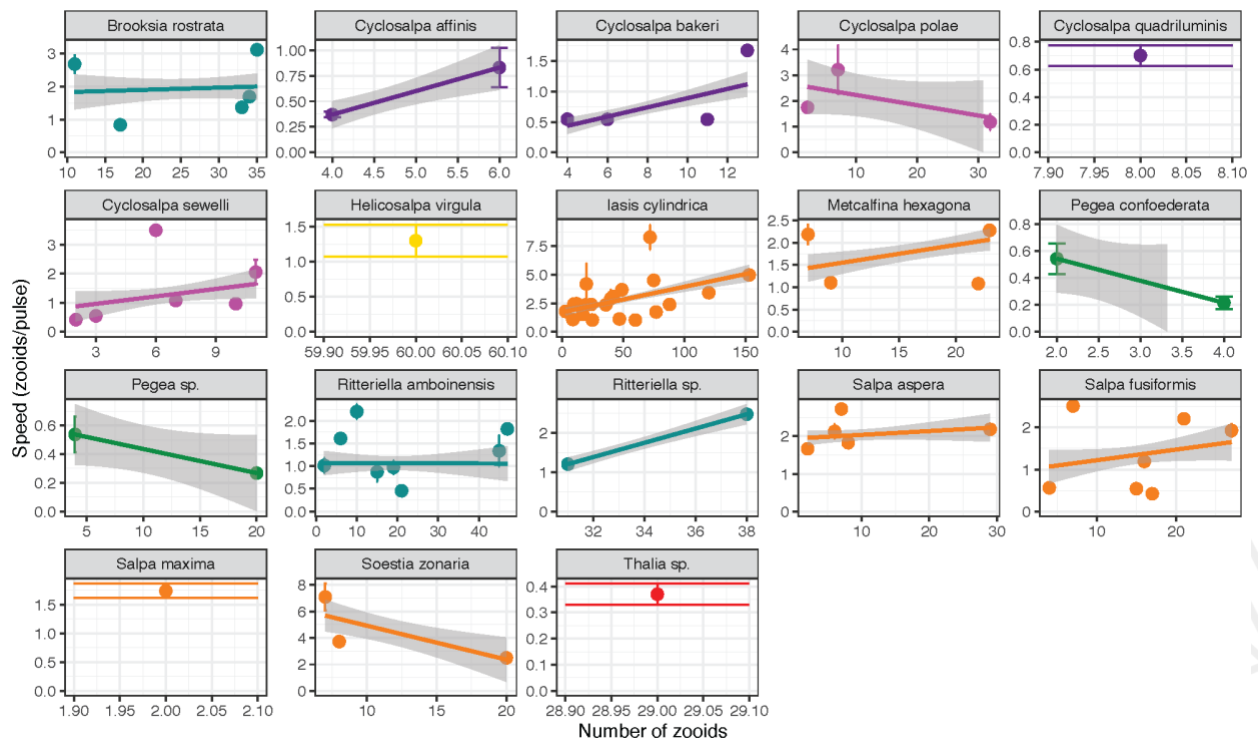


Figure S3 – Linear relationships between relative swimming speed (zooid lengths per pulsation, specimen means with standard errors) and number of zooids in the colony across each salp species. Gray areas represent the 95% confidence intervals of the linear regressions.

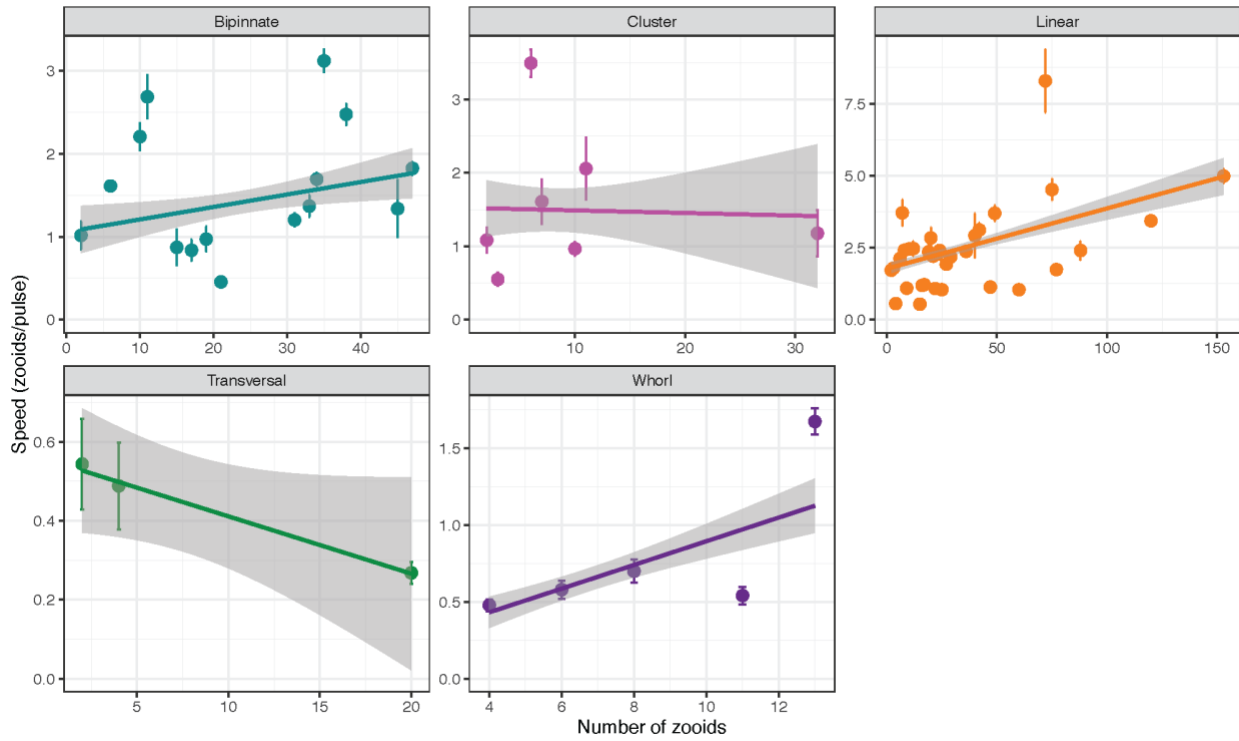


Figure S4. Linear relationships between relative swimming speed (zooid lengths per pulsation, specimen mean with standard errors) and number of zooids in the colony across each colonial architecture. Gray areas represent the 95% confidence intervals of the linear regressions.

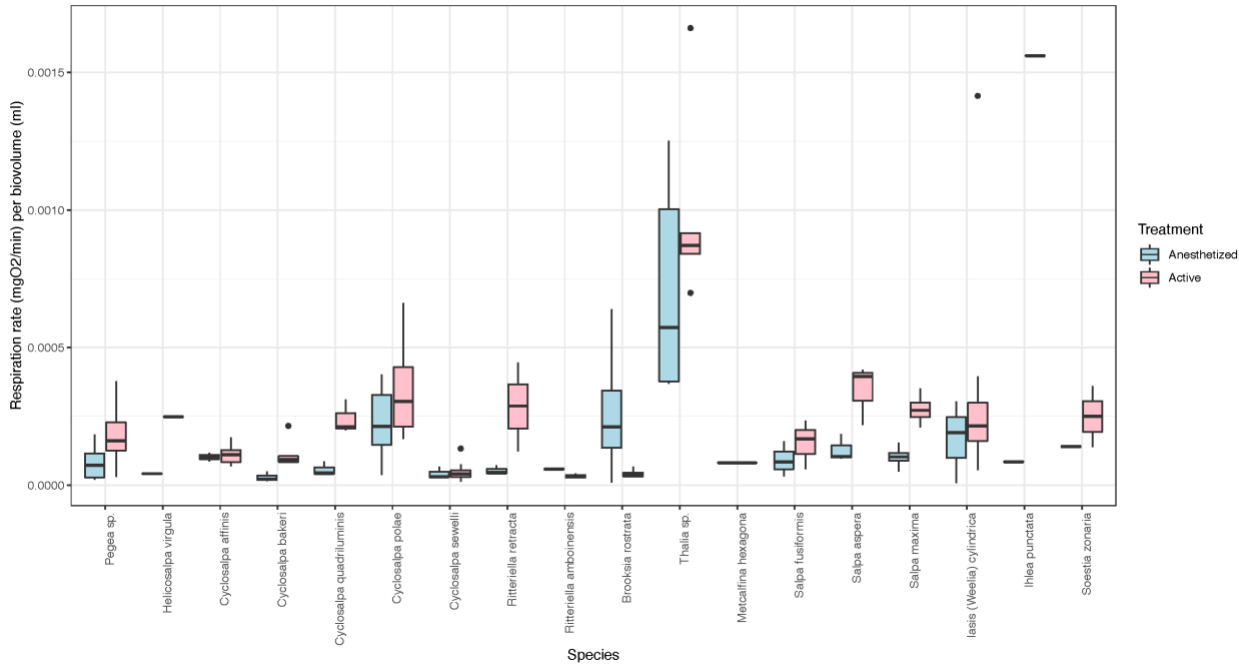


Figure S5. Biovolume-normalized respiration rates of swimming (red) and anesthetized (blue) salp colonies across different species.

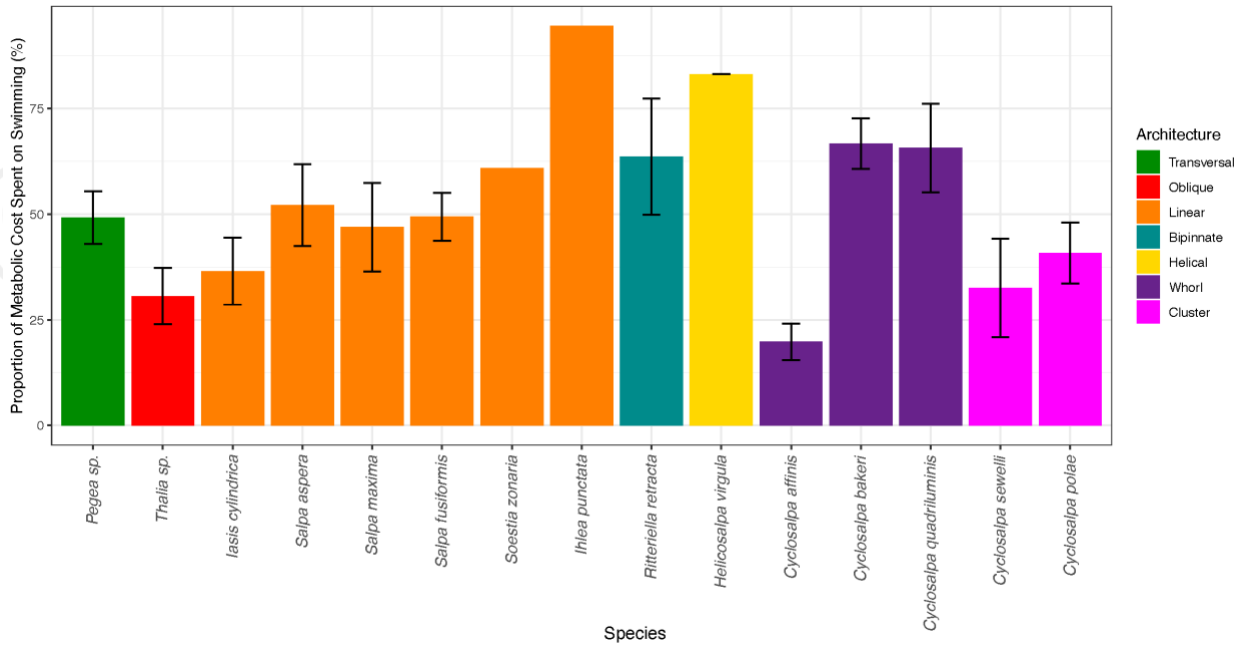


Figure S6. Percentage of the swimming respiration rates matched by the mean anesthetized respiration rate for each salp species. Bars represent species means with black lines representing standard errors. Colors indicate colonial architecture.

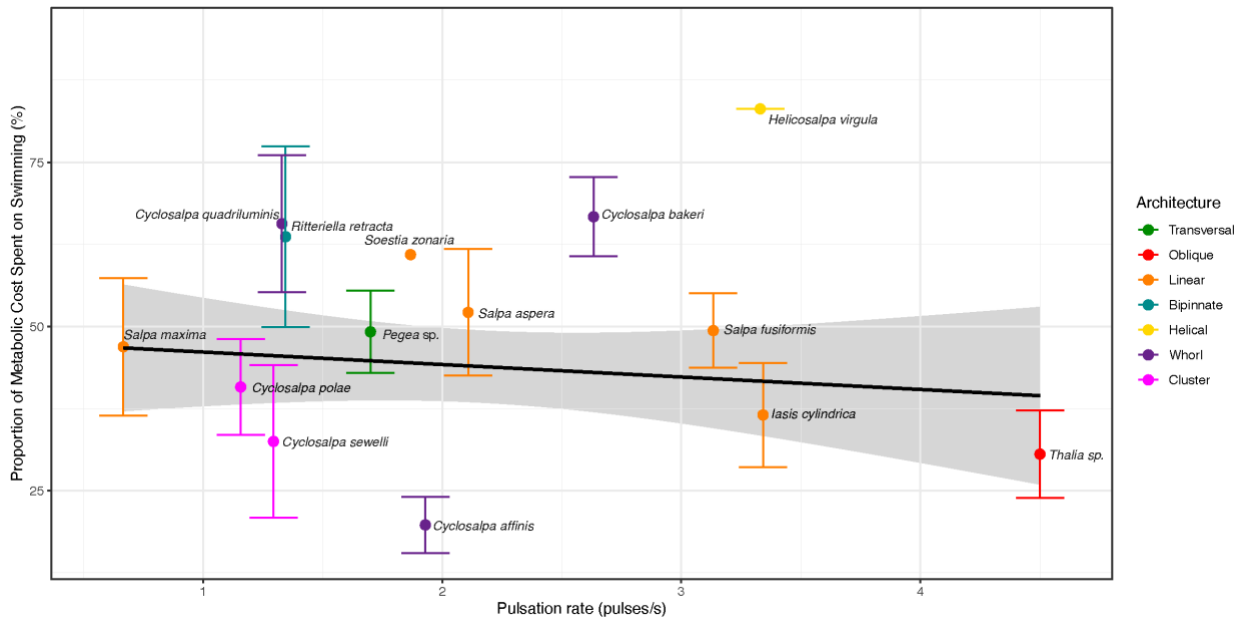


Figure S7. Percentage of the swimming respiration rates matched by the mean anesthetized respiration rate for each salp species (mean points with standard error bars) across species mean observed swimming pulsation rate derived from video data.

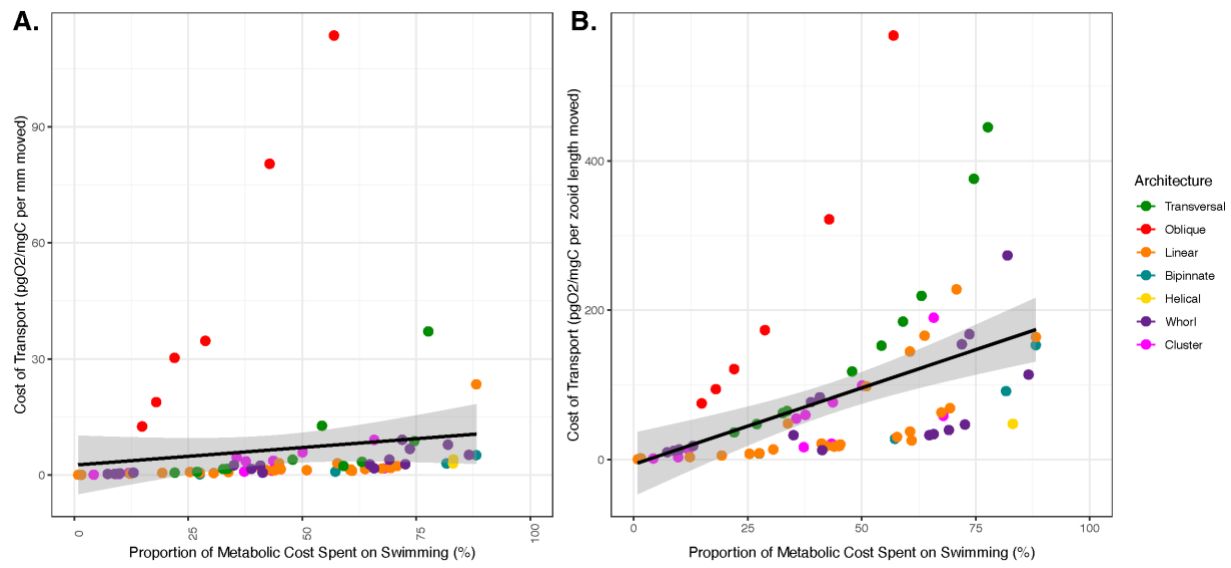


Figure S8. Cost of transport (per mm in A, per zooid length in B) for each salp species across their percent swimming respiration rate matched by the species' mean anesthetized respiration rate. Point color indicates colonial architecture.

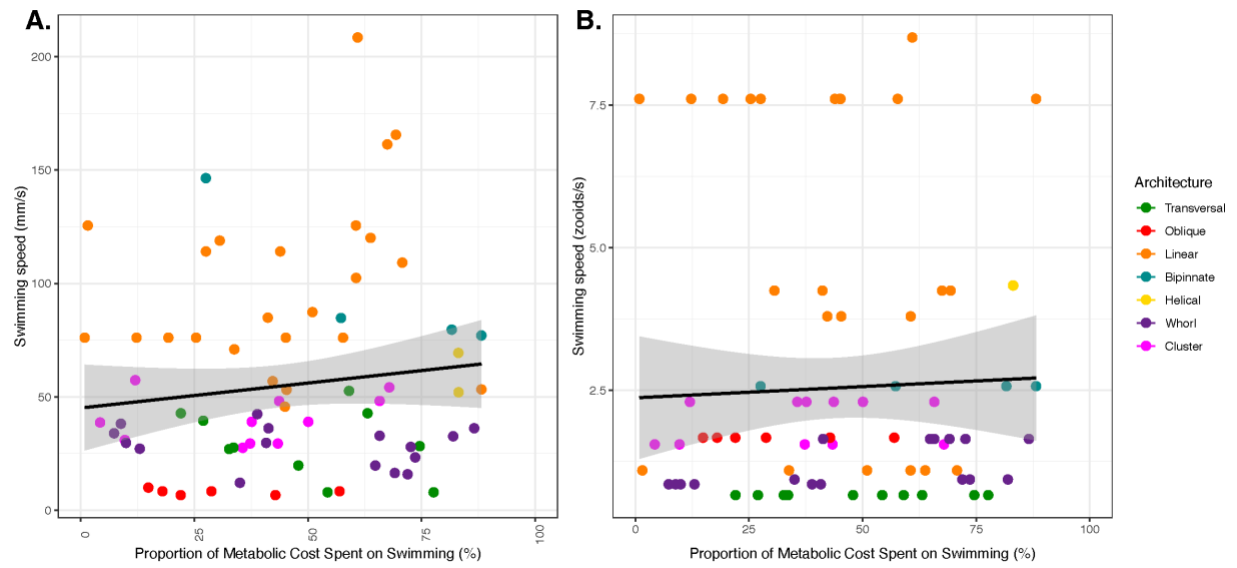


Figure S9. Swimming speed (in mm/s in A, and zooids/s in B) for each salp species across their percent swimming respiration rate matched by the species mean anesthetized respiration rate. Point color indicates colonial architecture.

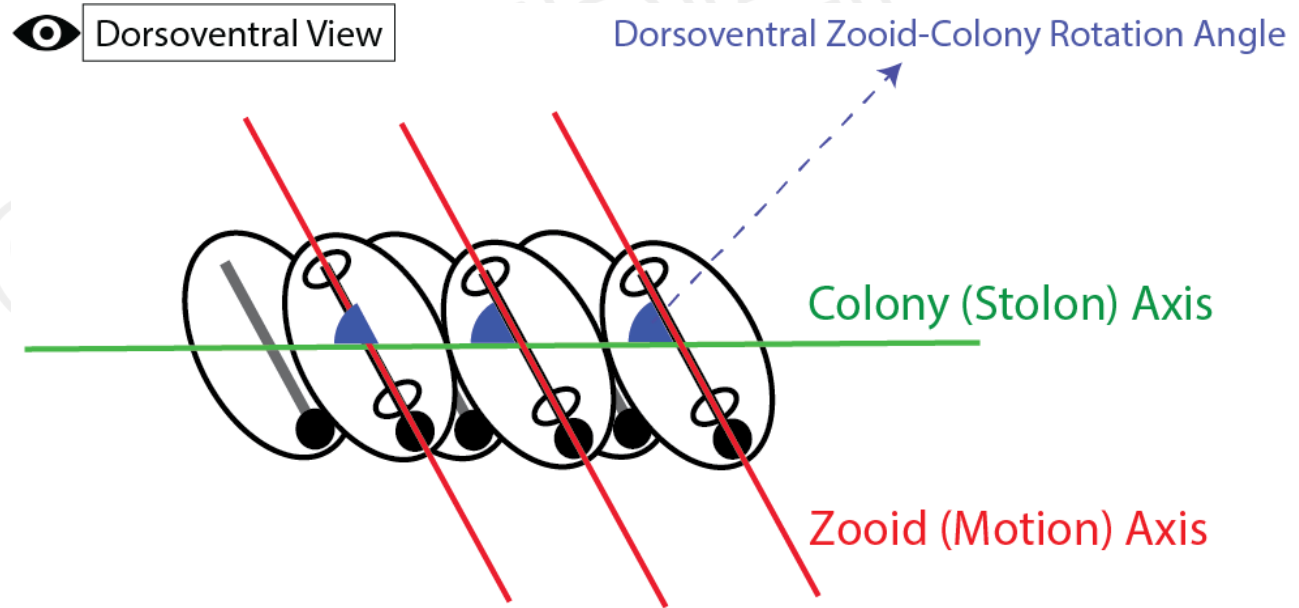


Figure S10. Schematic of an oblique chain from the dorsoventral perspective showing the zooid and stolon axes and the zooid rotation angle (degree of linearity) relative to those axes. Black lines indicate gill bars while gray lines represent endostyles.